Detection and Compensation of Control Valve Stiction

MASTER OF SCIENCE IN ENGINEERING
(CHEMICAL)

MONIR AHAMMAD

DEPARTMENT OF CHEMICAL ENGINEERING
BANGLADESH UNIVERSITY OF ENGINEERING AND TECHNOLOGY, DHAKA

January 2012

Detection and Compensation of Control Valve Stiction

by

MONIR AHAMMAD

A thesis

submitted to the Department of Chemical Engineering

for partial fulfillment of the requirements

for the degree

of

MASTER OF SCIENCE IN ENGINEERING (CHEMICAL)

DEPARTMENT OF CHEMICAL ENGINEERING

BANGLADESH UNIVERSITY OF ENGINEERING AND TECHNOLOGY, DHAKA

CERTIFICATION OF THESIS WORK

We the undersigned, are pleased to certify that **Monir Ahammad**, a candidate for the degree of **Master of Science in Engineering (Chemical)** has presented his thesis work on the subject **"Detection and Compensation of Control Valve Stiction"**. The thesis is acceptable in form and content. The student demonstrated a satisfactory knowledge of the field covered by this thesis in an oral examination held on **January 7, 2012**.

Dr. Md. Ali Ahammad Shoukat Choudhury — Chairman
Associate Professor
Department of Chemical Engineering
BUET, Dhaka-1000

Prof. Dil Afroza Begum — Member (Ex-officio)
Professor and Head
Department of Chemical Engineering
BUET, Dhaka-1000

Sirajul Haque Khan — Member
Associate Professor
Department of Chemical Engineering
BUET, Dhaka-1000

Sk. Shafi Ahmed — Member
Chief Operations Officer — (External)
Karnaphuli Fertilizer Company Limited
KAFCO, Anowara, Chittagong

Abstract

Presence of oscillation or large variability in control loops results in decreased economical advantage to process plants due to inferior quality products, larger rate of rejections, reduced average throughputs and overall increased energy requirements. Oscillation may arise due to physical and non-physical causes. Mechanical problem in control valves is a common physical cause. Among the physical problems of control valve which produces oscillations in the control loop, stiction is often referred as hidden culprit. This study presents a novel noninvasive stiction detection method which requires only routine operation data. It has been shown that the presence of stiction in control valve produces signals containing odd harmonics. The proposed method estimates frequencies, amplitudes and phases of control error signals and examines harmonic relations among them. The presence of odd harmonics indicates the presence of stiction in the control valve. The method has been validated by simulation and pilot plant experimentation. The proposed method has also been evaluated by using benchmark industrial data sets and found to perform better than currently available other stiction detection methods.

Detection of control valve stiction and it's remedial action are two separate tasks. Oscillations of the process variables due to the presence of stiction in the control valve can't be stopped until valve maintenance. Normally, maintenance of sticky valves in the industry is usually carried out in a scheduled outage. If immediate actions can't be implemented after the detection of sticky valve, industry continues to incur economic losses from the harmful effect of stiction such as early wear-off of the valve stem, reduced valve life and production of off-spec products. Thus, an effective stiction compensation method to remove the harmful effects of stiction on the process plant is a long felt desire of the industry. In this study, the performance of a self tuning adaptive controller in the presence of stiction was studied. PI and PID type adaptive controllers' efficacy has been studied as a compensator for valve stiction.

Acknowledgements

The author expresses his gratitude and thanks to Dr. M. A. A. Shoukat Choudhury for the supervision of this research. His guidance and inspirations led this work to see the face of light. His enthusiastic appreciation and counseling stimulated author's research interest.

The author would like to gratefully acknowledge Mr. B.M. Sirajeel Arifin, Lecturer, Department of Chemical Engineering, BUET for his cooperation with understanding some theoretical backgrounds and also for giving some mental support during the hard time of this research.

Contents

List of Figures

List of Tables

Abbreviations

AC	**A**nalyzer **C**ontrol
ARMA	**A**uto **R**egressive **M**oving **A**verage
BIC	**BIC**oherence
CC	**C**oncentration **C**ontrol
CCF	**C**ross **C**orrelation **F**unction
CHEM	**CHEM**ical Industry
EWMA	**E**xponentially **W**eighted **M**oving **A**verage
FC	**F**low **C**ontrol
FOPTD	**F**irst **O**rder **P**lus **T**ime**D**elay
GPC	**G**eneralized **P**redictive **C**ontrol
HAMM2	Second **HAMM**erstein based indentification technique
HAMM3	Third **HAMM**erstein based indentification technique
ISE	**I**ntegral **S**quare **E**rror
MET	**MET**al Processing Industry
MIN	**MIN**ing
MPC	**M**odel **P**redictive **C**ontrol
MV	**M**anipulated **V**ariable
OP	Controller Output or Valve Input
PAP	**P**ulping **A**nd **P**aper Industry
PC	**P**ressure **C**ontrol
PI	**P**roportional and **I**ntegral Controller
PID	**P**roportional **I**ntegral **D**erivative
PV	**P**rocess **V**ariable
RLS	**R**ecursive **L**east **S**quares

SNR	**S**ignal to **N**oise **R**atio
SP	**S**et **P**oint
STC	**S**elf **T**uning **C**ontroller
ThC	**Th**ickness **C**ontrol
VOC	**V**olatile **O**rganic **C**omponents
ω_i	Frequency of the i'th sinusoid term of Fourier series
ω_1	Fundamental Frequency
A_1	Amplitude of the first term of Fourier series
ϕ_1	Phase lag of the first term of Fourier series
g	Fisher's **g** factor
y(t)	Any time series
e	error signal
K_C	Controller gain
τ_I	Integral gain
K_P	Process gain
τ	Time constant of process
G_P	Transfer Function of Process
G_C	Controller's Transfer Function
S	Deadband plus stickband
J	Slip Jump

Chapter 1

Introduction

Modern process plants are getting increasingly automated due to the requirement of tight quality control, larger production rate and higher energy integration and stringent environmental requirement. Hundreds and thousands of control loops are the integral part of the automation in the large process plants. The presence of oscillation or large variability in the control loops results in off-specification products and reduced profitability. Production of off-spec products means reduction in average throughput, wastage of energy, materials and time, and ultimately economic loss. The cause of oscillation or limit cycles may be physical and non-physical. Aggressive tuning of controller, presence of external oscillatory disturbance and loop interactions are the non-physical causes of oscillation. Physical problems can be sensor failure or control valve problems. Among the causes of limit cycles, control valve problems should be considered with prime importance because it is the only moving part in a typical control loop. It implements the controller decision to the process. Hence if the control valve malfunctions, the performance of the loop will deteriorate – no matter how good or expensive the other components e.g., controller, sensors are. Commonly encountered control valve problems are: Stiction, Hysteresis, Deadband or Deadzone. Many surveys [3] [4] [5] [6] indicated that about 30% of all the control loops oscillate due to the valve nonlinearities. Stiction in the control valve is usually detected by physical test of the valve which is known as bump test. It is almost impossible to detect stiction in an industry

where a pretty good number of control loops are present. As a result, non-invasive techniques become popular for detection of stiction so that maintenance action can be immediately taken during the period of scheduled outage.

It is known that maintenance action in the control valve can't be taken until the period of overhauling. As a result, a sticky valve causes off-specification products due to the presence of oscillation. Thus an adaptive noninvasive stiction compensation technique which can sufficiently suppress the oscillations of the variables is a long-felt desire of the industry personnel.

1.1 Objective of the Study

This work aims to develop:

1. An improved method for the detection of control valve stiction and,
2. A noninvasive stiction compensation technique that will suppress the effect of stiction.

1.2 Scope of the Study

The presence of stiction in the control loops causes huge economical disadvantage to process plants. The product quality may be affected greatly due to the presence of stiction. Significant amount of stiction may cause unstable process.

Simple harmonic analysis techniques has been developed for the noninvasive detection of control valve stiction. The proposed method has been validated by using simulation and pilot plant experimentation. It was also evaluated using benchmark industrial data sets. It was found that the proposed method works better than any other currently existing method.

This study also attempted to develop an adaptive controller tuning based stiction compensation algorithm for suppressing the effect of stiction. A self tuning adaptive controller was designed to automatically update the controller parameters when the performance of the control loop deteriorates. The algorithm automatically retunes the controller gain, K_c and integral time constant, τ_I when the performance index goes below a threshold value. It was found that a self tuning controller based on the Hammerstein system identification doesn't work good for stiction compensation.

1.3 Thesis Organization

This thesis is organized as follows:

Chapter 1 is the introduction to this thesis. Summary of the background and thesis organization are included in this chapter.

Chapter 2 provides an overview of the existing stiction detection and compensation methods. Several existing methods for detection and compensation are briefly discussed.

Chapter 3 describes the ins and outs of the proposed stiction detection method. The detailed mathematical description of the proposed method is provided. Practical aspects of the proposed method is also discussed.

Chapter 4 validates the proposed stiction detection method. Simulated data and pilot plant experimentation have been used for the validation of the proposed method.

Chapter 5 evaluates the proposed method on benchmark industrial data sets. This chapter compares the efficiencies of different methods by applying them on a set of common industrial data sets.

Chapter 6 discusses the efficacy of a performance based adaptive compensation method based on the Hammerstein system identification.

Finally, Chapter 7 states the conclusions drawn from the current work and suggests possible directions for future work.

Chapter 2

Literature Review

2.1 Typical Control Loop

Feedback control is the most common automatic control system used in process industry. Figure 2.1 shows a simple feedback control configuration. In this Figure, the valve is the only moving part which implements controller decision hence known as the work-horse of a control loop. Most of the industrial valves are pneumatic control valves driven by pressure variation of compressed air. Figure 2.2 shows important parts of a typical industrial pneumatic control valve. Stiction in control valves may appear due to seal degradation, lubricant depletion, inclusion of foreign matters, activation of metal sliding surfaces at high temperature and/or tight packing around the stem [7]. The resistance due to stem packing is considered as the main cause of stiction. A very common cause of stiction in the control loop is the over tightening of the stem packing for controlling Volatile Organic Components (VOC) emissions. Stiction may vary with time and operating range as frictional wear may not uniform along the stem.

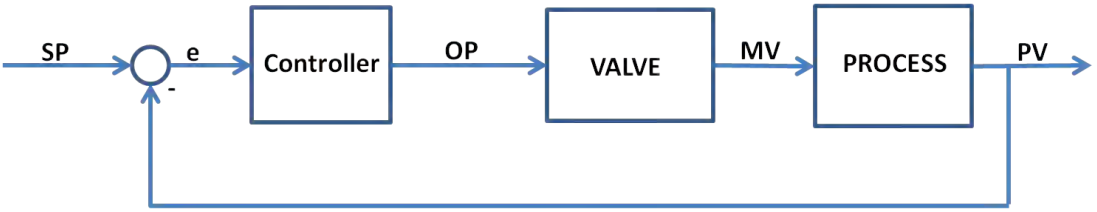

FIGURE 2.1: Simple feedback control scheme

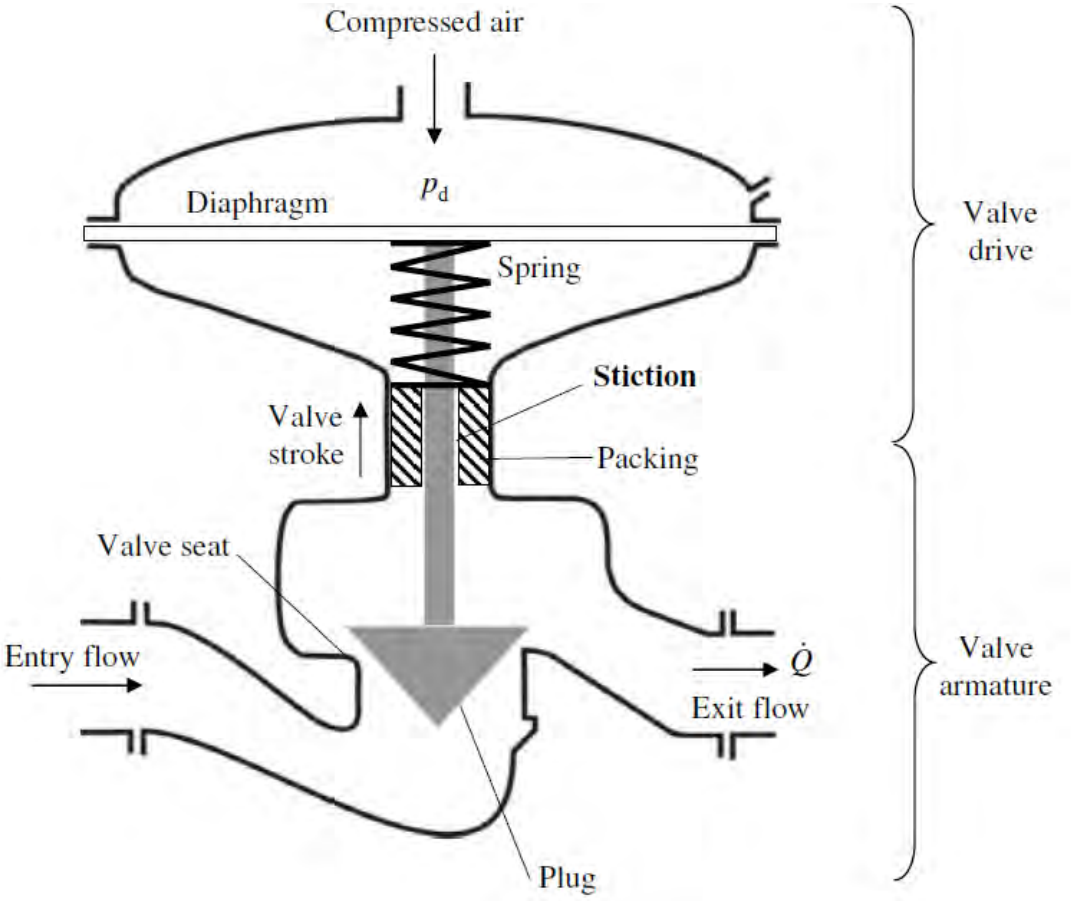

FIGURE 2.2: Diagram of a pneumatic control valve [1]

2.2 Definition of Stiction

The most comprehensive, formal and explanatory definition of valve stiction was first proposed by [8]. The definition is based on the input-output behavior of the valve as illustrated in Figure 2.3. From this figure, a sticky valve can't move from a stationary position until the input signal (OP) overcomes a band of S, known as deadband plus stickband. As soon as it overcomes the deadband and stickband, the valve jumps. The jump is termed as slip jump (J). This phenomena mainly

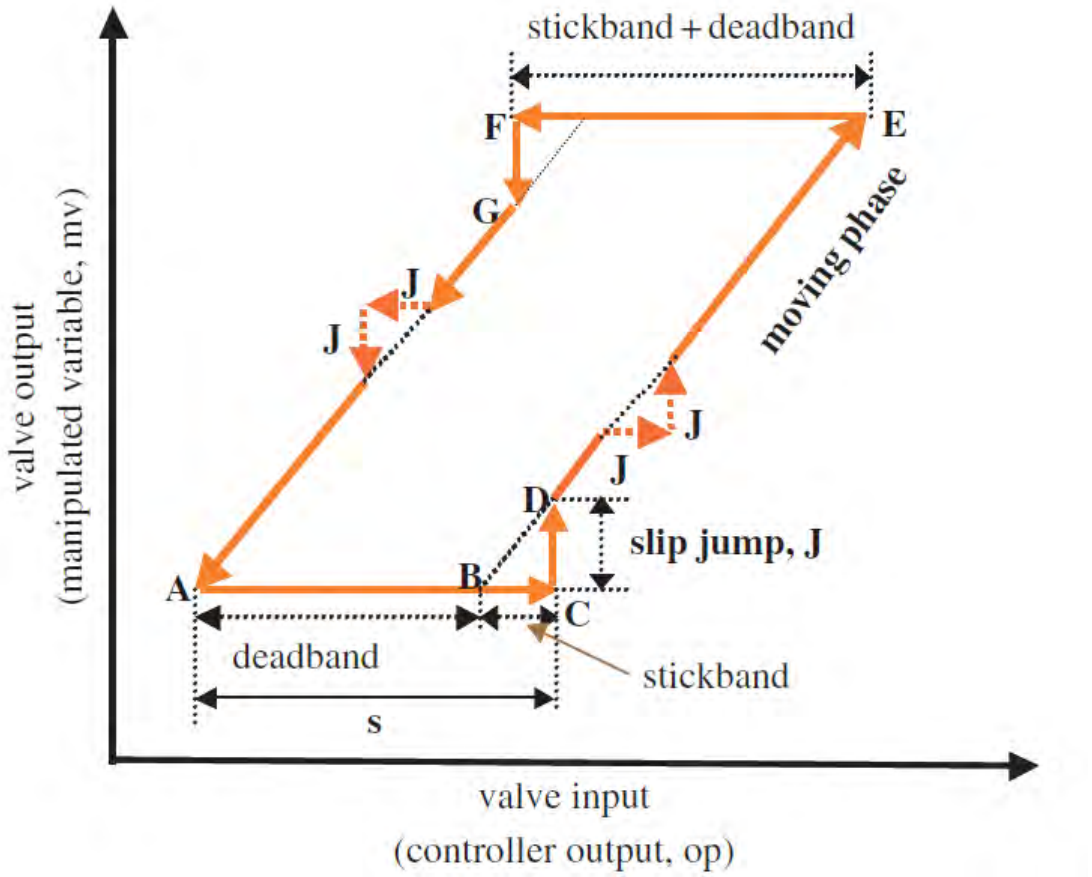

FIGURE 2.3: Input-output behavior of a sticky valve [2]

occur when the valve starts to move from a static position (A and E in the Figure). If the the velocity of the valve movement along the path DE or GA is very low, stiction may also happen. According to [8]:

> "The presence of stiction impairs proper valve movements, i.e., the valve stem may not move in response to the output signal from the controller or the valve positioner. The smooth movement of the valve in response to a varying input from the controller or the valve positioner is preceded by a stickband and an abrupt jump termed as slip jump. Its origin in the mechanical system is static friction, which exceeds the dynamic friction during smooth movement."

Based on the illustrative definition of the input-output behavior of the sticky valve, the mechanism of oscillation production becomes easier to understand. When a control valve suffers from stiction it doesn't move until the input signal or air pressure which is applied to its actuator is greater than what is required with respect to an ideal frictionless valve [9] [10]. An excess control signal is necessary to overcome the stiction and move the stem. As a result, the valve position goes to a point beyond the desired value. This phenomenon repeats causing oscillations and large variability in the control loop. Thus valve stiction is considered as one of the major causes of performance degradation by producing limit cycle oscillations in control loops [11] [12] [13] [14] [15].

2.3 Stiction Modelling

Considering the negative impact of valve stiction in process plants, several physical and data-driven (empirical) stiction models have been developed. Physical models such as Karnopp's model [16] are difficult to simulate and often cannot reproduce stiction effect precisely because a large number of parameters are to be specified. On the other hand, data-driven models are useful because it is non-invasive, few parameters needed to be specified and easy to implement. Two main classes of data-driven models have appeared in literature, they are: one-parameter models and two-parameter models. One parameter model such as Stenmann et al. [17] reported in the literature is not adequate to explain the details of stiction dynamics. The well known two-parameter models of stiction are Choudhury's [8] model, Kano's [18] model and He's [19] model. The first two are variants of the same principle. In this study, Choudhury's stiction model was used in the simulation and experimentation of the proposed method. Choudhury's model requires controller output (OP) as input signal to the model and specifications of two parameters namely the deadband plus stickband (S) and slip jump (J). To cope noise problems an Exponentially Weighted Moving Average (EWMA) filter was used after the controller.

2.4 Stiction Detection Methods

The literature describes different types of non-invasive approaches to detect and estimate valve stiction. However, many of them have some practical limitations one way or other, which have to be addressed for real life applications in the industry. Some of the methods are grouped and briefly discussed below:

2.4.1 Shape-based Stiction Detection

The relationship between the controller output (OP) and manipulated variable (MV) is used to detect stiction. In practice where MV is not available, flow rate is used. Kano et al. [18] suggested two shape-based detection method. In the first method, he suggested to observe the behavior of MV against OP. The method utilized the fact that MV doesn't change in the presence of stiction though OP is changing. The second method utilizes the fact that the relationship between the OP and the MV takes the shape of a parallelogram due the presence of stiction. The distance between the arms of parallelogram indicates the degree of stiction. Yamasita [20] proposed a method based on the qualitative shape of the time series. Time segment can be qualitatively approximated as increasing (I), decreasing (D) and steady (S). The combinations of the symbols provides the qualitative movement patters such as DI, IS, II etc. The second step is to find the patterns of the time window. Segments of typical patterns for stiction are the sequence of IS II, IS SI, DS DD and DS SD. A stiction index SI_C to capture these specific pattern sequence is used which is shown as below:

$$SI_C = (\tau_{IS\ II} + \tau_{IS\ SI} + \tau_{DS\ DD} + \tau_{DS\ SD})/(\tau_{total} - \tau_{SS}) \tag{2.1}$$

where τ_{total} is the width of the time window, and τ_{SS} is time period for patterns SS in the window. If the value of SI_C is larger than 0.25 the loop possibly has stiction.

Another shape based detection method using the area calculation was proposed by Salsbury and Singhal [21]. This method refers to the zero-crossing events of the controller error signal. After a zero-crossing event, the left hand area and right hand area under the peak is calculated. The ratio (R index) between the areas is used to determine the presence of stiction. It is suggested that if the R index is larger than 1, the loop contains stiction.

The main disadvantage of these methods is that, manual inspection of the time series is required in order to detect the shapes.

2.4.2 Correlation-based Stiction Detection

Alexander Horch [10] suggested correlation based stiction detection method. Ideally, the stiction phenomena results in the signals as shown in the left half plane of the Figure 2.4. For all other cases, the signal shapes are more or less sinusoidal as indicated in the right half plane of Figure 2.4. Based on this, he devised a cross-correlation function (CCF) method to detect stiction. This strategy is stated as:

> "If the cross-correlation function (CCF) between the controller output and process output is an odd function (i.e., asymmetric w.r.t the vertical axis), the likely cause of the oscillation is stiction. If the CCF is even (i.e., symmetric w.r.t the vertical axis) then the stiction is not likely to be the cause of the oscillation."

The limitations of this method are

- The oscillation has to be detected a-priori.
- Non integrating process.
- Controller must have significant integral action.
- The loop should not carry any compressible media.

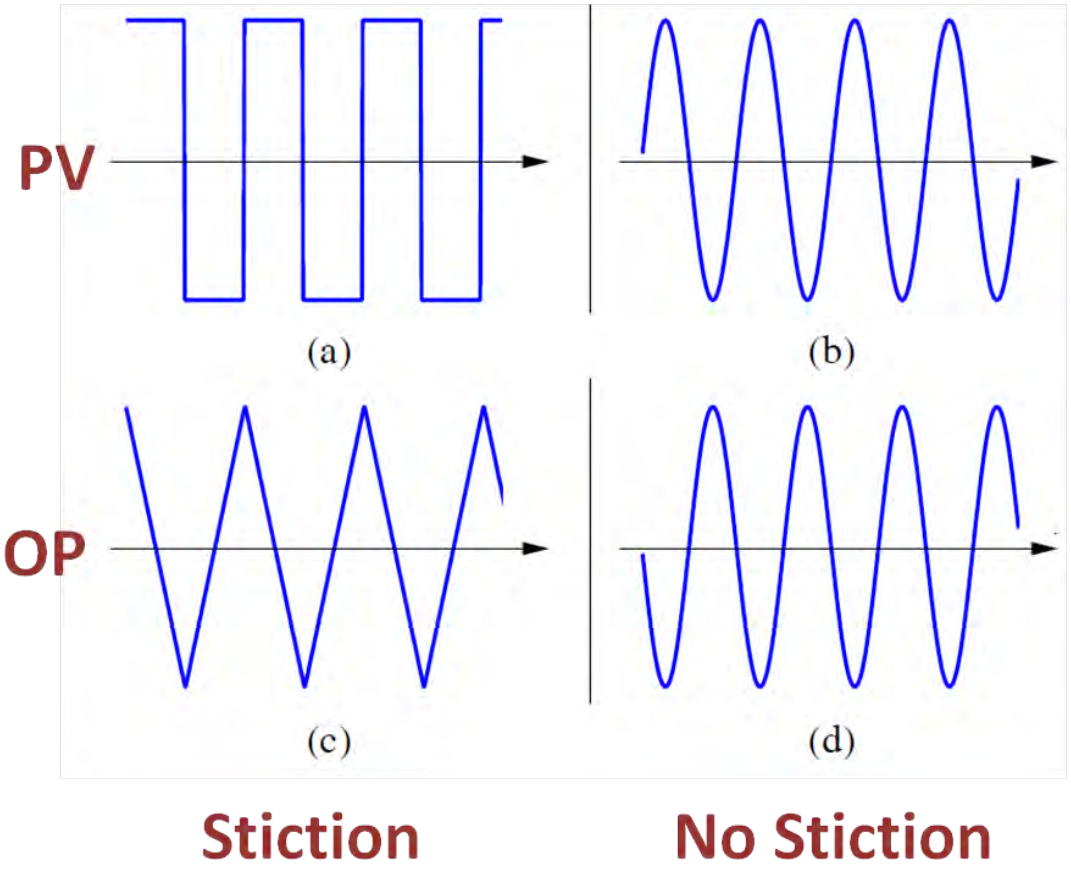

FIGURE 2.4: Ideal PV (top) and OP (bottom) signals in the presence (left) and absence (right) of stiction.

This method may also have problems due to the phase shift induced by controller tuning.

2.4.3 Curve Fitting method of Stiction Detection

He et al. [19] presented a curve fitting method based on qualitative analysis of the control signals. The fact about the control signals is that, in the case of control-loop oscillations caused by controller tuning or external oscillating disturbances, the OP and PV typically follow sinusoidal waves for both self regulating and integrating processes. In case of stiction, the unmeasured valve position signal may usually takes the shape of a rectangular signal. The integrating element of controller or process (if any) converts this rectangular form to triangular form after the valve, which is either OP or PV. For non-integrating process PI controller

acts as the first integrator and the OP's move follow the triangular shape whereas integrating process such as level control, the integrator in the process integrates the rectangular waves and the PV signal follows a triangular wave. The basic idea is to fit two different functions, triangular wave and sinusoidal wave to the measured oscillating signal (OP for self regulating and PV for integrating process). A better fit to a triangular wave indicates valve stiction, while a better fit to a sinusoidal wave indicates non-stiction.

The limitations of the curve fitting methods is that, it requires a certain shape of the signal and requires accurate zero-crossing detection which is a non-trivial task in the presence of noise.

2.4.4 Relay-based Techniques for Stiction Detection

Scali [22] proposed a relay based shape formalism for the automatic detection of control valve stiction. In this method, every significant half cycle of a recorded oscillation of the output variable PV is fitted by means of three primitives obtained by varying parameters, namely: a sine wave, a triangular wave and a relay-generated wave. The last primitive is the output response of a FOPTD under a relay control, by varying the ratio of the process parameter θ/τ. There is a similarity between the shapes of the oscillatory controlled variable (PV) due to valve stiction with those of loops under relay control. A relay scheme is used to generate the data to perform the fitting of the acquired PV. Each half of the oscillation is analyzed and the same data are also fitted by means of sinusoidal, triangular and relay generated wave. If minimum amount of fitting error occurs for triangular and relay generated signal, the loop is said to be associated with the presence of stiction. If minimum error occurs for sinusoidal signal, it is the oscillation referred with the presence of disturbance and not due to the valve stiction.

The disadvantage of this method is that, an on-line relay has to be implemented for the detection of stiction.

2.4.5 Bicoherence and Ellipse Fitting Method of Stiction Detection

Choudhury et al. [8] presented a method to detect and quantify stiction using routine operating data. The non-linearity of the loop is tested using bicoherence. If the non-linearity is detected, stiction is estimated as the maximum width of the cycles of the PV-OP plot in the direction of OP. The PV-OP plot is fitted with an ellipse and the amount of stiction is estimated to be the maximum width of the ellipse in the OP direction, which is called the ellipse-fitting method. The stiction estimated using the method of Choudhury et al. is stated as "apparent stiction" and it provides an indication of the severity of the consequence of stiction in an oscillatory loop.

It is to be noted that the ellipse-fitting method has a clear limitation in the fact that the shape and size of the PV-OP plot depend on several factors: the changes of proportional or integral control gain, the process gain, the process time constant, the time delay of the process, phase lags, etc. Hence, the apparent stiction that the ellipse-fitting method estimates will differ from the actual amount of stiction. Moreover, the proposed method assumed the process to be locally linear. Only the PV-OP plot whitout bicoherence analysis can't distinguish the root cause between the nonlinear process or a sticky valve.

2.4.6 Least-squares and Global Search Algorithm for Estimation of Valve Stiction

Jelali [15] proposed a technique for stiction detection and quantification. This method is based on the identification of a Hammerstein model as shown in Figure 2.5 using the available industrial data for OP and PV. The Hammerstein model describes the global system and separate identification of (1) the linear output and (2) the non-linear part, i.e., the function between the controller output (OP) and the manipulated variable (MV). Global search techniques, i.e., Pattern

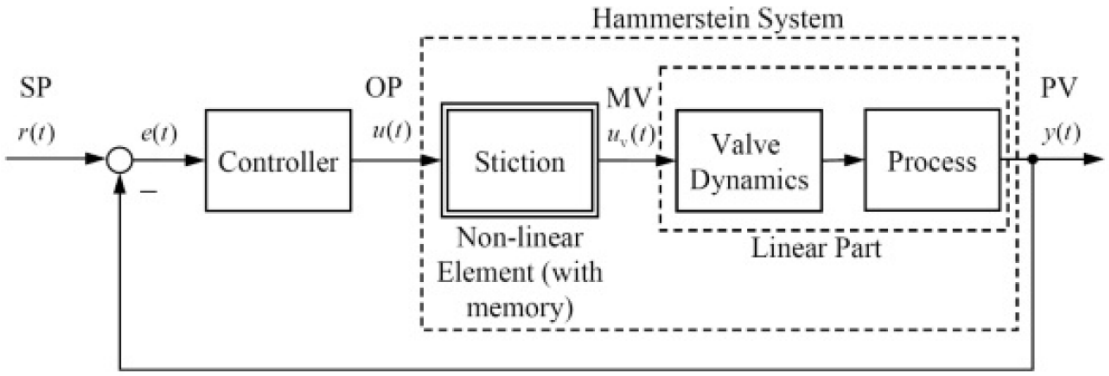

FIGURE 2.5: Hammerstein model in the process control loop

Search methods, or Genetic Algorithms are used to estimate the non-linear model parameters.

The weakness of this method is that, a good initializing data set is needed for the stiction estimation. The genetic algorithm used in this detection method is highly complex and requires a large number of function evaluations per iteration and storing a considerable amount of information in the computer memory.

Besides the methods described above there are other methods such as a simple grid-search method for estimating stiction parameters [23] [24].

2.5 Comparison of Various Stiction Detection Methods and a Need for a New Method

Jelali and Scali compared eight different stiction methods for a set of industrial data in chapter 13 of [25]. The methods are Bicoherence, Correlation, histogram-based method of Horch, Relay technique of Rossy and Scali [26], Curve fitting approach of He, Area-peak method of Salsbury and Singhal [21], Hammerstein-model-based technique (HAMM1) of Jelali, Hammerstein-model-based technique (HAMM2) of Lee et al [27], and Hammerstein-model-based technique (HAMM3) of Karra and Karim [28]. They found that Bicoherence, HAMM2, and HAMM3

worked well but still their is a scope of improvement. Hence a novel method is developed and it is compared with other methods for the same industrial data sets. It is found that the novel method performs better than the existing methods. This comparison is shown in Chapter 5.

From the practical implementation point of view, the proposed method has many advantages. It is an automatic detection tool, which can be used for both online and offline stiction detection since the method requires only routine operating data. The pretreatment of data-set is a simple procedure. The proposed method requires no filter design and it works quite well even for low Signal to Noise Ratio (SNR). The effectiveness of the proposed method is demonstrated by applying it to industrial data sets as shown in Chapter 5.

2.6 Valve Stiction Compensation Methods

The plant operations management may have to wait for maintenance of the faulty valve until overhauling, after the correct detection of stiction, as overall economic analysis suggests not to stop the plant for a valve. This incurs a significant amount of economic losses to the plant because of ignoring the effect of stiction for the intermediate time. A good stiction compensation method can reduce this losses by reducing the oscillations produced from the presence of stiction in the control valve. Literature suggests some stiction compensation methods which are briefly described below.

Two basic approaches to stiction compensation, namely dithering and impulsive control have been reported in the literature [29]. Dithering means adding a high-frequency zero-mean signal to the control signal. The idea is that the amplitude of the dither should be so high that the stiction is overcome, and that the frequency should be high enough, so that the generated disturbance is above the interesting frequency range of the system. In impulsive control, no stiction-compensation signal is added to the control signal, but the control signal itself is generated as a sequence of pulses. The pulses should be so large, that they overcome the stiction

level. Again, this high-frequency pressure impulses over the actuator piston is impossible to generate due to the dynamics and limitations in the positioner and actuator. A good overview on stiction compensation in electromechanical systems is provided by Armstrong et al. [29].

Unfortunately, pneumatic valves constitute more than 90% of all actuators employed in the industry and dithering may not be useful for these industries. A dithering signal may perhaps be generated by the positioner, since a stand-alone control valve is rather fast. However, this high-frequency signal will be low-pass filtered (integrated) in the actuator. Furthermore, since the output from the valve is limited in amplitude, it is not very effective to generate a dithering high-frequency pressure impulses over the actuator piston. Even if it were possible, the solution would cause a significant wear on the valve. Similar drawback exists with impulsive control technique.

Kayihan and Doyle [30] and Hagglund [31] have addressed stiction compensation algorithms for pneumatic control valves. The approach of Kayihan and Doyle [30] assumes that all valve parameters such as mass of stem, stem position, stem velocity etc, are known a priori. Such detailed parameter values are not usually available.

Two major works on stiction compensation by Hagglund [31]and Srinivasan [32] are reviewed below. As these methods have some weakness in one way or another, a conquest for an efficient stiction compensation method is done in this thesis. Chapter 6 discusses the applicability of a Self Tuning Adaptive PID controller as stiction compensator.

2.6.1 Hagglund's Technique

Based on the fact that an ideal stiction compensator would be a rectangular pulse in the controller output signal. Hagglund [31] proposed a technique which add short pulses (termed as 'knocker') to the control signal in the direction of the rate of change of the control signal. The method of adding pulse is shown in

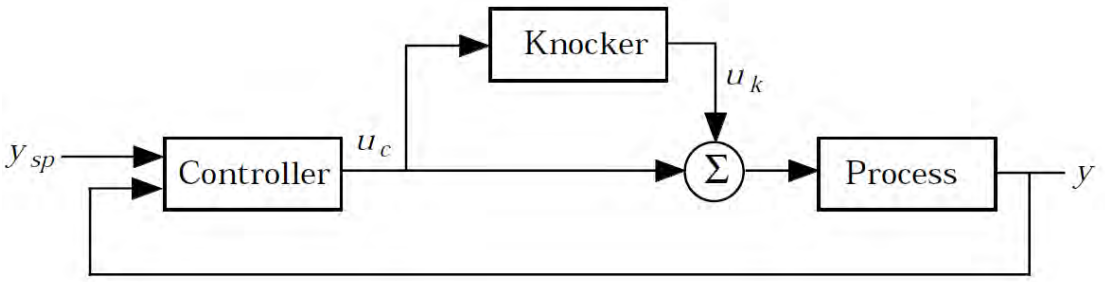

FIGURE 2.6: Block diagram of using knocker in the feedback loop

Figure 2.6. However, there is a need to tune three parameters that characterize the short pulses: amplitude (a), pulse width (t) and time between each pulse (h_k). The weakness of this method is that the 'knocker' performance was influenced by the pulse parameters [33] and for the varying amount of stiction it is extremely difficult to determine pulse parameters correctly. One of the major problems which decreased the popularity of this method is that operators attention is required for the use of this method.

2.6.2 Optimization-based Stiction Compensation Method

Srinivasan and Rengaswami [32] suggested an optimization technique for the compensation of control valve stiction. In this method, a cost function of controller error signal obtained from the subtraction of PV from SP is minimized for the design of the compensator signal which is to be added to the controller output. The cost term has three parts: integral square error (ISE), valve stem variability and valve aggressiveness. Based on this minimization criteria, a model predictive controller (MPC) updates the tuning parameters of the PID controller so that the cost function can be minimized.

The weakness of this method is that the transfer function of the process must be known a priori. Beside, the method cannot determine the severity of stiction. Another weakness is that the method requires a higher computational burden.

2.7 Conclusion

Timely detection of control valve stiction will reduce the economic loss by enabling the maintenance department for immediate action. Thus an automatic detection method based on routine operating data is necessary. Despite the presence of large number of stiction detection method available in the literature, this chapter discusses the motivation for the need of a novel and efficient detection method. An efficient stiction compensation technique will reduce the economic losses incurred during the intermediate time when the plant can't be stopped. By reduction of the oscillation, a stiction compensation helps to operate the process with a higher load and control the product quality tightly. This chapter reviews two existing stiction compensation techniques and their pros and cons. A better technique would be a great help for the plant personnel. For this reason, the applicability of STC as stiction compensator is studied in Chapter 6.

Chapter 3

A Novel Stiction Detection Method Based on Harmonics

Last decade has seen several studies on detection and quantification of valve stiction [15] [22] [8] [20] [13] [10] [7]. They suggested that a sticky control valve in a control loop produces a rectangular/squared shaped manipulated variable and a saw toothed/triangular wave type controller output signal, while an aggressive controller produces a sinusoidal signal. For the presence of stiction, the valve position usually takes the form of a rectangular wave [34] [10]. The reason is explained in [35]. Due to large time constants of level and temperature control processes, rectangular signal changes into triangular shape signal. However, the signal shapes may change differently according to the presence of noise and the nature of process. Thus, it is difficult to predict the presence of stiction merely from the signal shape of OP or PV signal. In this chapter, a novel harmonic method based on the signal shape of the controlled error signal is proposed.

The basic idea of the proposed stiction detection method is that, as rectangular shape results from the presence of stiction hence the information lies in a rectangular signal can be used for the correct detection of stiction. From the Fourier analysis of a rectangular signal, it is found the odd harmonic relations is present among the sine elements of Fourier series. This important property is used in this

study. Hence, control error signal is decomposed into a series of sinusoids and a significant number of sinusoids are examined for the presence of odd harmonics. It is suggested that the presence of odd harmonics indicates the presence of stiction in the control loop.

The proposed method has many advantages from the practical implementation point of view. Firstly, data pretreatment is quite simple. Controlled error signal should be detrended only and there is no filter requirement. Secondly, It can be implemented as an automatic detection tool because it uses only routine operating data. Controlled error signal can be found from subtracting PV from SP. Also, it can naturally deal with the oscillatory open-loop data.

3.1 Fourier analysis of Square wave and Triangular wave signals

A square wave signal, $f(t)$, as shown in Figure 3.1(a), can be mathematically represented over the length of $2L$ as:

$$f(t) = 2[H(t/L) - H(t/L - 1)] - 1 \tag{3.1}$$

where t is the time, $H(t)$ is the Heaviside step function. This signal can be rewritten as :

$$f(t) = a_0 + \sum_{n=1}^{\infty} a_n \cos(nt) + \sum_{n=1}^{\infty} b_n \sin(nt) \tag{3.2}$$

Since $f(t) = f(2L-t)$, the function is odd. So Euler co-efficient, $a_0 = \frac{1}{2L}\int_0^{2L} f(t)dt = 0$, $a_n = \frac{1}{L}\int_0^{2L} f(t)\cos(\frac{n\pi t}{L})dt = 0$ and $b_n = \frac{1}{L}\int_0^{2L} f(t)\sin(\frac{n\pi t}{L})dt$.

Evaluating b_n provides:

$$b_n = \frac{4}{n\pi}\begin{cases} 0 & n = 2, 4, 6, \ldots \\ 1 & n = 1, 3, 5, \ldots \end{cases} \tag{3.3}$$

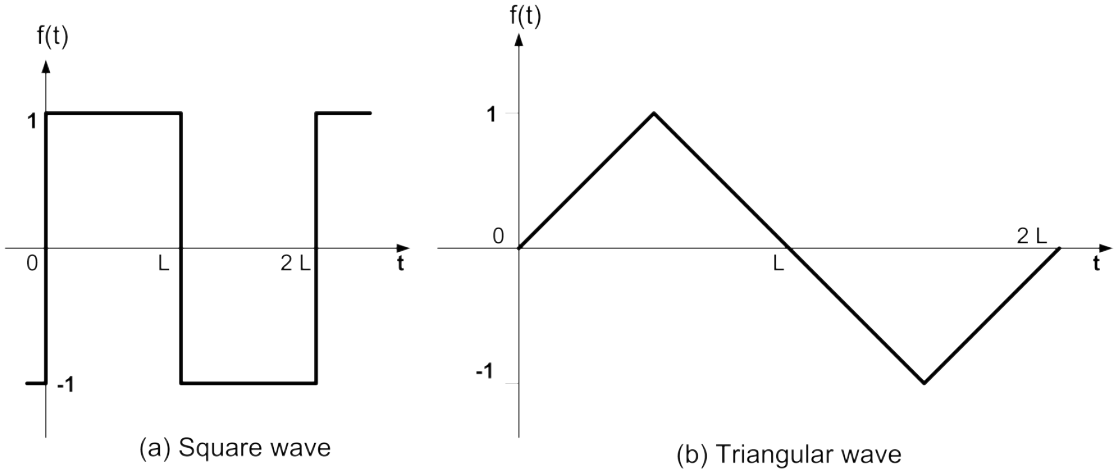

FIGURE 3.1: Time trends of Square wave and triangular wave signals

The Fourier series of a square wave signal is therefore

$$f(t) = \frac{4}{\pi} \sum_{n=1,3,5...}^{\infty} \frac{1}{n} \sin(\frac{n\pi t}{L}) \tag{3.4}$$

Or its equivalent

$$f(t) = \tfrac{4}{L} \sin(t) + \tfrac{4}{3L} \sin(3t) + \tfrac{4}{5L} \sin(5t) + \dots \tag{3.5}$$

Similarly, a triangular wave signal as shown in Figure 3.1(b) having a period of $2L$ mathematically can be expressed as

$$f(t) = \begin{cases} \frac{2}{L}t & 0 < t \leq \frac{L}{2} \\ 2(1 - \frac{t}{L}) & \frac{L}{2} < t \leq \frac{3L}{2} \\ \frac{2}{L}t - 4 & \frac{3L}{2} < t \leq 2L \end{cases} \tag{3.6}$$

Since the function is odd, $a_0 = a_n = 0$ and

$$\begin{aligned} b_n &= \frac{2}{L}\left\{\int_0^{L/2} \frac{t}{L/2}\sin(\frac{n\pi t}{L})dt + \int_{L/2}^{L}\left[1 - \frac{2}{L}(t - \frac{2}{L})\sin(\frac{n\pi t}{L})dt\right]\right\} \\ &= \frac{32}{\pi^2 n^2}\cos(n\pi/4)\sin^3(n\pi/4) \\ &= \frac{8}{\pi^2 n^2}\begin{cases} (-1)^{(n-1)/2} & for\ n\ odd \\ 0 & for\ n\ even \end{cases} \end{aligned}$$

The Fourier series for the triangular wave is therefore

$$f(t) = \frac{8}{\pi^2}\sum_{n=1,3,5...}^{\infty}\frac{(-1)^{(n-1)/2}}{n^2}\sin(\frac{n\pi t}{L}) \tag{3.7}$$

Therefore, the Fourier series expansion of a rectangular and triangular wave function shows the presence of odd harmonics. Though the signal shape may change due to presence of noise and the nature of process but odd harmonics prevails. For example, presence of integrating process results triangular signal for input rectangular signal. Despite of the form change, the fundamental property which is the harmonic relation among the various sinusoids lies in the control error signal. For example, due to the presence of integrating control loop such as level control loop, odd harmonics can be found as the integration of right side of Equation (3.5) results in amplitude and phase change but the frequency of each sinusoidal term remains unaltered.

3.2 Fourier Series Analysis of Any Time Trends

Fourier series states that any time signal can be represented as a summation of sinusoids. A time series $y(t)$ defined as:

$$y(t) = A_0 + \sum_{t=0}^{\infty} A_i\cos(\omega_i t + \phi_i) \tag{3.8}$$

where, ω is the fundamental frequency, which has the largest amplitude; A_i's are amplitudes of sinusoids having frequencies ω_i's. Since it is practically impossible to estimate amplitudes, frequencies and phases for infinite number of terms of Equation (3.8), only 'm' number of terms are estimated. Therefore, Equation (3.8) can be rewritten as:

$$\begin{aligned} y(t) = A_0 + A_1 \cos(\omega_1 t + \phi_1) + A_2 \cos(\omega_2 t + \phi_2) + .. \\ ..A_m \cos(\omega_m t + \phi_m) + \epsilon(t) \end{aligned} \tag{3.9}$$

$\epsilon(t)$ is the error due to omission of terms after the m^{th} term. As the chemical process units acts as a filter for higher order frequencies, Choudhury [36] suggested that it would be sufficient to write the equation upto tenth term, i.e., m=10. The actual value of m, that is the actual number of sinusoids needs to be estimated and is discussed in the Section 3.5. Iterative Auto-Regressive Moving Average (ARMA) technique with Least Squares Linear Regression has been employed to estimate the frequencies, amplitudes and phases of Equation (3.9).

3.3 Estimation of Frequency by an Iterative ARMA Technique

Let us consider a simple sinusoidal model of the form given in Equation 3.9 (m=1) for the estimation of frequencies.

$$y(t) = A \cos(\omega t + \phi) + \epsilon(t) \tag{3.10}$$

where, $\epsilon(t)$ is white noise.

Maximum likelihood and Autoregressive Moving Average techniques are the popular two methods for estimating the frequency of a signal using Equation 3.10. Maximum likelihood techniques for estimating frequency are computationally intensive and requires good initial estimation. On the other hand, ARMA techniques are

robust and computationally less intensive. In this study, Quinn & Fernandes [37] technique based on ARMA method was used. This method places the outset poles on the unit circle, and iteratively achieves an estimator whose asymptotic properties are the same as those of periodogram maximizer. The technique is similar and asymptotically equivalent to that of the Truong-Van [38], who used the fact that the solution to the difference equation is as follows.

$$y(t) - 2\cos\omega y(t-1) + y(t-1) = \cos(\omega t) \tag{3.11}$$

This involves the terms $t\cos(\omega t)$ and $t\sin(\omega t)$ as well as $\cos(\omega t)$ and $\sin(\omega t)$ and thus a filter of second order type $(1 - 2z\cos(\omega') + z^2)^{-1}$ applied to a signal will annihilate a (discrete-time) sinusoid at a given frequency and makes it ring when the frequency ω' is near the true frequency.

Thus, if a time trend $y(t)$ satisfies Equation 3.9, it also satisfies

$$y(t) - 2\cos\omega y(t-1) + y(t-2) = \epsilon(t) - 2\cos\omega\epsilon(t-1) + \epsilon(t-2) = \cos(\omega t) \tag{3.12}$$

This representation suggests that ω may be estimated by iterative ARMA-based techniques. Suppose that we wish to estimate α and β in

$$y(t) - \beta y(t-1) + y(t-2) = \epsilon(t) - \alpha\epsilon(t-1) + \epsilon(t-2) \tag{3.13}$$

while preserving $\alpha = \beta$. If α is known, and the $\epsilon(t)$ are independent and identically distributed, then β can be estimated by Gaussian maximum likelihood, that is, by minimizing

$$\sum_{t=0}^{T-1} \epsilon_{\alpha,\beta}^2(t) = \sum_{t=0}^{T-1} \{\xi(t) - \beta\xi(t-1) + \xi(t-2)\}^2 \tag{3.14}$$

with respect to β, where $\xi(t) = y(t) + \alpha\xi(t-1) - \xi(t-2)$ and $\xi(t) = 0, t < 0$. In other words, $\xi(t)$ is the output signal while by passing $y(t)$ as input signal through

a filter as given by $\frac{1}{1-\alpha q^{-1}+q^{-2}}$. As this is quadratic in β, the minimizing value is the regression coefficient of $\xi(t)+\xi(t-2)$ on $\xi(t-1)$, viz.,

$$\begin{aligned}\frac{\sum_{t=0}^{T-1}\{\xi(t)+\xi(t-2)\}\xi(t-1)}{\sum_{t=0}^{T-1}\xi^2(t-1)} &= \alpha + \frac{\sum_{t=0}^{T-1}y(t)\xi(t-1)}{\sum_{t=0}^{T-1}\xi^2(t-1)} \\ &= \alpha + h_T(\alpha)\end{aligned} \tag{3.15}$$

We then put α equal to this value and re-estimate β using Equation (3.15) and continue until α and β are sufficiently close. Then, estimate ω from the equation $\alpha = 2\cos\omega$. The factor 2 is introduced for rapid convergence.

This algorithm can be summarized as below:

1. Put $\alpha_1 = 2\cos\hat{\omega_1}$, where $\hat{\omega_1}$ is an initial estimator of the true value ω_0. This can be estimated from power spectrum.
2. For $j > 1$, put $\xi(t) = y(t) + \alpha_j\xi(t-1) - \xi(t-2)$, $t = 0, ..., T-1$ where $\xi(t) = 0, t < 0$.
3. Put $\beta_j = \alpha_j + 2\frac{\sum_{t=0}^{T-1}y(t)\xi(t-1)}{\sum_{t=0}^{T-1}\xi^2(t-1)}$
4. If $|\beta_j - \alpha_j|$ is suitably small, estimate $\hat{\omega} = \cos^{-1}(\beta_j/2)$. Otherwise, let $\alpha_{j+1} = \beta_j$ and go to step 2.

Once the frequency is estimated, the amplitudes and phases can be estimated using least-square regression method.

3.4 Least Squares Linear Regression Method for Estimating Amplitudes and Phases

Data are available as time series sampled at a fixed interval of time. Least-square regression technique is used to estimate each component of any time series data

$y(t)$, shown in Equation (3.16).

$$y(t) = \sum_{t=0}^{m} A_i \cos(\omega_i t + \phi_i) + \epsilon(t) \tag{3.16}$$

For example, if y is the time series data, $y_1 = A_1 \cos(\omega_1 t + \phi_1)$ will be first estimated. Therefore, let us write,

$$\begin{aligned} y &= A_0 + A_1 \cos(\omega_1 t + \phi_1) + e_1 \\ &= A_0 + \alpha \cos(\omega_1 t) + \beta \sin(\omega_1 t) + e_1 \end{aligned} \tag{3.17}$$

where, $\alpha = A_1 \cos(\phi_1)$ and $\beta = -A_1 \sin(\phi_1)$. Equation (3.17) contains four unknowns namely A_0, α, ω_1 and β. The frequency ω_1 will be estimated first by using Quinn-Hannan's techniques discussed in the last section. If ω_1 is known, parameters of Equation (3.17) can be calculated using simple linear regression techniques. Predictions of y can be made from the regression model,

$$\hat{y} = \hat{A}_0 + \hat{\alpha} \cos(\omega t) + \hat{\beta} \cos(\omega t) \tag{3.18}$$

where $\hat{A}_0, \hat{\alpha}$ and $\hat{\beta}$ denote the esimated values of A_0, α and β, $\hat{y}$ denotes the predicted value of y. Each observation or sample of y will satisfy

$$y_i = A_0 + \alpha \cos(\omega_1 t_i) + \beta \sin(\omega_1 t_i) + e_i$$

The least square method calculates values of A_0, α and β, that minimizes the sum of the squares of the errors S for an arbitrary number of data points, T:

$$S = \sum_{i=1}^{T} e_i^2$$

After some calculations, it can be shown that least-squares estimates of A_0, α and β is as follows:

$$\begin{bmatrix} \widehat{A}_0 \\ \widehat{\alpha} \\ \widehat{\beta} \end{bmatrix} = D^{-1}(\omega_1)E(\omega_1)$$

where

$$D(\omega_1) = \begin{bmatrix} T & \sum_{t=0}^{T-1}\cos(\omega_1 t) & \sum_{t=0}^{T-1}\sin(\omega_1 t) \\ \sum_{t=0}^{T-1}\cos(\omega_1 t) & \sum_{t=0}^{T-1}\cos^2(\omega_1 t) & \sum_{t=0}^{T-1}\sin(\omega_1 t)\cos(\omega_1 t) \\ \sum_{t=0}^{T-1}\sin(\omega_1 t) & \sum_{t=0}^{T-1}\sin(\omega_1 t)\cos(\omega_1 t) & \sum_{t=0}^{T-1}\sin^2(\omega_1 t) \end{bmatrix} \tag{3.19}$$

$$E(\omega_1) = \begin{bmatrix} T \\ \sum_{t=0}^{T-1} y(t)\cos(\omega_1 t) \\ \sum_{t=0}^{T-1} y(t)\sin(\omega_1 t) \end{bmatrix} \tag{3.20}$$

Thus, $\hat{A}_1, \omega_1$ and ϕ_1 of first term of Fourier series expansion are estimated. Similarly, all m–terms can be estimated.

3.5 Determination of Significant Number of Sinusoids i.e., 'm'

In practice, all signals contain noise. Therefore, the periodogram will have peaks that can be mistakenly identified as a presence of sinusoid. To test whether there is a sinusoid or not, consider the subset of sinusoidal models

$$y(t) = \mu + A\cos(\lambda_j t + \phi) + x(t), \quad t = 0,\ 1,\ \ldots,\ T-1 \tag{3.21}$$

where $\lambda_j = 2\pi j/T$ but j is unknown and $x(t)$ is Gaussian and an independent sequence, and therefore 'white'. It is not practically possible to estimate all sinusoidal components in the Equation 3.21. Null hypothesis test was employed to see whether an error signal may contain sinusoid or not in the Equation 3.21. Hence, We wish to test

$$H_0 : A_i = 0 \tag{3.22}$$

against

$$H_0 : A_i > 0 \tag{3.23}$$

A test which has usually good asymptotic properties and is usually simple to derive is the likelihood ratio test, which rejects the null on large values of the ratio of the maximum likelihood under H_A to the maximized likelihood under H_0. The former is just

$$-\tfrac{T}{2}\log(2\pi\hat{\sigma}_A^2) - \tfrac{T}{2}$$

while the latter is

$$-\tfrac{T}{2}\log(2\pi\hat{\sigma}_0^2) - \tfrac{T}{2}$$

where

$$\hat{\sigma}_0^2 = \tfrac{1}{T}\textstyle\sum_{t=0}^{T-1}\{y(t) - \bar{y}\}^2$$

$$\hat{\sigma}_A^2 = \tfrac{1}{T}[\textstyle\sum_{t=0}^{T-1}\{y(t) - \bar{y}\}^2 - \max_{1\leq j\leq n} I_y(\lambda_j)]$$

and $n = \lfloor (T-1)/2 \rfloor$. We thus rejects H_0 if $\hat{\sigma}_A^2/\hat{\sigma}_0^2$ is too large, or, equivalently if Fisher's g factor is too small. Fisher's g [39] factor as defined by

$$g = \frac{max_{1\leq j\leq n} I_y(\omega_j)}{\sum_{t=0}^{T-1}\{y(t) - \bar{y}\}^2} \tag{3.24}$$

was used in the test. We thus rejects H_0 if g is too small.

3.6 Odd Harmonics as a Root Cause of Stiction

Harmonics are oscillations whose fundamental frequencies are integer multiple of the fundamental frequency. Figure 3.2 shows four different type of signals with

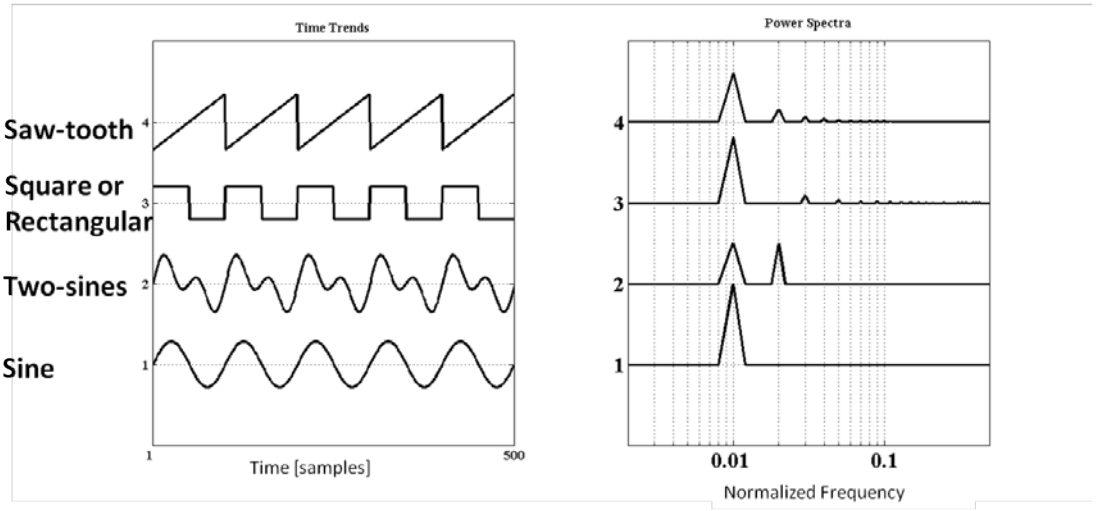

FIGURE 3.2: Time trend and power spectra of different signals

their power spectra. All these signals have a fundamental frequency of 0.01 in a normalized scale. From Figure 3.2, it can be observed that the sine curve has only one frequency; the multiple sine has two frequencies; the rectangular signal has the fundamental frequency and its 3^{rd}, 5^{th}, ..., odd harmonics; and the triangular or saw-toothed signal has all harmonics (odd and even) in addition to the fundamental frequency. Therefore it is evident that a 'Squared' or 'rectangular' signal results in odd harmonics. On the other hand the 'saw-toothed' produces both odd and even harmonics. As assumed in the beginning of this chapter, the presence of stiction in the control loop produces rectangular or square signal. Rectangular signal contains only odd harmonics. Therefore, the presence of odd harmonics indicates the presence of stiction in a control loops valve.

3.6.1 Summary of the proposed method

The proposed method can be summarized as follows:

1. Get routine operating data for control loops. Estimate the error signal by subtracting PV from SP.

2. Remove outliers from the data and detrend the error signal.

3. Estimate m number of sinusoids. $m = 10$ is used in this study.

4. Employ statistical hypothesis test described in section 3.5 to determine significant sinusoids.

5. Examine whether the frequencies of significant sinusoids are harmonically related. The presence of odd harmonics indicates the presence of valve stiction.

3.7 Practical Implementation Issues

The proposed stiction detection method has been validated by using sinusoids with known frequencies to the algorithm.

3.7.1 Length of Data Window

The minimum number of samples required for the determination of oscillation is estimated in this section. A sinusoid of the following equation was fed to the oscillation detection algorithm where one period of samples consists of 512 data instants.

$$y(t) = \sin(2\pi \frac{1}{512} t) \tag{3.25}$$

Though a single sinusoid was given as input to the algorithm, a series of ten sinusoidal signals were generated as because the harmonic relations among these sinusoids would be sought for the detection of stiction in the later part. In this subsection, only the fundamental frequency is considered. As the input signal was a pure sinusoid, the amplitudes of the sinusoids other than the fundamental were found practically zero. The error estimation equations shown in the Figure 3.3 are defined as follows:

$\%$ difference of $\omega_1 = \frac{(\omega_1)_{actual} - (\omega_1)_{estimated}}{(\omega_1)_{actual}} \times 100\%$

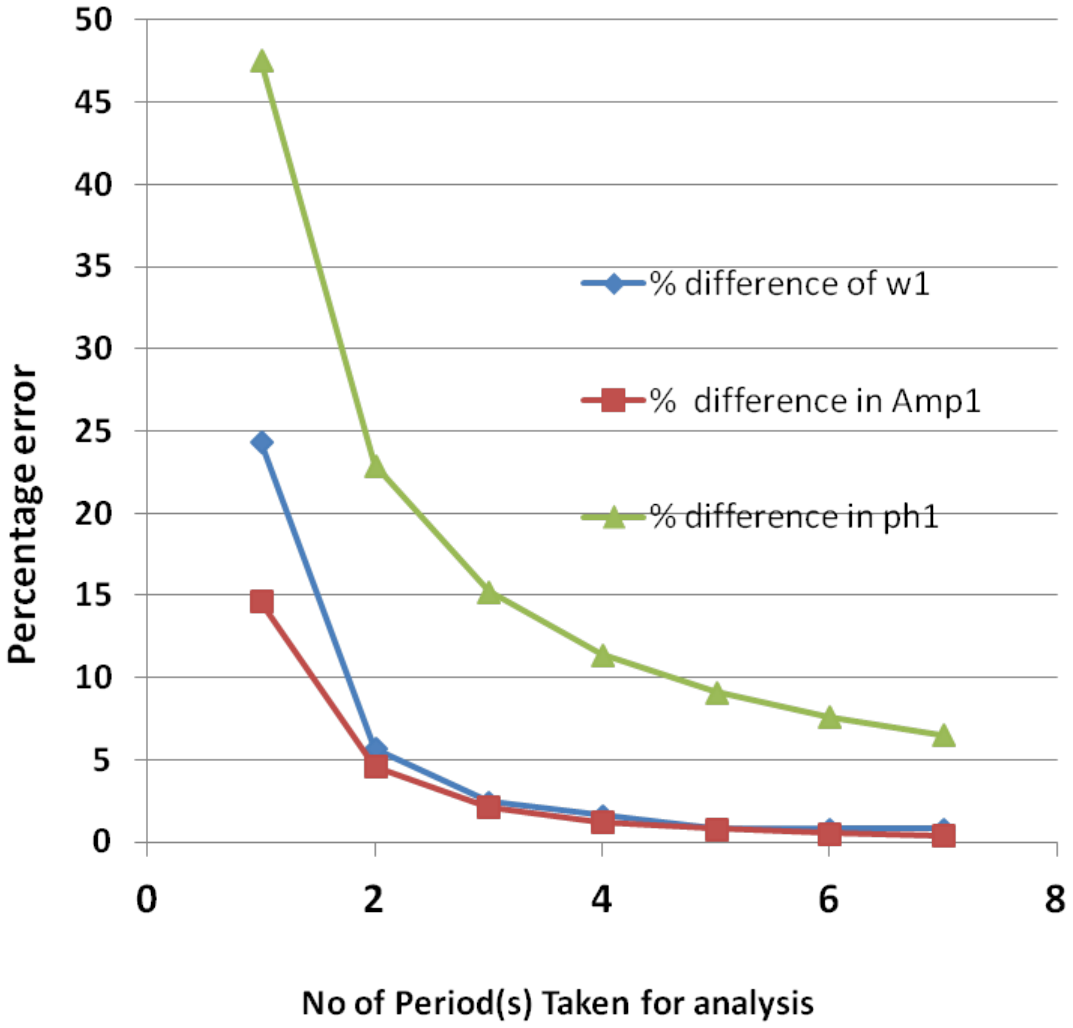

FIGURE 3.3: Effects of Sample periods on oscillation detection

$$\%\ \text{difference of } Ph_1 = \frac{\phi_1(actual) - \phi_1(estimated)}{\phi_1(actual)} \times 100\%$$

$$\%\ \text{difference of } amp = \frac{A_1(actual) - A_1(estimated)}{A_1(actual)} \times 100\%$$

Figure 3.3 shows the dependance of various differences between the estimated and the actual amplitudes, frequencies and phases with the number of sample periods. If a single period signal is used for the estimation of different sinusoids, about 20% estimation error in frequency, 47% error in phase estimation and 17% error occurs in the estimation of amplitude. With the increase of the number of sample periods, this estimation error minimizes to almost zero. In practical cases, large number of data may not be available. Hence, from Figure 3.3, three period of samples can be considered as sufficient for the analysis of oscillation detection.

3.7.2 Determination of a critical or threshold value of Fisher's 'g' for the determination of a significant sinusoid

As mentioned earlier, for any signal, 10 sinusoids are estimated. Some of them may be insignificant for the correct representation of the signal. For example, if a pure sinusoid is fed to the algorithm, only the fundamental signal should suffice to represent the input signal. A sum of two sinusoids is fed to the algorithm, the algorithm should be smart enough to show that only two sinusoids are only be considered. As practical data contains noise, the method should be robust also in presence of noise. Therefore it is important to find the critical threshold value of 'g' below which all sinusoids will be considered insignificant.

For this purpose, pure random noise of different variance is fed to the oscillation detection algorithm. For different level of noise signals, corresponding estimation of Fisher's 'g' factor by the oscillation detection method is shown in the Figure 3.4(a). It is clear that if the critical value of 'g' is chosen as 10, most noise signal can be avoided to be wrongly detected as sinusoids.

Now, a pure sinusoid of $y(t) = A\sin(2\pi\frac{1}{512}t + \theta)$ where, A=1, $\theta = 60^o$ corrupted with random noise of zero mean and 0.5 variance, having SNR = 1 fed to the algorithm. Fisher's 'g' for this input signal is shown in the Figure 3.4(b). Harmonic analysis result for this signal is shown in Table 3.1. It is found that g factor drops drastically after the first sinusoids calculations. Which indicates that, first sinusoid is sufficient for describing the input signal. That is, other sinusoids need not be considered. Again, a multiple sinusoid consists of $y(t) = y_1(t)+y_2(t)+noise$, where $y_1(t) = 0.8\sin(2\pi\frac{1}{512}t + 60^o)$ and $y_2(t) = 0.2\sin(2\pi\frac{1}{10}t + 0^o)$ with a noise variance of 0.05 having the SNR=6.8, was fed to the algorithm. Column 6-10 of Table 3.1 shows the harmonic analysis result of this signal. The g's value returned by the algorithm is also shown in the Figure 3.4(c). From the figure, it is clear that, g values are very small for the last 8 sinusoids. Thus, this figure refers that first two sinusoids should be considered for the estimation and detection of the oscillations. Similarly, a multiple sine having the form of $y(t) = y_1(t)+y_2(t)+y_3(t)+noise$ also fed to the algorithm. Here, $A_1 = 0.4$, A_2=0.35, A_3=0.25, ω_1=1/512, ω_2=1/10,

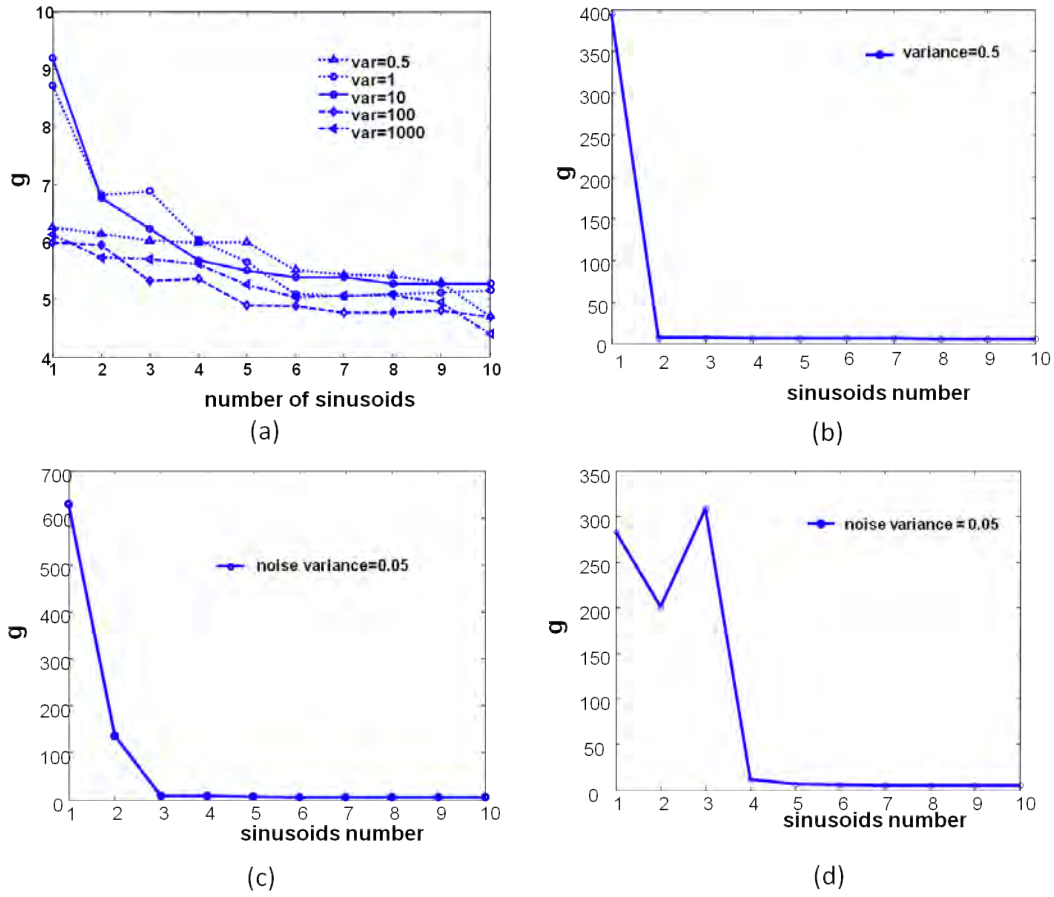

FIGURE 3.4: Variation of g factor with the number of sinusoids for different input cases.

TABLE 3.1: Variations of 'g' for the combination of different input signals

$y(t) = A\sin(2\pi\frac{1}{512}t + \theta)$					$y(t) = y_1(t) + y_2(t) + noise$					$y(t) = y_1(t) + y_2(t) + y_3(t) + noise$				
ω_i	A_i	ϕ_i	g	ω_i/ω_1	ω_i	A_i	ϕ_i	g	ω_i/ω_1	ω_i	A_i	ϕ_i	g	ω_i/ω_1
0.012	0.989	-0.51	369	1	0.012	0.794	-0.50	627	1	0.012	0.406	-0.50	282	1
1.645	0.118	0.37	10	133.7	0.628	0.197	1.38	136	51.297	0.628	0.35	1.51	200	51.1
2.924	0.118	-0.35	9	237.8	1.541	0.033	-1.19	7.94	125.7	1.571	0.254	-1.57	307	127.7
2.366	0.129	1.08	9	192.4	0.797	0.032	0	7.45	65.0	2.400	0.042	0	11	195.2
1.277	0.110	-0.22	8.5	103.8	2.282	0.028	-0.49	6.17	186.3	1.852	0.032	0.46	6	150.6
0.789	0.106	-0.25	8.3	64.1	3.099	0.031	-1.57	5.72	252.9	2.919	0.028	-1.57	5	237.5
2.381	0.101	-1.57	7.8	193.6	1.442	0.030	0.57	5.72	117.7	3.064	0.025	0	5	249.2
1.056	0.092	0.58	6.0	85.9	0.499	0.026	0	5.33	40.7	0.675	0.025	-1.57	5	54.9
0.086	0.086	-1.14	5.1	6.9	0.273	0.026	-0.67	5.31	22.3	1.762	0.028	1.57	4	143.8
2.536	0.081	-0.43	5.1	206.2	2.692	0.026	0.67	5.08	219.7	2.422	0.024	0	4	197.0

ω_3=1/2, $\theta_1 = 60^o, \theta_{2,3} = 0^o$. Column 11-15 of Table 3.1 shows the result of harmonic analysis. The algorithm returns g value showed in Figure 3.4(d). From the figure, it is clear that the first three value corresponds to the three sinusoids responsible for the construction of the input signal. Thus it can be concluded that the threshold critical value of g can be taken as 10 for the determination of significant sinusoids present in a signal.

3.8 Conclusion

In this chapter, a novel harmonics based stiction detection method has been proposed. The proposed method analyze the error signal of a control loop. Firstly the signal is decomposed into 10 sinusoidal signals. The significant sinusoids are determined using Fisher's g test. Then, harmonic relations among the significant sinusoids are examined. The presence of odd harmonics indicates the presence of stiction. For the successful implementation of the proposed method, various practical issues are finally discussed.

Chapter 4

Simulation and Experimental Validation of the Proposed Method

The objective of this chapter is to demonstrate the effectiveness of the proposed method by using simulation and pilot plant experimentation.

4.1 Simulations

A simple single-input, single-output (SISO) linear system with a feedback-control configuration has been used to generate the control error signal. Different first order plus time delay processes representing Flow control, Level Control, Temperature control and Integral processes having a PI controller with a sampling period of 1 second is considered for the process simulations. Stiction in the process is introduced by using valve-stiction model [8] with varying amount of slip jump (J) and deadband plus stickband (S). Table 4.1 lists a number of processes which were simulated. Each process shown in the column 3 of Table 4.1 were simulated for various noise cases. Column 4 shows the controller transfer functions for these processes. A variant of SNR referred as SNR^* were measured for each simulations.

TABLE 4.1: Simulated Cases

Stiction (S and J)	Process type	Gp	Gc
(1,1), (2,1), (2,2)	Flow	$\frac{3e^{-0.5s}}{0.5s+1}$	$0.2(1+\frac{1}{0.5s})$
(3,1), (3,2), (3,3)	Level	$\frac{e^{-10s}}{100s+1}$	$5(1+\frac{1}{100s})$
(4,2), (4,4) (5,5)	Temperature	$\frac{e^{-20s}}{500s+1}$	$12.5(1+\frac{1}{500s})$
	Integrating	$\frac{e^{-5s}}{s}$	$0.15(1+\frac{1}{15s})$

$$SNR^* = \frac{variance\ of\ measured\ signal}{variance\ of\ noise} \tag{4.1}$$

4.1.1 Results and Discussion of Simulations

For the sake of brevity, a representative result is shown in the Table 4.2 and corresponding error signal and g factor is shown in the Figure 4.1.

Figure 4.1(a)(i) shows error signal resulting from a flow control loop suffering from stiction of amount S=1, J=1. It is clear that the shape of the control error signal is rectangular. Oscillation detection method was employed to find the frequencies, amplitudes, phases, Fisher's g factors and thus the harmonic relations among the first ten constituting sinusoids. The result of the oscillation determination method is shown in Table 4.2(a). The first row of the numeric data corresponds to the fundamental frequency. It was found that the fundamental frequency of this error signal is 0.0265 radian/cycle or 37.74 samples/cycles. From Figure 4.1(a)(ii) and column 'g' of Table 4.2(a), it can be stated that three values of g are more than 10. Therefore, three sinusoids are significant. Thus, the first three sinusoidal elements would be sufficient for the harmonic analysis to find stiction. To distinguish between the harmonics to be considered,a horizontal line is drawn after the third numeric row of Table 4.2(a). Harmonic analysis of the first three sine's shows that the frequency of second and third sine is the 3rd and 5th harmonics of fundamental

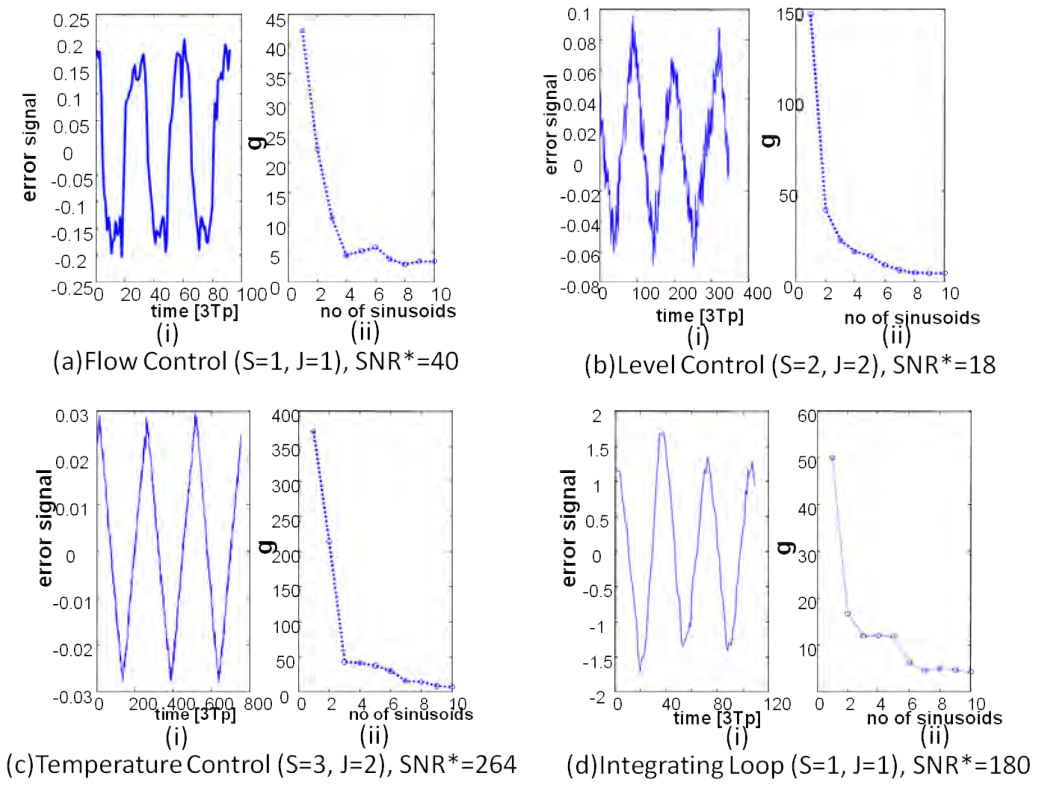

FIGURE 4.1: Simulations of different types of process with different amount of stiction in presence of noise

frequency. Hence, the presence of odd harmonic relation among the frequencies depicts that stiction is present in the control loop.

Figure 4.1(b)(i) shows error signal resulting from a level control loop suffering from stiction of amount S=2, J=2. The shape of control error signal became triangular due to the integrating effect of control loop with large dynamics. The amount of noise introduced was calculated as $SNR^* = 18$. As the presence of stiction induces large oscillation in the controlled variable, the variance of signal is quite high than the variance of pure noise. As a result, the response of the loop becomes unstable while SNR^* was attempted to reduce to below 15. Figure 4.1(b)(ii) and column 'g' of Table 4.2(b) shows that the first five sinusoids are significant. Table 4.2(b) shows that the 4th sinusoid has the frequency which is third harmonics of the fundamental sinusoid. Hence, third harmonic relation indicates the presence of stiction in this control loop. Similarly, the harmonic analysis was employed for the control error signal of a temperature control loop and an integrating loop.

TABLE 4.2: Results of Simulation Cases

(a) Flow Control $\theta = 0.5$ $\tau = 0.5$ $Kc = 0.2$ $\tau_I = 0.5$ $S = 1, J = 1$ $SNR^* = 40$					(b) Level Control $\theta = 10$ $\tau = 100$ $Kc = 5$ $\tau_I = 100$ $S = 2, J = 2$ $SNR^* = 17.5$				
ω_i rad/cycle	A_i	ϕ_i rad	ω_i/ω_1	**g**	ω_i rad/cycle	A_i	ϕ_i rad	ω_i/ω_1	**g**
0.2065	0.1881	0.64	**1**	42.05	0.0555	0.0516	1.57	**1**	147.4
0.6221	0.0405	-1.03	**3.01**	22.29	0.073	0.0091	0	1.32	39.7
1.0386	0.0205	-1.57	**5.02**	10.71	0.0159	0.0061	0	0.29	22.8
1.4605	0.0132	1.57	7.07	4.49	0.1654	0.0051	0	**2.98**	16.7
0.3338	0.0111	0	1.61	5.15	0.0387	0.0045	0	0.69	14.2
1.84	0.0103	0	8.91	5.84	0.1475	0.0034	0	2.66	8.9
1.1184	0.0077	0	5.41	3.75	1.4919	0.0026	0	26.90	6.4
1.1877	0.0076	0	5.75	2.94	0.4394	0.0023	0	7.92	4.9
0.5424	0.0068	0	2.63	3.37	1.6199	0.0022	0	29.21	4.8
0.1368	0.0066	0	0.66	3.43	0.1292	0.0022	0	2.32	4.7
(c) Temperature Control $\theta = 20$ $\tau = 500$ $Kc = 12.5$ $\tau_I = 500$ $S = 3, J = 2$ $SNR^* = 264$					(d) Integrating Loop $\theta = 5$ $K = 1$ $Kc = 0.15$ $\tau_I = 15$ $S = 1, J = 1$ $SNR^* = 830$				
ω_i rad/cycle	A_i	ϕ_i rad	ω_i/ω_1	**g**	ω_i rad/cycle	A_i	ϕ_i rad	ω_i/ω_1	**g**
0.0252	0.0231	0	**1**	371.2	0.1834	1.2933	-0.08	**1**	51.8
0.0749	0.0023	0	**2.98**	214.7	0.5458	0.0708	0.37	**2.98**	21.2
0.0345	0.0007	0	1.37	42.7	0.1301	0.0483	-0.33	0.71	17.6
0.1249	0.0006	0	**4.96**	40.9	0.2461	0.0332	1.57	1.34	12.5
0.0173	0.0006	0	0.69	38.2	0.9225	0.022	0.99	5.03	5.5
0.0513	0.0005	0	2.04	30.2	1.0933	0.0164	0	5.96	4.5
0.0604	0.0003	0	2.40	15.3	2.7466	0.0131	0	14.98	3.1
0.1752	0.0003	0	6.96	14.5	0.3346	0.0169	0	1.82	3.1
0.0986	0.0002	0	3.91	8.7	2.5103	0.0108	0	13.69	3.2
0.0669	0.0002	0	2.66	7.4	2.4376	0.0122	0	13.29	3.7

The control error signal and variations of 'g' factor for these loops is shown in Figure 4.1(c) and 4.1(d). The harmonic analysis results is shown in Table 4.2(c) and 4.2(d). The first 8 and 4 sines are respectively sufficient for the temperature control loop and the integrating loop. The temperature control loop was corrupted with $SNR^* = 264$ and the second and fourth sine of the Fourier series of its error signal are the 3rd and 5th harmonics of the fundamental frequency. In the integrating loop, the second sinusoid of the Fourier series has the 3rd harmonic relation with the fundamental sinusoid. Hence, the simulation study suggests that harmonic analysis can be successfully used as a detection tool for stiction in control

valves.

4.2 Experimental Results

To demonstrate the efficacy of the proposed method, stiction was deliberately introduced in a pilot plant scale experimental set-up shown in the Figure 4.2 located in the department of chemical engineering, BUET. The experimental facilities provided both flow and level control loop.

FIGURE 4.2: Experimental setup of a two tank pilot plant heating system

The schematic diagram of the two tank pilot plant heating system is shown in Figure 4.3. The process depicted in Figure 4.3 is a two tank system. The blue lines indicate water flow to the tanks. There are two water flow control valves. FCV01 is used to regulate the flow of water to Tank-1. FCV02 is used to regulate the flow of water to Tank-2. The transmitters FT01, FT02, FT03 and FT04 are the flow transmitters of the corresponding streams. Here, the process objective was to maintain the level and flow rates of the two tanks at a desired value.

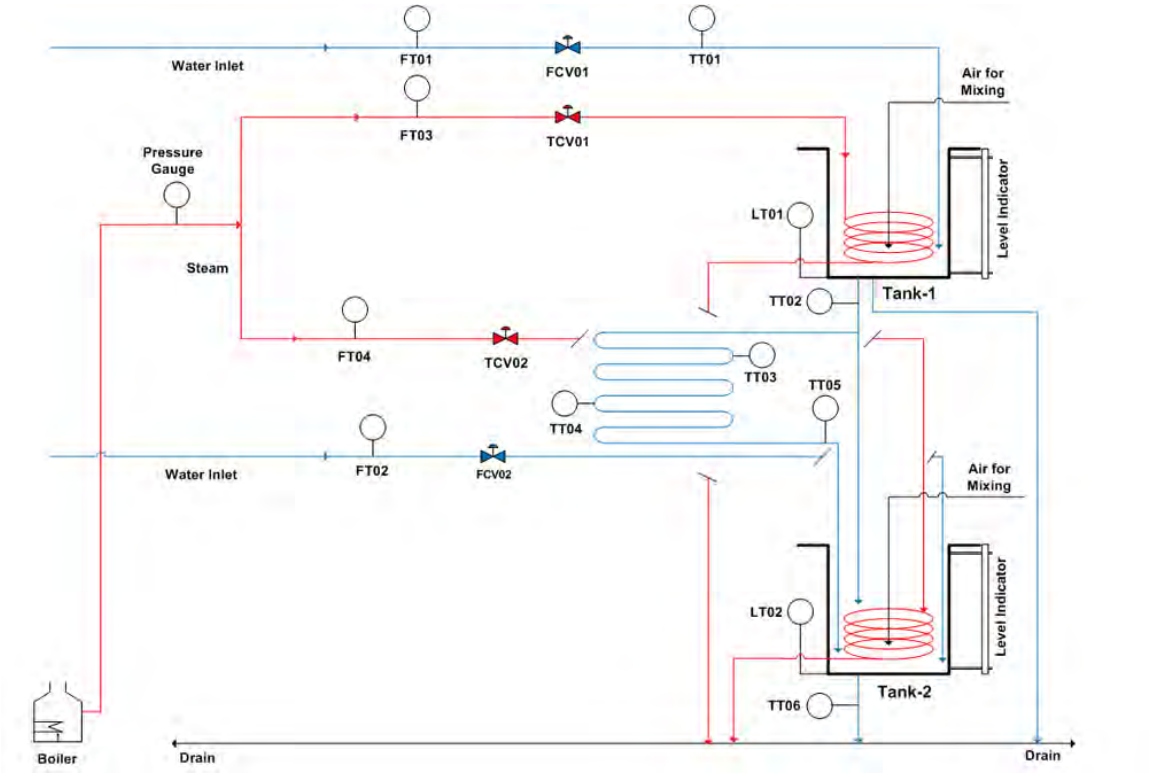

FIGURE 4.3: Schematic diagram of the experimental setup

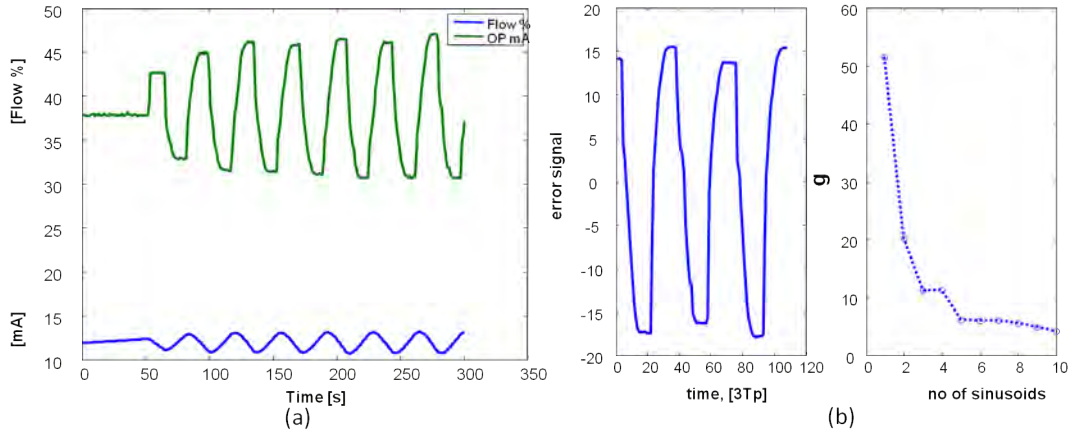

FIGURE 4.4: PV and OP time trends of flow control loop

Table 4.3: Experimental Result of Flow Control Loop

ω_i rad/cycle	A_i	ϕ_i rad	ω_i/ω_1	**g**
0.1698	8.1244	1.1466	1	53.2416
0.5166	0.8973	0.5362	**3.0423**	17.0927
0.125	0.7286	0	0.7361	14.1934
0.3337	0.4841	-0.8485	1.9656	11.009
0.8639	0.4935	0.8132	**5.088**	13.0819
0.2088	0.4309	-0.6509	1.23	9.7219
1.2203	0.2862	0.2121	7.1869	5.6904
0.0647	0.207	-0.278	0.3809	5.5432
1.5572	0.2049	0.7935	9.1714	4.3501
0.6702	0.1698	-1.3351	3.9473	4.3224

4.2.1 Experimentation of the Proposed Method in Flow Control Loop

Figure 4.4(a) shows the controller output (OP) and flow rate (PV), in terms of % maximum flow of the control loop (PV). It is clear that PV has a rectangular nature while OP is triangular. The set-point of this loop was 37%. After the introduction of stiction (S=2, J=2), the controlled variable has a sustained oscillation. The error signal estimated from the difference of SP and PV was analyzed to see whether odd harmonics is present. The result of the analysis is shown in Table 4.3. From column 4, the first 5 sines are significant. It was found that the third sine has third harmonic relation with the fundamental sine. Thus, it can be deduced from the result of the harmonic analysis that odd harmonics can be successfully employed for the detection of control valve stiction.

4.2.2 Experimentation of the Proposed Method in Level Control Loop

The proposed method has also been implemented in the level control loop of Tank 1 shown in Figure 4.3. Figure 4.5 shows the response of this control loop in presence of stiction S=7, J=7. After the initial unsteady response, the tank level become steady after 1600 sec. Error signal for this loop is estimated by subtracting the

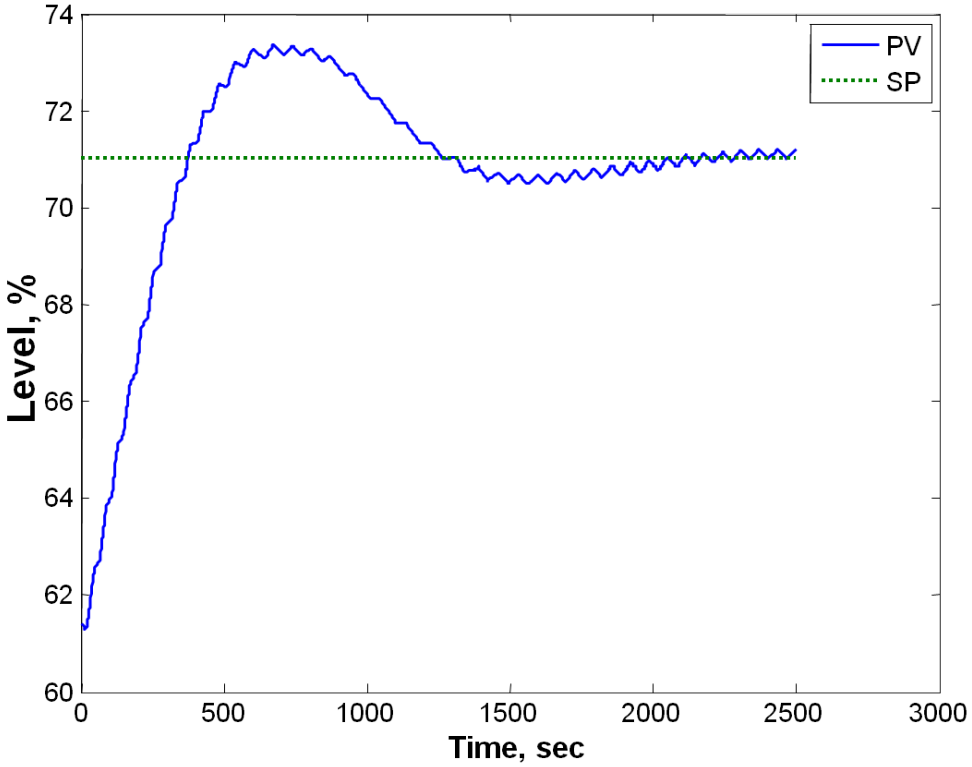

FIGURE 4.5: Response of a level control loop in presence of stiction (S=7, J=7)

signal from set-point. The steady state error signal of three sample cycles have been analyzed for the detection of stiction. The signal which has been analyzed is shown in the left hand side of Figure 4.6. Table 4.4 shows the result of harmonic analysis. The variation of 'g' for the analysis is plotted in the right hand side of Figure 4.6. As the value of 'g' is greater than 10 for all sinusoids, hence all sinusoidal elements needed to be analyzed. From the column of 4 of Table 4.4, it is found that odd harmonic relation is found in the significant sinusoids of the analysis. Thus, the presence of odd harmonics clearly indicates the presence of stiction in the control valve.

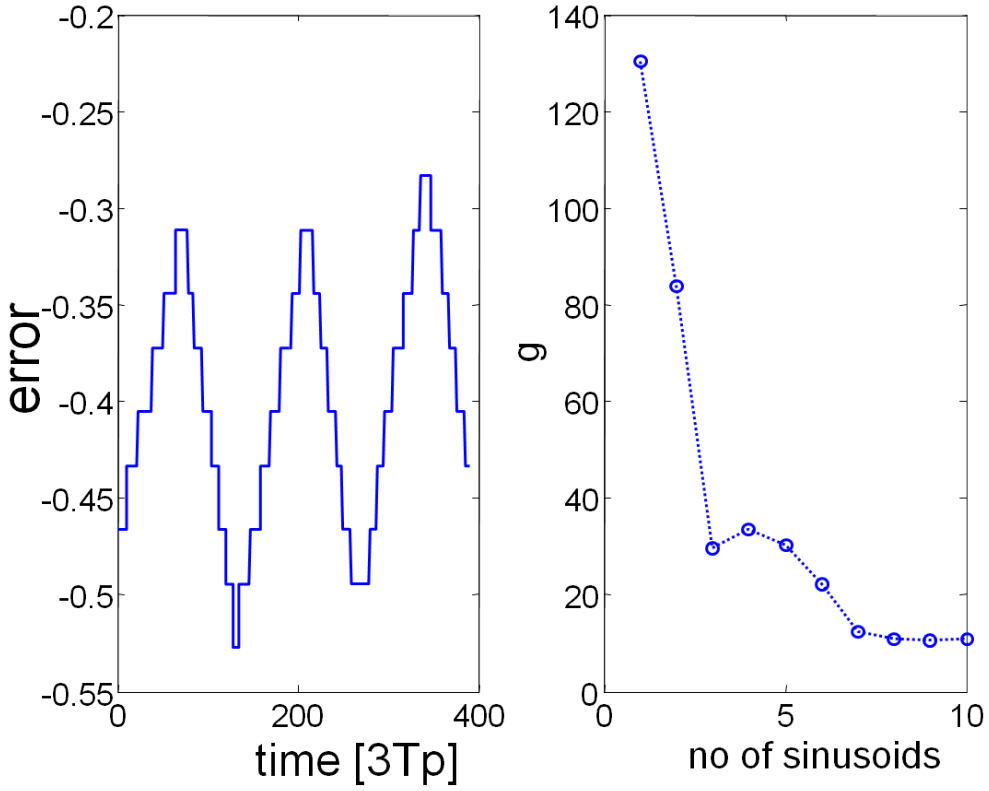

FIGURE 4.6: Error signal and Fisher's g factor of level control loop in presence of stiction (S=7, J=7)

TABLE 4.4: Experimental Result of Level Control Loop

ω_i rad/cycle	A_i	ϕ_i rad	ω_i/ω_1	**g**
0.0450	0.0819	0.44	1	130.26
0.0092	0.0391	0	0.21	83.99
0.0899	0.0101	0	1.99	29.54
0.0326	0.0098	0	0.72	33.59
0.0565	0.0139	0	1.25	30.21
0.1375	0.0079	0	**3.05**	22.20
0.1888	0.0040	0	4.19	12.39
0.0184	0.0038	0	0.41	10.78
0.7372	0.0030	0	16.38	10.53
0.5192	0.0034	0	11.54	10.96

4.3 Conclusion

The proposed stiction detection method has been successful for the simulated and experimental cases. Different types of processes such as flow, level, temperature and integrating were used for simulations. Experimental validations are also done for flow and level control loops.

Chapter 5

Evaluation of the Harmonics Method using Benchmark Industrial Data Sets

The proposed stiction detection method was used to diagnose the cause of oscillations in different types of selected control loops from various process industries. These loops include Flow Control (FC), Pressure Control (PC), Level Control (LC), Concentration Control (CC), Thickness Control (ThC) and Analyzer Control (AC). Error signals have been generated for each loop by subtracting controlled output (PV) from set point (SP). Literature [25] reported the result of different stiction detection methods. Table 5.1 shows a comparison of the results obtained using the proposed harmonics method with that of the other existing methods. A short summary of the findings is given in Table 5.3. A detailed analysis is provided in Appendix - A.

Table 5.1 shows the harmonic analysis results of 29 industrial control loops from different industries. The detailed description of the loops can be found in [25]. Column 1 of Table 5.1 stands for the industry type from which the data were collected. Here, CHEM means chemical industry, PAP means Pulp and Paper industry, MIN means mining industry and MET means metal processing industry.

TABLE 5.1: Comparison of different stiction detection methods

Loop name	**Loop Type**	**Given info**	**Detection and Results**							
			HAMM 2		HAMM 3		BIC		HARMONICS	
			Stiction?	Right or Wrong?	Stiction?	Right or Wrong?	Stiction?	Right or Wrong?	Stiction?	Right or Wrong?
CHEM 1	FC	Stiction	YES	√	YES	√	YES	√	YES	√
CHEM 2	FC	Stiction	YES	√	YES	√	YES	√	YES	√
CHEM 3	TC	Quantization	NO	√	NO	√	NLQ	√	NO	√
CHEM 6	FC	Stiction	YES	√	YES	√	YES	√	YES	√
CHEM 10	PC	Stiction	YES	√	YES	√	YES	√	YES	√
CHEM 11	FC	Stiction	YES	√	YES	√	YES	√	YES	√
CHEM 12	FC	Stiction	YES	√	YES	√	NL-NO	√	YES	√
CHEM 13	AC	Faulty sensor, No stiction	NO	√	YES	X	YES	√	NO	√
CHEM 14	FC	Faulty sensor, No stiction	YES	X	YES	X	YES	X	YES	X
CHEM 16	PC	Interaction likely, No stiction	YES	X	NO	√	YES	X	NO	√
CHEM 18	FC	Stiction (Likely)	YES	√	YES	√	YES	√	YES	√
CHEM 23	FC	Stiction (Likely)	YES	√	YES	√	YES	√	YES	√
CHEM 24	FC	Stiction (Likely)	YES	√	YES	√	YES	√	YES	√
CHEM 28	TC	Stiction (Likely)	YES	√	YES	√	NO	X	NO	X
CHEM 29	FC	Stiction	YES	√	YES	√	YES	√	YES	√
CHEM 32	FC	Stiction (Likely)	YES	√	YES	√	YES	√	YES	√
CHEM 33	FC	Disturbance (Likely)	YES	X	YES	X	YES	X	NO	√
CHEM 40	TC	No clear oscillation	NO	√	NO	√	NO	√	NO	√
CHEM 54	LC	No clear oscillation	YES	X	YES	X	YES	X	NO	√
CHEM 62	FC	No clear oscillation	YES	X	NO	√	NO	√	NO	√
PAP 2	FC	Stiction	YES	√	YES	√	YES	√	YES	√
PAP 4	CC	Deadzone, No stiction	YES	X	YES	X	YES	X	YESl	X
PAP 5	CC	Stiction	NO	X	NO	X	YES	√	NO	X
PAP 7	FC	External Disturbance	YES	X	NO	√	NO-NO	√	NO	√
PAP 9	TC	No stiction	NO	√	YES	X	YES	X	NO	√
MIN 1	TC	Stiction	YES	√	YES	√	YES	√	NO	X
MET 1	Th. C	External Disturbance (likely)	YES	X	YES	X	NO	√	NO	√
MET 2	Th. C	External Disturbance (likely)	YES	X	YES	X	NL-NO	√	NO	√
MET 3	Th. C	No oscillation	YES	X	YES	X	NL-NO	√	NO	√

Column 2 indicates the type of control. In the 'given info' column, specific details of the data that were known from the data supplier is shown. This information is claimed by the plant personnel. Stiction detection results by using HAMM2, HAMM3, and Bicoherence (BIC) methods are shown in the consecutive columns. The results obtained from the Harmonic based method are shown in the rightmost part of the table. The detection results are shown under the column heading 'Stiction ?'. When results under this column don't match with the 'Given info' column, the analysis result is considered to be wrong and a cross mark is shown in the column 'Right or Wrong?' otherwise a tick mark is placed.

For the sake of brevity, the details of harmonic analysis for one industrial control loop (CHEM 1) is shown in this thesis. The detailed description for the other loops are shown in Appendix-A. Figure 5.1 shows the time trends of the error signal and

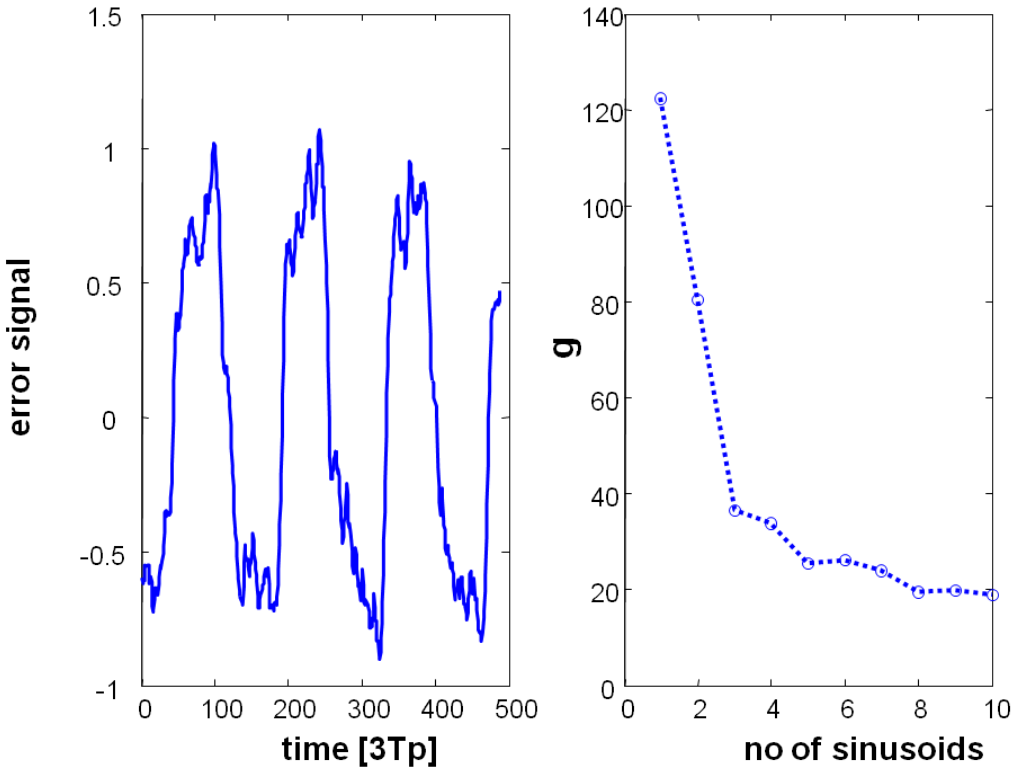

FIGURE 5.1: Harmonic analysis of Industrial Data (CHEM 1)

'g' values. Harmonic analysis was done and it was found that the third harmonic relation is present in the signal. Hence, it is concluded that stiction was present in the control valve of this loop.

A summary of the analysis of the stiction detection methods for these 29 industrial control loops is shown in Table 5.3. From this table, it is found that the proposed harmonics based stiction detection method results in the highest number of correct detection. Among the 29 loops under consideration, harmonics method correctly detects the root cause of oscillations for 24 loops. The nearest candidate for the correct detection is bicoherence method which can detect 22 loops correctly. HAMM2 and HAMM3 methods can only detect 18 and 19 loops correctly. Based on this analysis, harmonics based stiction detection method finds 14 loops suffering from stiction whereas other methods detect stiction in more than 20 loops. As a result it can be inferred that the existing stiction detection methods produce more false positive results. In other words, the proposed harmonics based

TABLE 5.2: Harmonic analysis result of Industrial Control Loop (CHEM 1)

ω_i rad/cycle	A_i	ϕ_i rad	$\mathbf{g}$	ω_i/ω_1
0.0437	0.8205	-0.4079	122.19	**1**
0.1321	0.1848	-0.9637	80.32	**3.0257**
0.1787	0.0837	1.5708	36.50	4.0944
0.0929	0.0848	1.1475	33.77	2.1282
0.075	0.0597	0.3156	25.58	1.7176
0.2633	0.0639	-0.8741	26.04	6.0317
0.2295	0.0538	1.2879	24.06	5.2568
0.2478	0.0496	-1.2719	19.45	5.6754
0.0572	0.0539	-1.5708	19.69	1.311
0.3543	0.0459	1.5708	18.98	8.1171

TABLE 5.3: Summary of different stiction detection methods for Industrial Data Sets

	HAMM 2		HAMM 3		BIC		Harmonics	
Detection	Right	18	Right	19	Right	22	Right	**24**
	Wrong	11	Wrong	10	Wrong	7	Wrong	**5**
Stiction	Yes	24	Yes	23	Yes	20	Yes	14
	No	5	No	6	No	9	No	15

stiction detection method produces less false positive results. It is to be also noted that false positive results degrade the confidence in automatic stiction detection methods.

Chapter 6

Compensation of Valve Stiction

The classical PID control schemes is the most popular and widely used for in process control systems for a long time. The performance of a fixed PID controller may drastically fall in the presence of nonlinearity in control loops. An adaptive PID controller can overcome this shortcoming. The efficacy of using a Self-Tuning Controller(STC) scheme in a control loop where stiction is the main nonlinearity is studied in this chapter. The basic structure of a STC is as follows. First, the property of the hammerstein control system is identified by using least squares method. Then the control parameters are calculated from the estimated parameters by using generalized predictive control algorithm. Finally, these controller parameters are used to control the hammerstein nonlinear process. These procedure is repeated in every step. This method can retune the controller adaptively. The retuning of controller is carried out only when the control performance become poor. Because, the idea of control performance assessment is becoming very important in the process control area [40], [41] and the basic idea of adaptive control refers only when the performance becomes bad. One of the most useful methods of performance assessment is minimum variance control based method proposed by Harris [42], [43]. The performance index of this method is defined as the ratio of minimum variance of the closed loop output and the variance of the current actual output. This index is bounded between 0 and 1. The index value near 1 means good control performance and a value near 0 means bad performance which needs

retuning of control parameters. This study presents the design, implementation and evaluation of an adaptive PID controller which is driven by current control performance. The calculations of PID parameters are based on the generalized predictive control (GPC) [44]. The current control performance is obtained in an online manner over a user-specified time-window with some overlap. The retuning of PID parameters and system identification are only carried out when controller performance deteriorates to a userspecified limit. The batch type least squares is employed for the system identification. This Chapter is organized as follows: the design method of the proposed performance-driven adaptive PID controller is considered in the next section. The following two sections evaluate the proposed method with simulation examples. Final section summarizes the conclusions.

6.1 Design of Performance-Driven Adaptive PID Controller

6.1.1 System description

In this section, the mathematical model which is important for the controller design is considered. In the process control system, many systems may have the high order properties. However, as it is actually difficult to identify the exact high order properties, the model up to a 2nd order system is often used as the transfer function of the controlled system. So, many STC algorithm are based on a discrete time model of the form:

$$A(z^{-1})y(t) = z^{-1}B(z^{-1})u(t) + \xi(t)/\Delta \tag{6.1}$$

where,

$$\left.\begin{aligned} A(z^{-1}) &= 1 + a_1 z^{-1} + a_2 z^{-2} \\ B(z^{-1}) &= b_0 + b_1 z^{-1} + \cdots + b_m z^{-m} \end{aligned}\right\} \tag{6.2}$$

$u(t)$ and $y(t)$ denote the control input and the corresponding output signals respectively. And, $\xi(t)$ means noise term, Δ is the differential operator which means $\Delta = 1 - z^{-1}$.

The control system Equations (6.1) and (6.2) satisfy the following assumptions.

[**Assumptions**]

[**A.1**] a_i's and b_i's are unknown.

[**A.2**] m, which is the order of $B(z^{-1})$, is known.

[**A.3**] $A(z^{-1})$ and $B(z^{-1})$ are irreducible to each other.

[**A.4**] The noise $\xi(t)$ satisfies the following conditions.

$$\left.\begin{aligned} &E[\xi(t)] = 0 \\ &E[\xi^2(t)] = \sigma^2 \\ &E[\xi(t)\xi(t+\tau)] = 0 \end{aligned}\right\} \tag{6.3}$$

[**A.5**] Reference signal $y_{sp}(t)$ is given by a piecewise constant signal.

6.1.2 PID control law

The following velocity-type PID controller is employed.

$$\Delta u(t) = k_c \frac{T_s}{T_I} e(t) - k_c(\Delta + \frac{T_D}{T_s}\Delta^2) y(t) \tag{6.4}$$

where $e(t)$ denotes the control error signal given by

$$e(t) := y_{sp}(t) - y(t) \tag{6.5}$$

and k_c, T_I and T_D are the proportional gain, the reset time and the derivative time, respectively. T_s denotes the sampling interval.

For convenience, Equation (6.4) is rewritten by

$$C(z^{-1})y(t) + \Delta u(t) - C(1)y_{sp}(t) = 0 \tag{6.6}$$

where,

$$\begin{aligned} C(z^{-1}) &= c_0 + c_1 z^{-1} + c_2 z^{-2} \\ &= k_c(1 + \frac{T_s}{T_I} + \frac{T_D}{T_s}) - k_c(1 + \frac{2T_D}{T_s})z^{-1} + \frac{k_c T_D}{T_s} z^{-2}. \end{aligned} \tag{6.7}$$

The tuning of the control parameters included in the PID control law (6.4) or (6.6) is important since it strongly influences the control performance. The design method is considered based on the relation to the Generalized Predictive Control (GPC) by the following procedure.

6.1.3 Generalized Predictive Control law

Generalized Predictive Control method, which is one of the model predictive control law, is proposed for long time delay systems. The cost function of the Generalized Predictive Control law is defined as

$$J(t) = E[\sum_{j=1}^{N}\{y(t+j) - y_{sp}(t)\}^2 + \lambda \sum_{j=1}^{N}\{\Delta u(k+j-1)\}^2] \tag{6.8}$$

where, $y_{sp}(t)$ is the reference signal. λ and N mean the weighting factor of the control input and the prediction horizon, respectively. By minimizing the cost function (6.8), the following GPC law can be derived,

$$\sum_{j=1}^{N} p_j F_j(z^{-1})y(t) + \{1 + z^{-1}\sum_{j=1}^{N} p_j S_j(z^{-1})\}\Delta u(t) - \sum_{j=1}^{N} p_j y_{sp}(t) = 0 \tag{6.9}$$

where, $F_j(z^{-1})$ can be obtained by solving the following the Diophantine equation,

$$1 = \Delta A(z^{-1})E(z^{-1}) + z^{-j}F_j(z^{-1}) \tag{6.10}$$

$$\left.\begin{aligned} E_j(z^{-1}) &= 1 + e_{j,1}z^{-1} + \cdots + e_{j,j-1}z^{-(j-1)} \\ F_j(z^{-1}) &= f_{j,0} + f_{j,1}z^{-1} + f_{j,2}z^{-2} \end{aligned}\right\}$$

Also $S_j(z^{-1})$ can be obtained by solving the following equation,

$$E_j(z^{-1})B_j(z^{-1}) = R_j(z^{-1}) + z^{-j}S_j(z^{-1}) \tag{6.11}$$

$$\left.\begin{aligned} R_j(z^{-1}) &= r_0 + r_1z^{-1} + \cdots + r_{j-1}z^{-(j-1)} \\ S_j(z^{-1}) &= s_{j,0} + s_{j,1}z^{-1} + \cdots + s_{j,m-1}z^{-(m-1)} \end{aligned}\right\}$$

moreover, p_j can be calculated as:

$$[p_1, p_2, \cdots, p_N] := [1, \underbrace{0, \cdots, 0}_{N-1}](G^TG + \lambda \cdot I)^{-1}G^T \tag{6.12}$$

where,

$$G := \begin{bmatrix} r_0 & & & \\ r_1 & r_0 & & 0 \\ \vdots & & \ddots & \\ r_{N-1} & r_{N-2} & \cdots & r_0 \end{bmatrix} \tag{6.13}$$

6.1.4 Calculation of the PID parameters

This section discusses the calculation of the PID parameters based on the GPC law [45], [46]. The GPC law of Equation (6.9) is rewritten by replacing the second term of the right hand side with the approximation of the static term:

$$\frac{1}{\nu}\sum_{j=1}^{N} p_jF_j(z^{-1})y(t) + \Delta u(t) - \frac{1}{\nu}\sum_{j=1}^{N} p_jy_{sp}(t) = 0 \tag{6.14}$$

where,

$$\nu := 1 + \sum_{j=1}^{N} p_jS_j(1) \tag{6.15}$$

Next, the following relation is obtained by comparing Equation (6.6) and (6.14),

$$R_j(z^{-1}) = F_j(z^{-1}) \tag{6.16}$$

$$C(z^{-1}) = \frac{1}{\nu}\sum_{j=1}^{N} p_j F_j(z^{-1}) \tag{6.17}$$

where $R_j(z^{-1})$ and $C(z^{-1})$ are designed, such that two control laws are equivalent. Finally, PID parameters are calculated by the following equations.

$$\left.\begin{aligned} k_c &= -\frac{1}{\nu}(\tilde{f}_1 + 2\tilde{f}_2) \\ T_I &= -\frac{\tilde{f}_1 + 2\tilde{f}_2}{\tilde{f}_0 + \tilde{f}_1 + \tilde{f}_2} T_s \\ T_D &= -\frac{\tilde{f}_2}{\tilde{f}_1 + 2\tilde{f}_2} T_s \end{aligned}\right\} \tag{6.18}$$

where,

$$\tilde{f}_i := \frac{1}{\nu}\sum_{j=1}^{N} p_j f_{i,j} \quad (i = 0, 1, 2) \tag{6.19}$$

6.1.5 Current Performance Assessment

In this work, the performance assessment index is employed for the threshold of adaptive function. The retuning of PID parameters and system identification are only carried out when controller performance index deteriorates to a user-specified limit.

Desborough and Harris [43] proposed a calculation method of the performance assessment index based on minimum variance of closed loop system [43]. The performance assessment index is defined as

$$\eta(t) = \frac{{\sigma^2}_{mv}(t)}{{\sigma^2}_{e}(t)} \tag{6.20}$$

where, ${\sigma^2}_e(t)$ and ${\sigma^2}_{mv}(t)$ mean the variance of control error signal and minimum variance of closed loop system. Control performance index can also be calculated in an online manner with some overlap.

6.1.6 System Identification Method

The recursive least squares method (RLS) is known as the main estimation method for the self-tuning controller. RLS requires the calculation at every step, because the calculated result is accumulated. However, in this work, the estimation should be carried out intermittently based on the current performance assessment index (6.20). So, a batch type least squares method is employed.

$\hat{\theta}(t)$ is the estimates of unknown parameters $\theta = [a_1, b_0, \ldots, b_m]^T$

$$\hat{\theta}(t) \quad = \quad [\hat{a}_1(t), \hat{a}_2(t), \hat{b}_0(t), \ldots, \hat{b}_m(t)]^T \tag{6.21}$$

First, the following first order filer is used for input and output signals.

$$y_f(t) = \frac{1-f}{1-fz^{-1}} y(t) \tag{6.22}$$

$$u_f(t) = \frac{1-f}{1-fz^{-1}} u(t) \tag{6.23}$$

Next, the data matrix is consisted as:

$$Z(t) = \begin{bmatrix} -\Delta y_f(t-1) & -\Delta y_f(t-2) & \Delta u_f(t-1) & \ldots & \Delta u_f(t-m-1) \\ -\Delta y_f(t-2) & -\Delta y_f(t-3) & \Delta u_f(t-2) & \ldots & \Delta u_f(t-m-2) \\ . & . & . & \ldots & . \\ . & . & . & \ldots & . \\ -\Delta y_f(t-l) & -\Delta y_f(t-l-1) & \Delta u_f(t-l) & \ldots & \Delta u_f(t-m-l) \end{bmatrix} \tag{6.24}$$

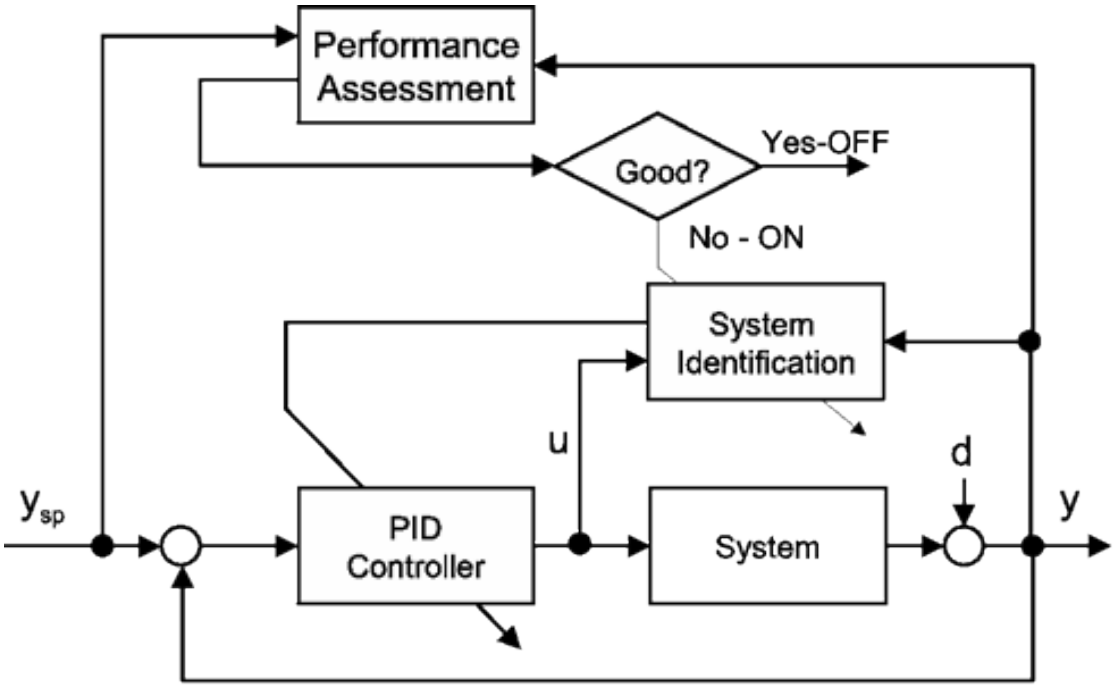

FIGURE 6.1: Block diagram of the proposed method

where, l is the length of the data window for estimation. Output vector is defined as:

$$\mathbf{y}(t) = [\Delta y_f(t), \Delta y_f(t-1), \cdots, \Delta y_f(t-l)]^T \tag{6.25}$$

The estimated system parameter vector is calculated by the following equation.

$$\hat{\theta}(t) = \{Z^T(t)Z(t)\}^{-1} Z(t)^T \mathbf{y}(t) \tag{6.26}$$

The recursive least squares is employed at $t < l$, because enough data sets can not obtained for batch type identification.

This identification procedure are only carried out when controller performance deteriorates to a user-specified limit $\bar{\eta}$. So, PID parameters calculation based on GPC is also done when the performance index is under $\bar{\eta}$.

The block diagram of proposed scheme is showen as Figure 6.1. The block 'System' in the Figure 6.1 indicates the Hammerstein system shown in Figure 2.5.

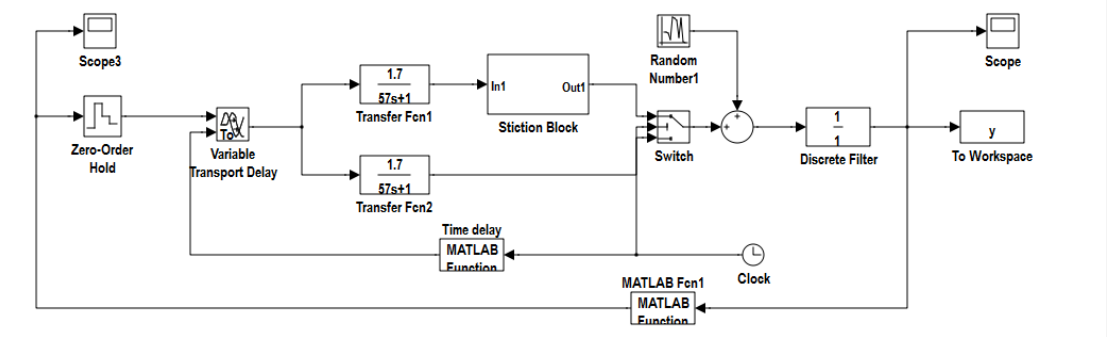

FIGURE 6.2: Simulink model for simulation of the adaptive controller in presence of stiction

6.2 Application of a performance-driven adaptive PID controller to sticky control loops

In order to study the efficacy of the performance driven STC as stiction compensator in a sticky control loop, a process having the transfer function shown in Equation 6.27 is used. For this FOPTD process, a PI controller is employed. Samples are taken at the interval of 10 s. Figure 6.2 shows the Simulink model of the adaptive STC in the presence of stiction.

$$G(s) = \frac{1.7e^{-7.8s}}{57s + 1} \tag{6.27}$$

At first the process was simulated for a fixed PI controller. Figure 6.3 shows the input-output of the hammerstein system. At time 800 s, stiction of amount S=5, J=5 is introduced in the control loop. As a result, the output of the hammerstein system, i.e., the controlled variable began to oscillate in a rectangular manner. As, the transfer of the process as shown in Equation 6.27 is for a level control loop with sufficient amount of integrating action, the input to the hammerstein system i.e., the controller output oscillates in a triangular manner.

Figure 6.4 shows the control performance index for the sticky control loop. The performance calculation algorithm calculates the performance index at every 10 samples using the last 300 data. Because of the introduction of stiction at 800s, the

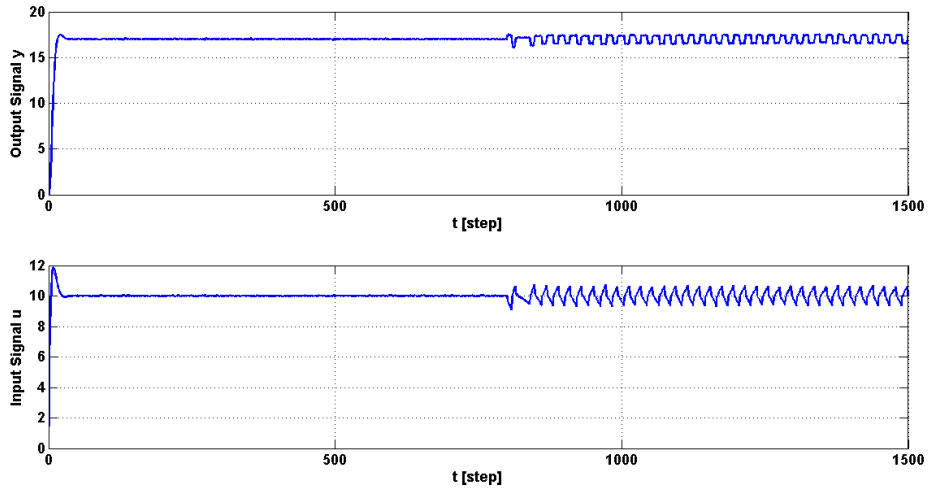

FIGURE 6.3: Input-output response of a sticky control loop in presence of a fixed PI controller (S=5, J=5)

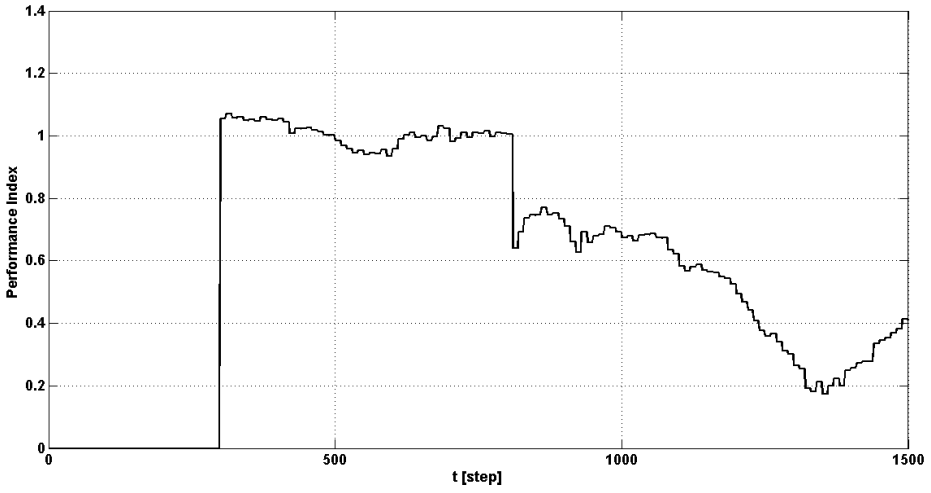

FIGURE 6.4: Performance Index of the process in presence of a fixed PI controller (S=5, J=5)

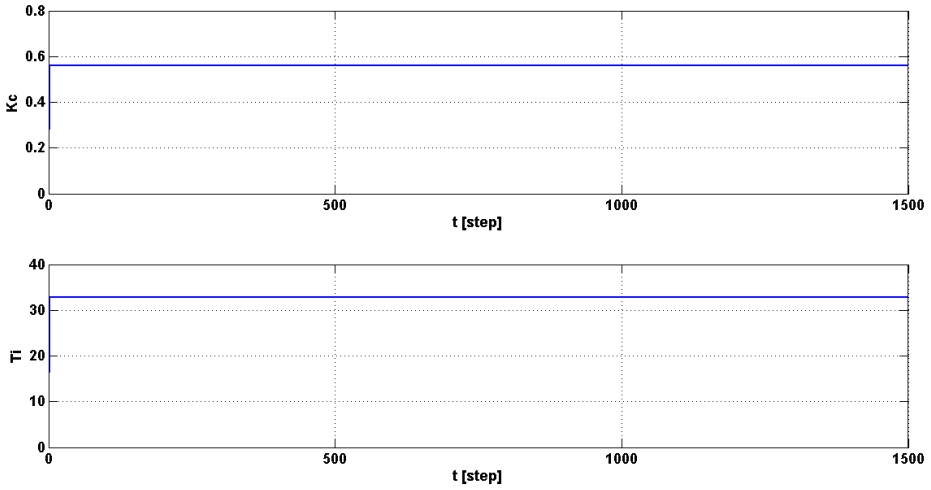

FIGURE 6.5: Profile of fixed controller parameters in presence of stiction (S=5, J=5)

performance drastically drops from 1.0. Figure 6.5 shows the controller parameter K_C and τ_I for this control loops.

The efficacy of an adaptive controller is studied with regard to reduce the impact of performance degradation caused by stiction. A batch-wise control performance assessment algorithm which retunes the controller settings based on a threshold performance index is used. In this case, the threshold index was selected as 0.8. Hence if the performance index falls below 0.8, self tuning initiates. Figure 6.6 shows the input – output signals of the hammerstein system in presence of the adaptive PI controller. It is clear from the figure that oscillation initiates after the introduction of stiction. Unfortunately, the ST-PI controller can't damp out the oscillations.

Figure 6.7 shows that, due to introduction of stiction at 800s the performance index falls quickly below 0.8. Thus, self tuning method initiates and the controller parameters K_c and τ_I change to a new value as shown in Figure 6.8. Due to this action the performance index increases from 0.6 to 0.93 as shown in Figure 6.7. As long as the performance index stays above 0.8, the control parameters don't changes. After some time, the performance of the control loops deteriorates monotonically. After 1500s, the performance index falls to 0.5 and further retuning of

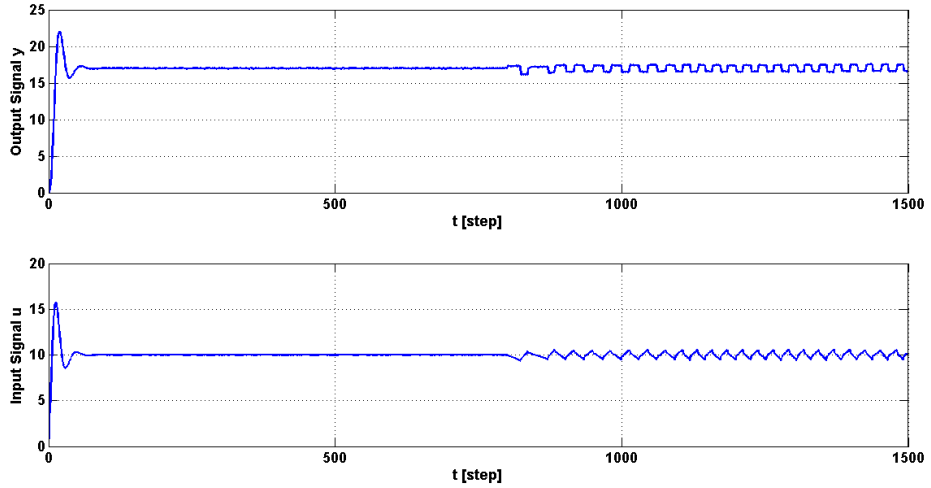

FIGURE 6.6: Input-output response of a sticky control loop (S=5, J=5) with a ST-PI controller

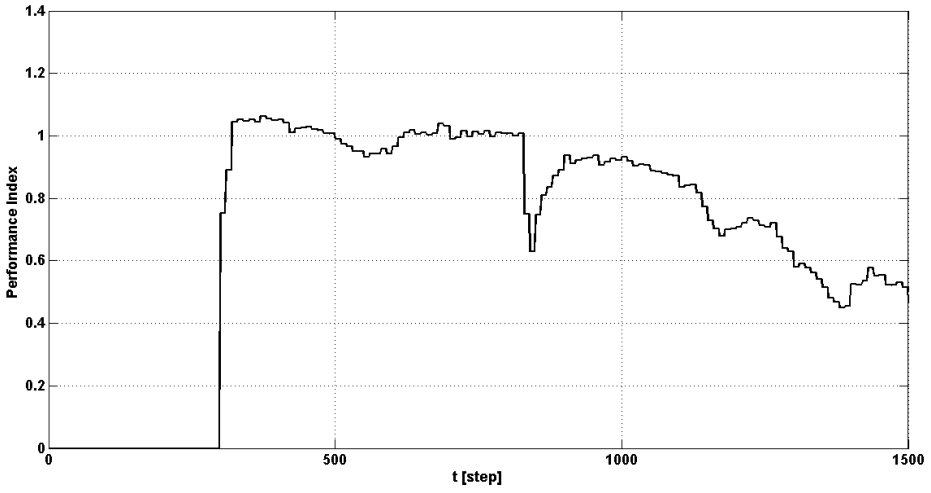

FIGURE 6.7: Performance index of a sticky control loop in presence of ST-PI controller (S=5, J=5)

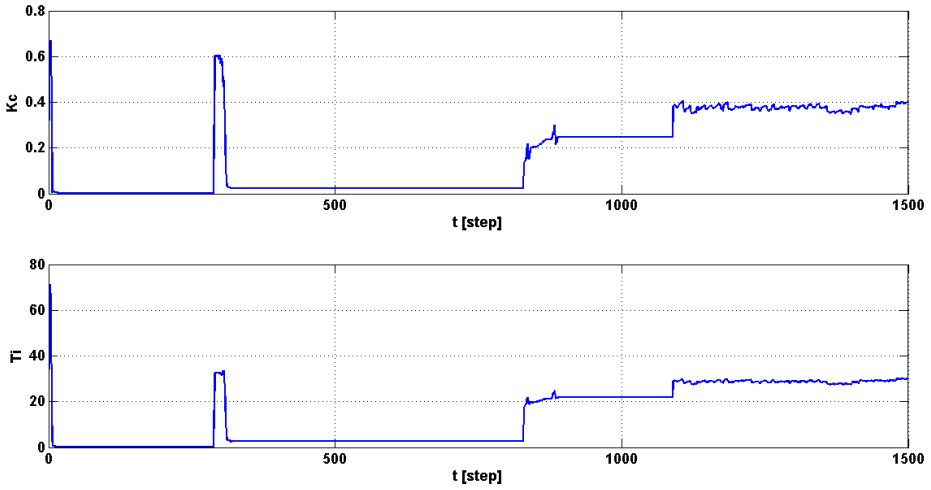

FIGURE 6.8: Controller parameters of adaptive PI controller in presence of stiction (S=5,J=5)

the controller didn't help much.

6.3 Conclusion

In this chapter, the efficacy of using an adaptive performance based PI controller is studied. Firstly, the design and controller tuning algorithm based on recursive least squares method and generalized predictive algorithm is used. Harris performance index is used to assess the performance of the control loops. A threshold value of 0.8 is used. The application of this ST controller to a sticky control loops based on the hammerstein system identification is studied. Unfortunately, it is found that though the performance index improves for some time but at the long run it falls below the threshold due to presence of stiction. Moreover, the variabilities in the PV and OP signal don't reduce.

Chapter 7

Conclusions and Future Works

Modern chemical processes are sophisticated and consists of hundreds of control loops. It is important to know that all control loops are performing satisfactorily. This requires controller performance audit. However, it is not possible to audit the controller performance manually on a loop by loop basis. Therefore, a data based method for controller performance assessment and for diagnosis of the causes of poor performance is an effective aid for control engineers.

7.1 Conclusions

The main contributions of this thesis can be summarized as below:

1. A new method for oscillation detection is developed. The proposed method reports the amount of oscillation by using the frequencies, amplitudes and phases of the significant sinusoidal elements present in the signal. It has been shown that Fisher's 'g' factor is an excellent way to distinguish between the presence of sinusoidal elements and noises in the signal to be analyzed.

2. A novel harmonics based stiction detection method is proposed. The proposed method detect stiction by using the estimated frequencies resulting from the oscillation detection methods. Presence of odd harmonics among

the significant sinusoids indicates the presence of stiction in the control valve. The proposed method is validated by simulation and pilot plant scale experimentation. The method was also applied to benchmark industrial data sets and it is found that the proposed method works better than the currently existing stiction detection methods.

3. For the successful implementation of the proposed method, various practical issues were addressed.

4. An adaptive STC controller was designed by considering hammerstein model identification for stiction compensation. It was found that the efficacy of STC controller is not satisfactory enough to suppress the effect of stiction in the control loops.

7.2 Recommendations for Future Work

There is a scope of improvement and extension of this research. The following recommendations can give some directions to future works.

1. The proposed method can be extended for stiction detection in presence of loop interactions.

2. The proposed methodology of stiction detection can be attempted to apply for the root-cause diagnosis of plant-wide oscillations.

3. There is a need for a good stiction compensation method in process industries. Till date, there is no good stiction compensator which can be successfully and satisfactorily applied to process industries. Therefore, it is still an open area for research. One form of stiction compensator may be found by employing an inverse of the two-parameter stiction model. As the amount of stiction may change over time, the best compensator would be an adaptive stiction compensator.

References

[1] L. Lunze. Automatisierungstechnik. *Oldenburg*, 2007.

[2] M. A. A. S. Choudhury, S. L. Shah, and N. F. Thornhill. Data-driven model of valve stiction: Diagnosis of process nonlinearities and valve stiction. In *Advances in Industrial Control*, pages 161–171. Springer Berlin Heidelberg, 2008.

[3] W. L. Bialkowski. Dreams versus reality: a view from both sides of the gap. *Pulp and Paper Canada*, 94:19–27, 1993.

[4] L. Desborough, P. Nordh, and R. Miller. Control system reliability: process out of control. *Industrial computing*, 8:52–55, 2001.

[5] D. B. Ender. Process control performances: Not as good as you think. *Control Engineering Practice*, 9:180–190, 1993.

[6] M. A. Paulonis and J. W. Cox. A practical approach for large-scale controller performance assessment, diagnosis and improvement. *Journal of Process Control*, 13:307–313, 1996.

[7] M. Jelali and B. Huang. *Detection and Diagnosis of Stiction in Control Loops: State of the Art and Advanced Methods*. Springer, 2010.

[8] M. A. A. S. Choudhury, M. Jain, and S. L. Shah. Stiction - definition, modelling, detection and quantification. *Journal of Process Control*, 18(3-4):232 – 243, 2008.

[9] C. Garcia. Comparison of friction models applied to a control valve. *Control Engineering Practice*, 16(10):1231 – 1243, 2008.

[10] A. Horch. A simple method for detection of stiction in control valves. *Control Engineering Practice*, 7(10):1221 – 1231, 1999.

[11] R. A. Romano and C. Garcia. Valve friction and nonlinear process model closed-loop identification,. *Journal of Process Control*, 21(4):667 – 677, 2011.

[12] S. B. Chitralekha, S. L. Shah, and J. Prakash. Detection and quantification of valve stiction by the method of unknown input estimation. *Journal of Process Control*, 20(2):206 – 216, 2010.

[13] R. Rengaswamy, T. Hagglund, and V. Venkatasubramanian. A qualitative shape analysis formalism for monitoring control loop performance. *Engineering Applications of Artificial Intelligence*, 14(1):23 – 33, 2001.

[14] M. Ruel. Stiction: the hidden menace. *Control Magazine*, 13:69–75, 2000.

[15] M. Jelali. Estimation of valve stiction in control loops using separable least-squares and global search algorithms. *Journal of Process Control*, 18(7-8):632 – 642, 2008.

[16] D. Karnopp. Computer simulation of stick-slip friction in mechanical dynamic sustems. *Trans ASME*, 107:100–103, 1985.

[17] A. Stenman, F. Gustafsson, and K. Forsman. A segmentation-based method for detection of stiction in control valves. *International Journal of Adaptive Control and Signal Processing*, 17(7-9):625–634, 2003.

[18] M. Kano, H. Maruta, H. Kugemoto, and K. Shimizu. Practical model and detection algorithm for valve stiction. In *Proc IFAC DYCOPS, Cambridge, USA*, 2004.

[19] Q. P. He, J. Wang, M. Pottmann, and S. J. Qin. A curve fitting method for detecting valve stiction in oscillating control loops. *Industrial & Engineering Chemistry Research*, 46(13):4549–4560, 2007.

[20] Y. Yamashita. An automatic method for detection of valve stiction in process control loops. *Control Engineering Practice*, 14(5):503 – 510, 2006.

[21] A. Singhal and T. I. Salsbury. A simple method for detecting valve stiction in oscillating control loops. *Journal of Process Control*, 15(4):371 – 382, 2005.

[22] C. Scali and C. Ghelardoni. An improved qualitative shape analysis technique for automatic detection of valve stiction in flow control loops. *Control Engineering Practice*, 16(12):1501 – 1508, 2008.

[23] R. Srinivasan, R. Rengaswamy, and R. Miller. Contr loop performance assessment. 2. hammerstein model approach for stiction diagnosis. *Industrial & Engineering Chemistry Research*, 44:6719–6728, 2005.

[24] R. Srinivasan, R. Rengaswamy, and R. Miller. Control loop performance assessment. 1. a qualitative approach for stiction diagnosis. *Industrial & Engineering Chemistry Research*, 44(17):6708–6718, 2005.

[25] M. Jelali and C. Scali. *Detection and Diagnosis of Stiction in Control Loops: Sate of the Art and Advanced Methods*. Springer, 2010.

[26] M. Rossi and C. Scali. A comparison of techniques for automatic detection of stiction: simulation and application to industrial data. *Journal of Process Control*, 15(5):505 – 514, 2005.

[27] K. H. Lee, Z. Ren, and B. Huang. *Detection and Diagnosis of Stiction in Control Loops: State of the Art and Advanced Methods*, chapter Chapter 11, pages 249–288. Spinger, 2010.

[28] S. Karra and M. N. Karim. Alternative model structure with simplistic noise model to identify linear time invariant systems subjected to non-stationary disturbances. *Journal of Process Control*, 19(6):964 – 977, 2009.

[29] B. Armstrong-Helouvre, P. Dupont, and C. C. De-Wit. A survey of models, analysis tools and compensation methods for the control of machines with friction. *Automatica*, 30:1083–1138, 1994.

[30] A. Kayihan and F. J. Doyle. Friction compensation for a process control valve. *Control Engineering Practice*, 8:799–812, 2000.

[31] T. Hagglund. A friction compensator for pneumatic control valves. *Journal of Process Control*, 12:897–904, 2002.

[32] R. Srinivasanan and R. Rengaswamy. Integrating stiction diagnosis and stiction compensation in process control valves. *16th europian symposium on computer aided process engineering*, 2006.

[33] R. Srinivasan and R. Rengaswamy. Stiction compensation in process control loops: A framework for integrating stiction measure and compensation. *Accepted for publication in Industrial and Engg. Chemistry Research*, 2005.

[34] T. Hagglund. A control-loop performance monitor. *Control Engineering Practice*, 3(11):1543 – 1551, 1995.

[35] M. A. A. S. Choudhury, N. F. Thornhill, and S. L. Shah. *Detection and Diagnosis of Stiction in Control Loops: State of the Advanced Techniques*, chapter 2, pages 21–36. Springer, 2010.

[36] M. A. A. S. Choudhury. Troubleshooting plantwide oscillations using harmonics,. In *Proceedings of ADCONIP*, May 4-8, Jasper, Canada, 2008.

[37] B. G. Quinn and J. M. Fernandes. A fast efficient technique for the estimation of frequency. *Biometrika*, 78(3):489–497, 1991.

[38] B. Truong-Van. A new approach to frequency analysis with amplified harmonics. *Journal of Royal Statistics Society B*, 52:203–22, 1990.

[39] R. A. Fisher. Tests of significance in harmonic analysis. *Proceedings of Royal Society London A*, 125:54–49, 1929.

[40] B. Huang and S. L. Shah. *Performance assessment of control loops: Theory and Applications*. Spinger, 1999.

[41] M. Jelali. An overview of control performance assessment technology and industrial applications. *Control Engineering Practice*, pages 441–466, 2006.

[42] T. J. Harris. Assessment of closed-loop performance. *The Canadian Journal of Chemical Engineering*, 67:856–861, 1989.

[43] L. Desborough and T. J. Harris. Performance assessment measures for univariate feedback control. *The Canadian Journal of Chemical Engineering*, 70:1186–1197, 1992.

[44] D. W. Clarke, C. Mohitadi, and P. S. Tuffs. Generalised predictive control. *Automatica*, 23:137–160, 1987.

[45] R. M. Miller, K. E. Kwok, S. L. Shah, and R. K. Wood. Development of stocastic predictive pid controller. In *Proc. of the American Control Conference*, volume 6, pages 4204–4208, 1995.

[46] T. Yamamoto, S. Omatu, and M. Kaneda. A design method of self-tuning pid controllers. In *Proc. of american Control Conference*, volume 3, pages 3262–3267, 1994.

Appendix A

Appendix A

Harmonic Analysis of Benchmark Industrial Data Sets

Given Info	Analysis Result by using the proposed method					Comment
CHEM 1	**Frequency, w rad/cycle**	**Amplitudes**	**Phase, radian**	**g**	**w./w(1)**	
Flow Control	0.0437	0.8205	-0.4079	122.1904	**1.0000**	Correctly detected **stiction**
	0.1321	**0.1848**	-0.9637	**80.3204**	**3.0257**	
Ts = 1 s Time Window: 1:487	0.1787	**0.0837**	1.5708	**36.5038**	**4.0944**	
	0.0929	0.0848	1.1475	33.7702	2.1282	
	0.0750	0.0597	0.3156	25.5837	1.7176	
	0.2633	0.0639	-0.8741	26.0453	**6.0317**	
	0.2295	0.0538	1.2879	24.0645	5.2568	
Stiction	0.2478	0.0496	-1.2719	19.4515	5.6754	
	0.0572	0.0539	-1.5708	19.6853	1.3110	
	0.3543	0.0459	1.5708	18.9775	8.1171	

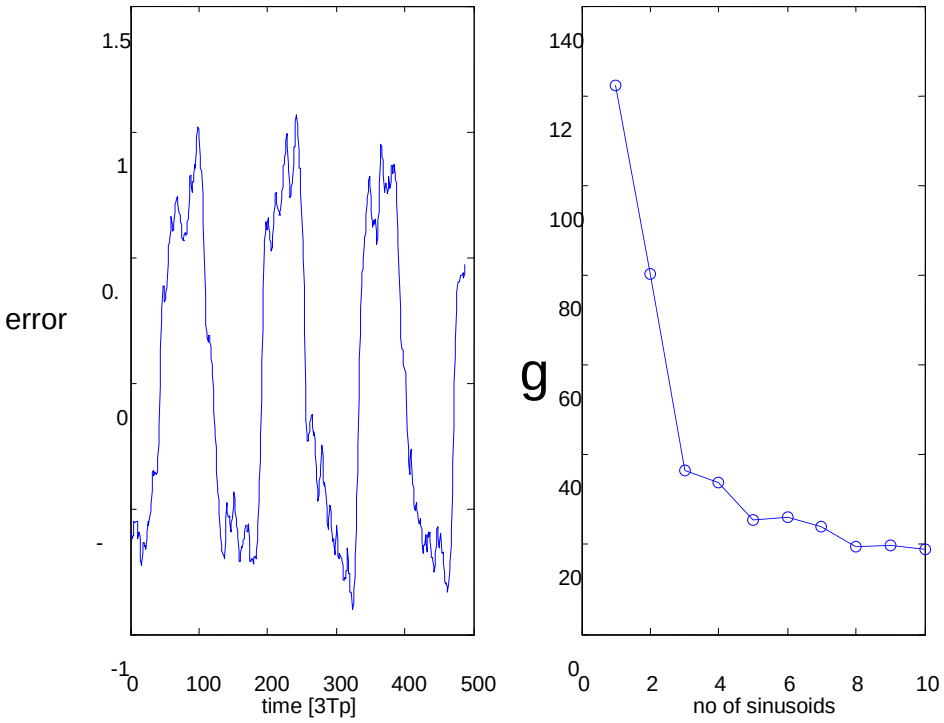

Given Info	Result of Harmonic Analysis					Comment
CHEM 2	Frequency, w rad/cycle	Amplitudes	Phase, radian	g	w./w(1)	
Flow control	0.0281	0.8101	1.1833	179.3811	1.0000	Correctly detected the presence of stiction
	0.0859	**0.3471**	0.9857	71.0719	**3.0554**	
Ts = 1 s **Time window: 300 to 956**	0.0685	0.1846	0.3719	25.2550	2.4367	
	0.1345	0.1871	1.5708	28.0244	4.7819	
	0.1582	0.2185	-1.1268	23.2587	5.6256	
	0.0996	0.1904	-0.4994	24.6055	3.5402	
	0.0761	0.1333	-0.5726	20.5349	2.7061	
Stiction	0.0172	0.1157	-0.9703	18.8839	0.6118	
	0.1139	0.1192	1.3814	17.5441	4.0481	
	0.1931	0.1148	0.5748	17.3010	6.8644	

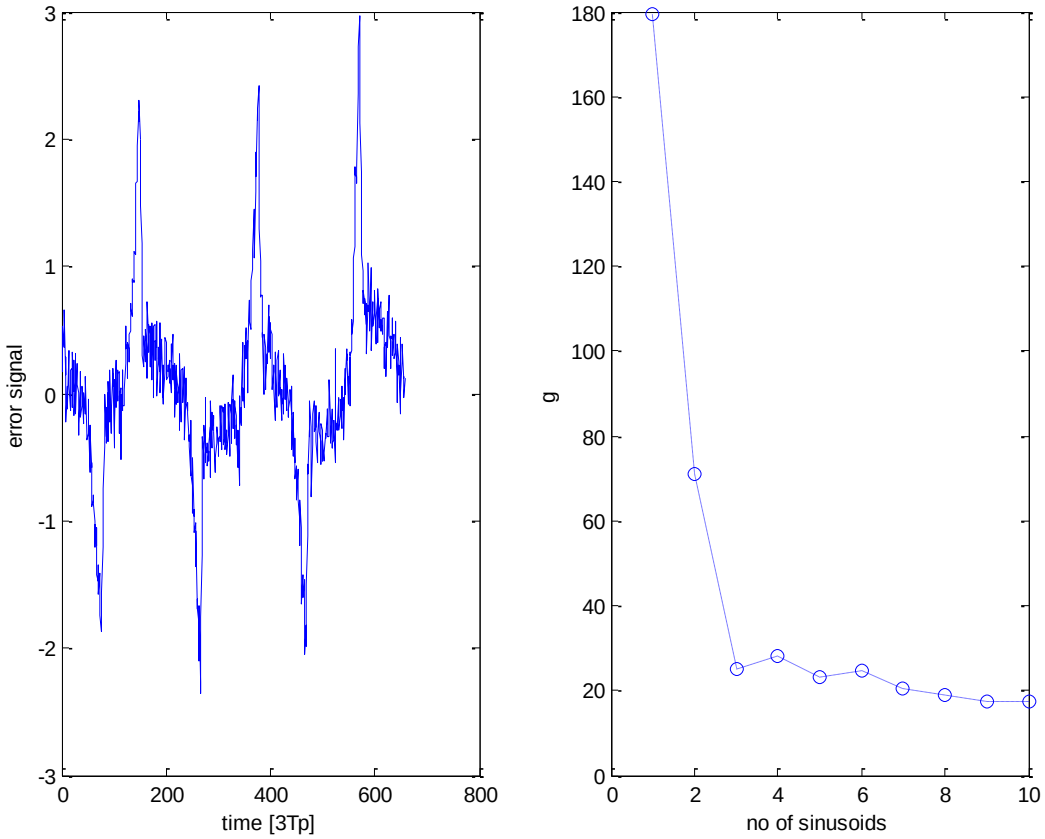

Given Info	Result of Harmonic Analysis					Comment
CHEM 3	**Frequency, w rad/cycle**	**Amplitudes**	**Phase, radian**	**g**	**w./w(1)**	
Temperature control	**0.2017**	**0.0579**	**-0.9337**	**26.7911**	**1.0000**	**No Stiction**, since the 3 significant sinusoids have to odd harmonic relation
	0.1232	**0.0261**	**-1.0771**	**11.9257**	**0.6108**	
Ts= 30 **Time window: 1 to 89**	**0.2724**	**0.0220**	**0**	**11.3407**	**1.3510**	
	0.3538	0.0139	0	7.5765	1.7546	
	0.4397	0.0143	-1.5708	6.8303	2.1805	
	1.0057	0.0113	0	4.8630	4.9873	
	1.5230	0.0085	0	5.7520	7.5528	
Quantisation	1.9099	0.0099	0	6.3098	9.4711	
	0.6841	0.0064	0	6.9924	3.3925	
	0.1998	0.0057	0	7.5657	0.9910	

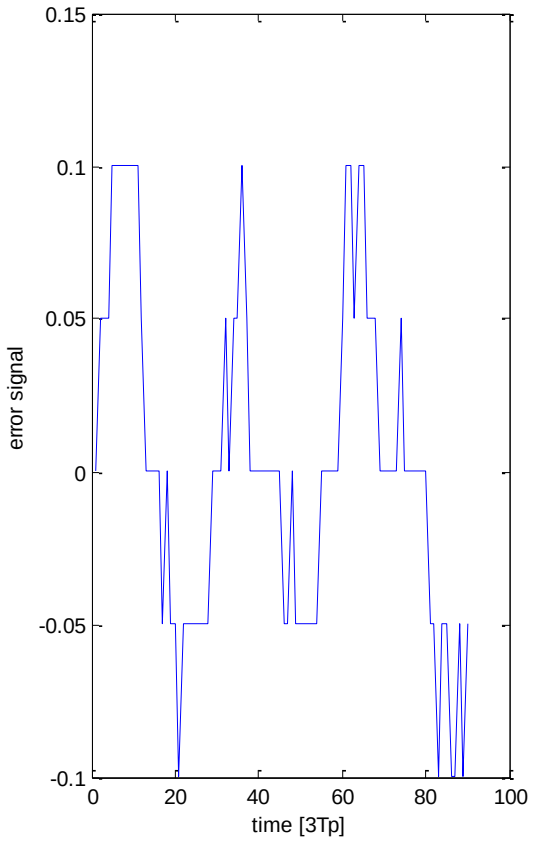

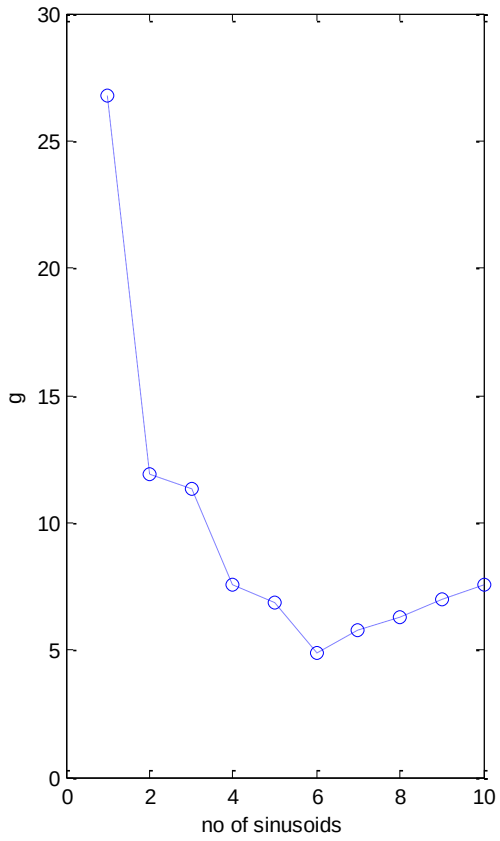

Given Info	Result of Harmonic Analysis					Comment
CHEM 6	**Frequency, w rad/cycle**	**Amplitudes**	**Phase, radian**	**g**	**w./w(1)**	
Flow control	0.0066	16.7384	-0.5381	103.4407	1.0000	Correctly detected stiction.
	0.0826	12.0639	0.3057	73.6380	12.4190	
Ts=1 s **Time window: 1 to 972**	0.1101	12.2089	0.4067	73.1953	16.5560	
	0.0198	**8.7523**	0.4919	56.7319	**2.9717**	
	0.1153	8.7490	-1.5146	58.5091	17.3352	
	0.1279	8.9274	0.6252	63.9522	19.2286	
	0.0889	7.8861	-1.0584	66.6910	13.3680	
Stiction	0.0136	6.3219	0.2068	49.7722	2.0482	
	0.1208	6.2213	0.4197	47.7018	18.1709	
	0.1059	7.3630	0.7856	41.0245	15.9178	

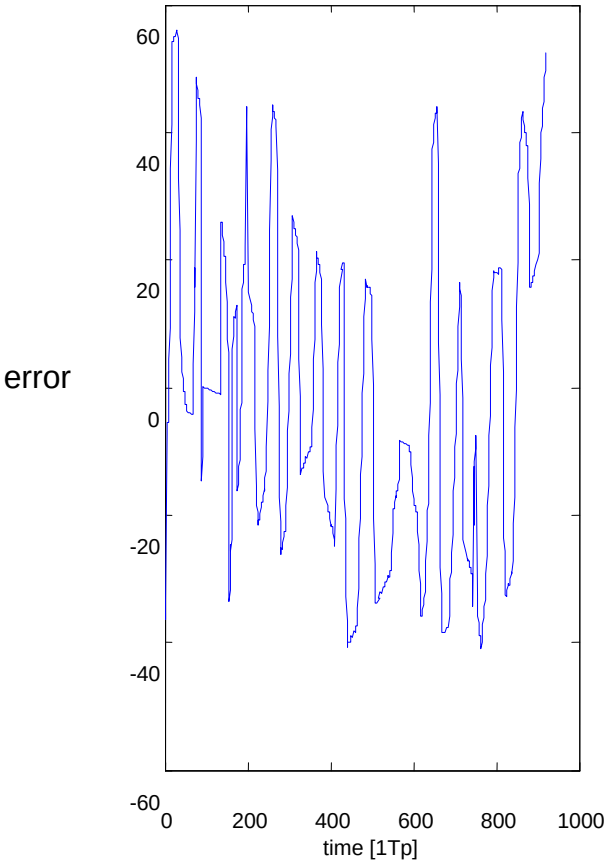

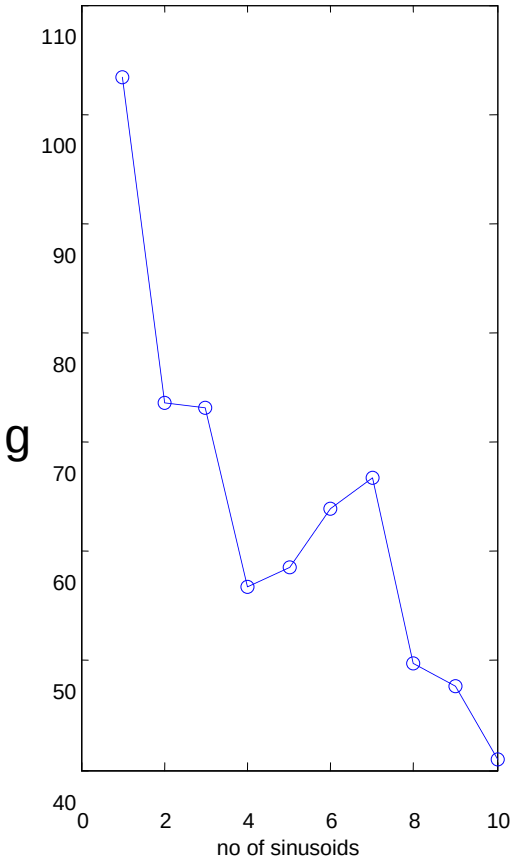

Given Info	Result of Harmonic Analysis					
CHEM 10	**Frequency, w rad/cycle**	**Amplitudes**	**Phase, radian**	**g**	**w./w(1)**	**Comment**
Pressure Control	0.0434	1.6104	-1.3991	200.6086	1.0000	Correctly detected **stiction**
	0.1333	**0.2796**	-1.3039	82.6262	**3.0737**	
Ts=1 s **Time window: 1 to 443**	0.0530	0.2032	-0.0995	30.4820	1.2214	
	0.2201	0.1190	-0.1638	37.0521	**5.0773**	
	0.0357	0.1343	0	24.3160	0.8245	
	0.0643	0.1010	0	25.3295	1.4827	
	0.2619	0.0487	-0.7657	11.5529	6.0415	
Stiction	0.0806	0.0697	-0.2532	11.8904	1.8580	
	0.1395	0.0535	0.4816	11.0369	3.2178	
	0.0067	0.0710	0.2122	11.6858	0.1548	

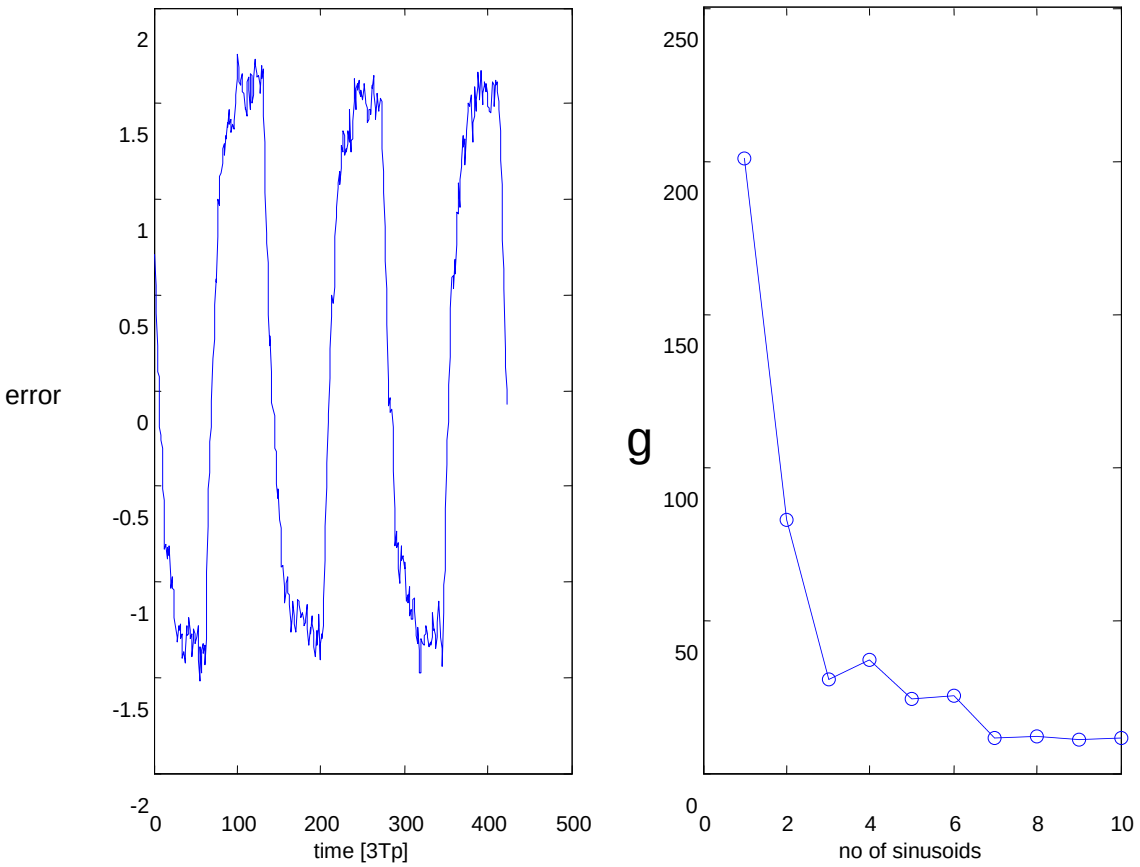

Given Info	Result of Harmonic Analysis					Comment
CHEM 11	**Frequency, w rad/cycle**	**Amplitudes**	**Phase, radian**	**g**	**w./w(1)**	
Flow Control	0.0502	2.2788	0.4331	182.9860	1.0000	Correctly detected the presence **stiction**
	0.1498	**0.1151**	0.6089	14.9363	**2.9839**	
Ts= 1 s **Time window: 200 to 577**	0.2168	0.0959	-0.8180	11.3464	4.3196	
	0.1311	0.0744	-1.0600	7.3014	2.6118	
	0.8803	0.0731	1.3679	7.5286	17.5397	
	0.2350	0.0719	0.9678	7.1981	4.6824	
	0.4671	0.0689	0.3855	6.8015	9.3073	
Stiction	0.2855	0.0704	-0.2886	6.7093	5.6888	
	0.8597	0.0691	-0.3879	6.7378	17.1299	
	0.5647	0.0587	1.5708	5.8349	11.2515	

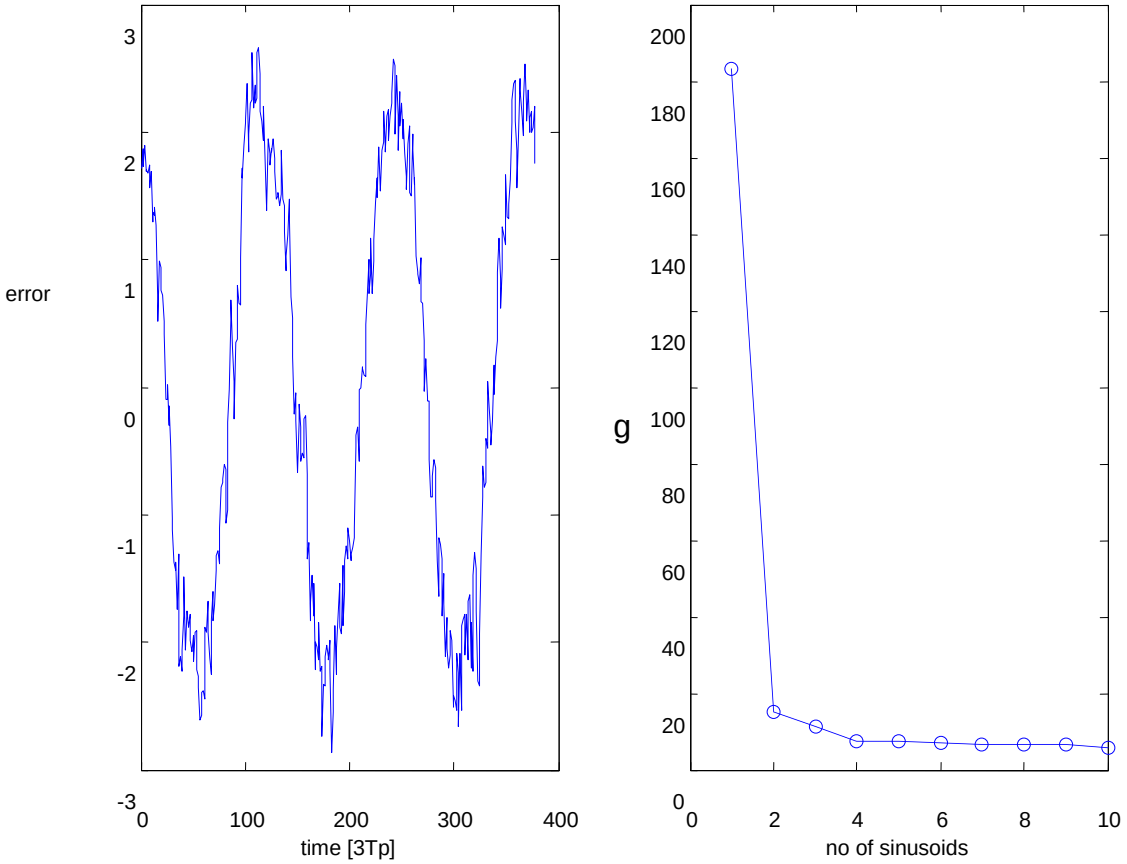

CHEM 12	Frequency, w rad/cycle	Amplitudes	Phase, radian	g	w./w(1)	Comment
Flow Control	0.0127	2.9586	-0.5588	570.9368	**1.0000**	Correctly detects stiction
	0.0261	0.8887	-1.0456	212.9822	**2.0465**	
Ts = 1 s **Time window: 1 to 1500**	0.0509	0.5171	1.1826	115.2510	**4.0009**	
	0.0178	0.4614	-1.5708	96.6191	1.3962	
	0.0383	0.3954	0.7854	91.5380	**3.0116**	
	0.0619	0.2129	0.5272	71.3649	4.8584	
	0.0586	0.4071	-0.7979	85.8932	4.5998	
Stiction	0.0456	0.3508	-1.1804	90.8166	3.5827	
	0.0298	0.3114	0.9022	93.6099	2.3433	
	0.0216	0.3128	-0.6898	106.3308	1.6997	

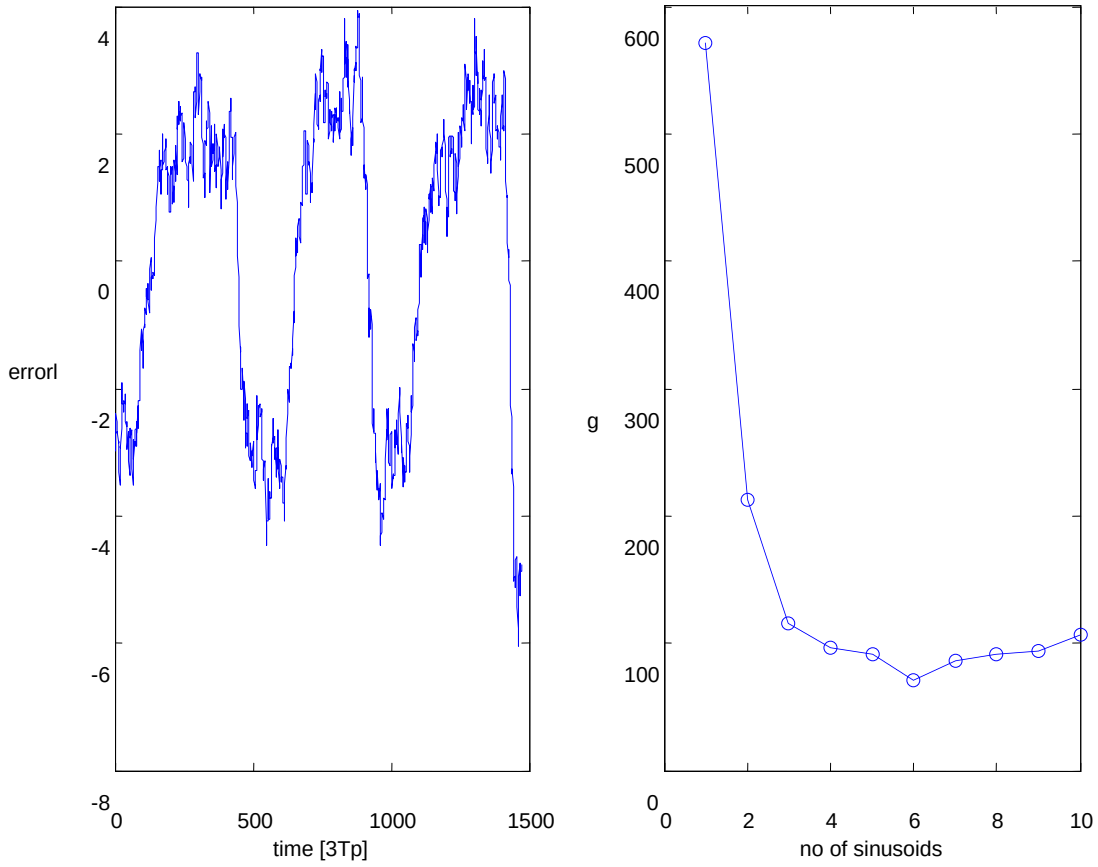

CHEM 13	Frequency, w rad/cycle	Amplitudes	Phase, radian	g	w./w(1)	Comment
Analyser control	0.2588	1.7163	0.2829	34.2995	1.0000	Correctly detects the absence of stiction
	0.0482	0.4376	0.3993	15.5336	0.1863	
Ts = 20 s **Time window: 1 to 73**	0.1428	0.1413	-1.1369	10.5417	0.5519	
	0.2895	0.1491	0.7114	10.9327	1.1187	
	0.5653	0.0584	0.2171	10.8168	2.1842	
	0.3548	0.0609	0	15.0178	1.3710	
	0.1036	0.0368	-1.5708	9.6317	0.4004	
Faulty steam sensor, no stiction	0.2289	0.0373	0.8834	12.1145	0.8844	
	0.4242	0.0189	-0.7800	9.2939	1.6391	
	0.5239	0.0179	0	10.5966	2.0244	

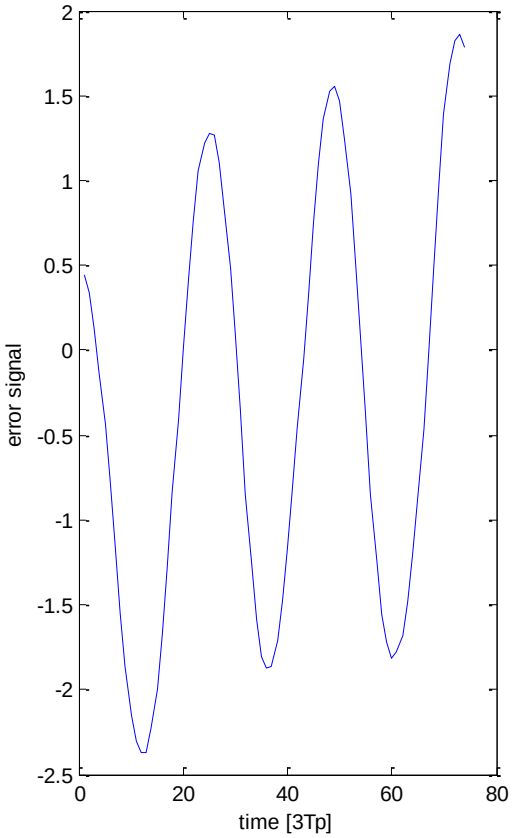

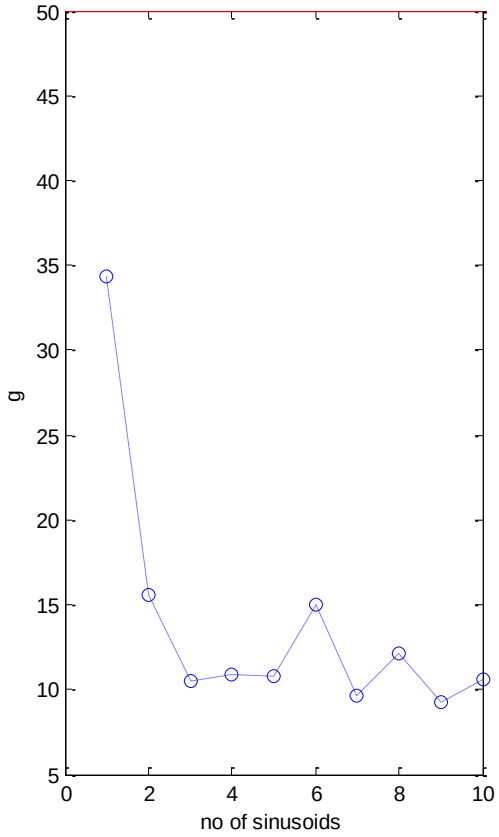

CHEM 14	Frequency, w rad/cycle	Amplitudes	Phase, radian	g	w./w(1)	Comment
Flow control	0.2750	0.6159	-1.1637	10.5265	1.0000	**Stiction**
	0.5425	0.3936	0.1205	11.8441	1.9728	
Ts=20 s **Time window: 1 to 60**	0.8104	**0.2032**	0.8134	6.2183	**2.9470**	
	0.6498	0.1914	-1.2770	5.6197	2.3630	
	1.3170	0.1372	-1.0838	4.8813	4.7895	
	0.9113	0.1226	-0.5278	4.1645	3.3142	
	1.2305	0.1047	-0.2491	4.1413	4.4749	
Faulty steam sensor, no stiction	1.9632	0.0989	1.3538	3.9238	7.1397	
	1.6703	0.0889	-0.4516	3.4149	6.0745	
	1.8734	0.0753	0.1816	3.1649	6.8131	

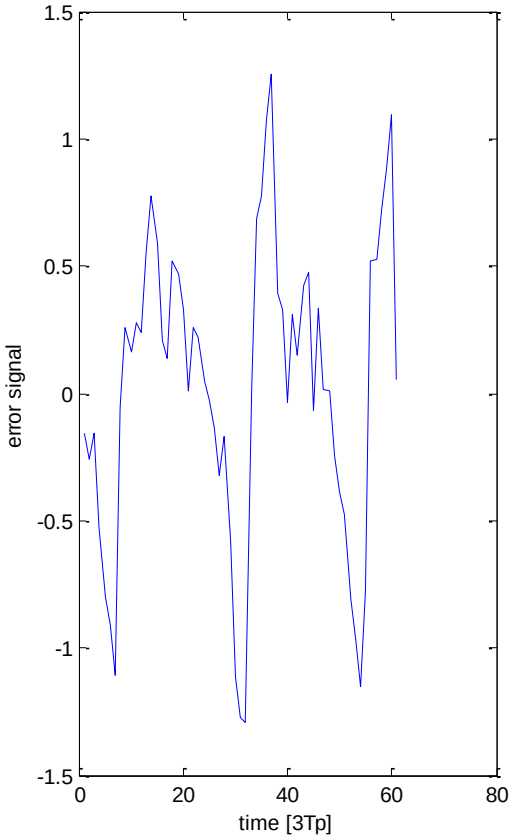

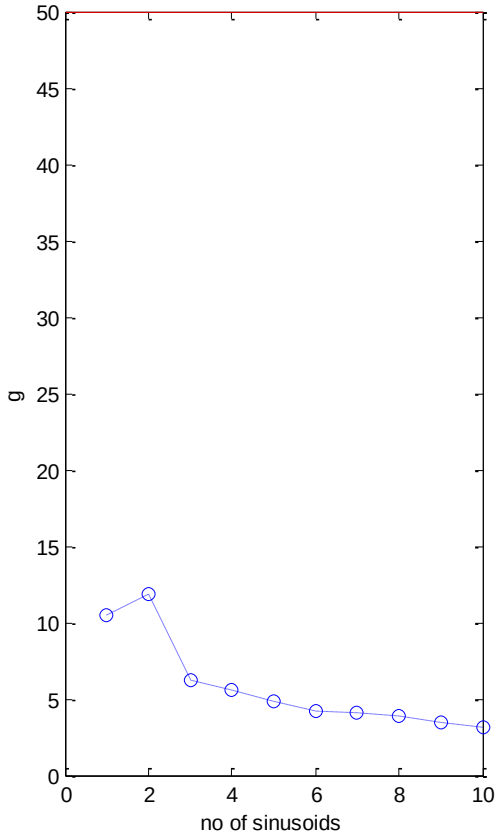

CHEM 16	Frequency, w rad/cycle	Amplitudes	Phase, radian	g	w./w(1)	Comment
Pressure Control	0.5441	0.3483	-0.2524	189.9044	1.0000	Correctly detects the absence of stiction
	0.8349	0.2120	-0.2719	6.3131	1.5343	
Ts = 20 s **Time window: 1 to 57**	0.6324	0.2149	-1.1767	8.1023	1.1621	
	0.4036	0.2208	1.0818	8.2202	0.7417	
	0.9518	0.1254	-1.2859	4.9090	1.7492	
	0.3041	0.1088	0	4.6541	0.5588	
	0.5125	0.0901	-1.1869	5.5181	0.9419	
Interaction (likely), no stiction	1.7824	0.0807	-1.5708	6.2429	3.2756	
	0.7626	0.0670	-1.5708	6.6965	1.4015	
	1.7070	0.0716	-0.7325	7.4754	3.1370	

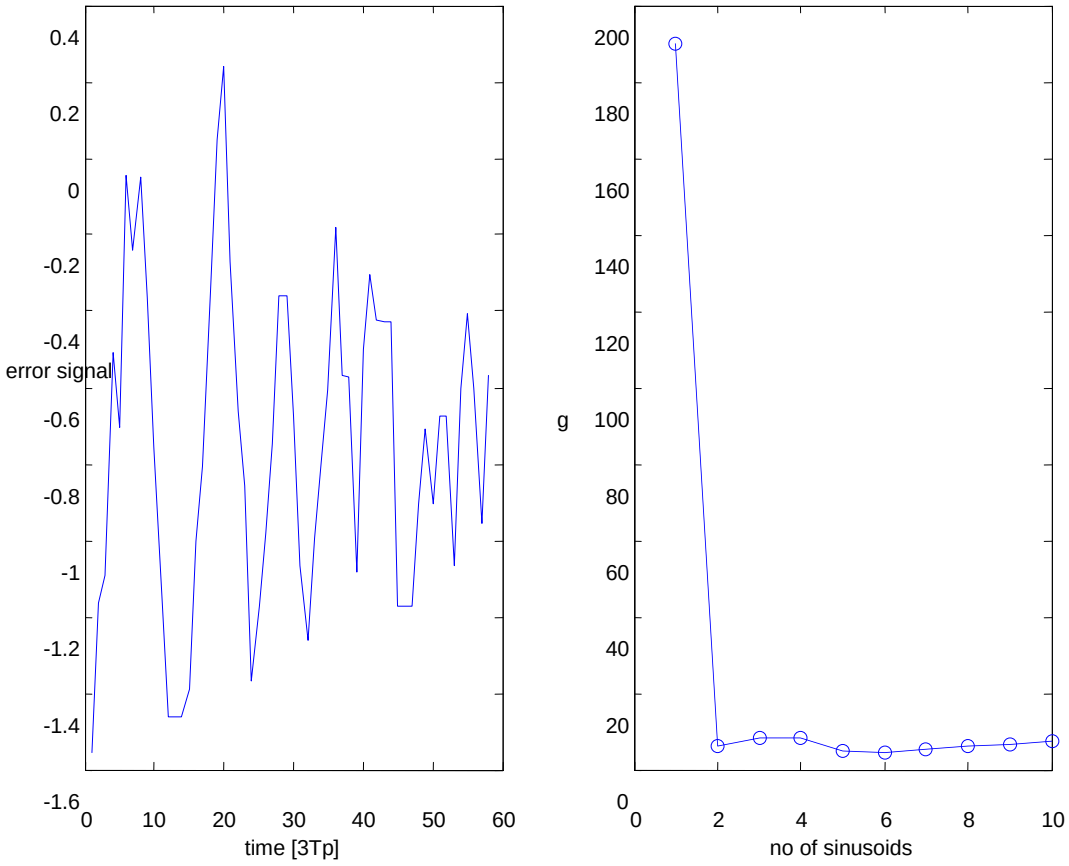

CHEM 18	Frequency, w rad/cycle	Amplitudes	Phase, radian	g	w./w(1)	Comment
Flow control	0.2245	2.3120	1.0230	22.8190	1.0000	Insignificant amount of stiction may present
	0.6808	0.5138	-0.1388	11.9302	**3.0331**	
Ts=12 s **Time window: 1 to 94**	0.3139	0.3665	0.0411	11.6879	1.3983	
	0.1438	0.2964	-0.7911	12.6096	0.6407	
	0.4775	0.2354	1.3376	9.0654	2.1274	
	0.4060	0.1402	0.5278	5.4492	1.8089	
	0.8582	0.1330	-0.9084	5.7730	3.8235	
Stiction (likely)	1.1188	0.1235	-0.8745	5.8762	4.9844	
	0.9382	0.1199	-0.0923	5.6120	4.1799	
	0.7522	0.0994	0.5998	3.4744	3.3511	

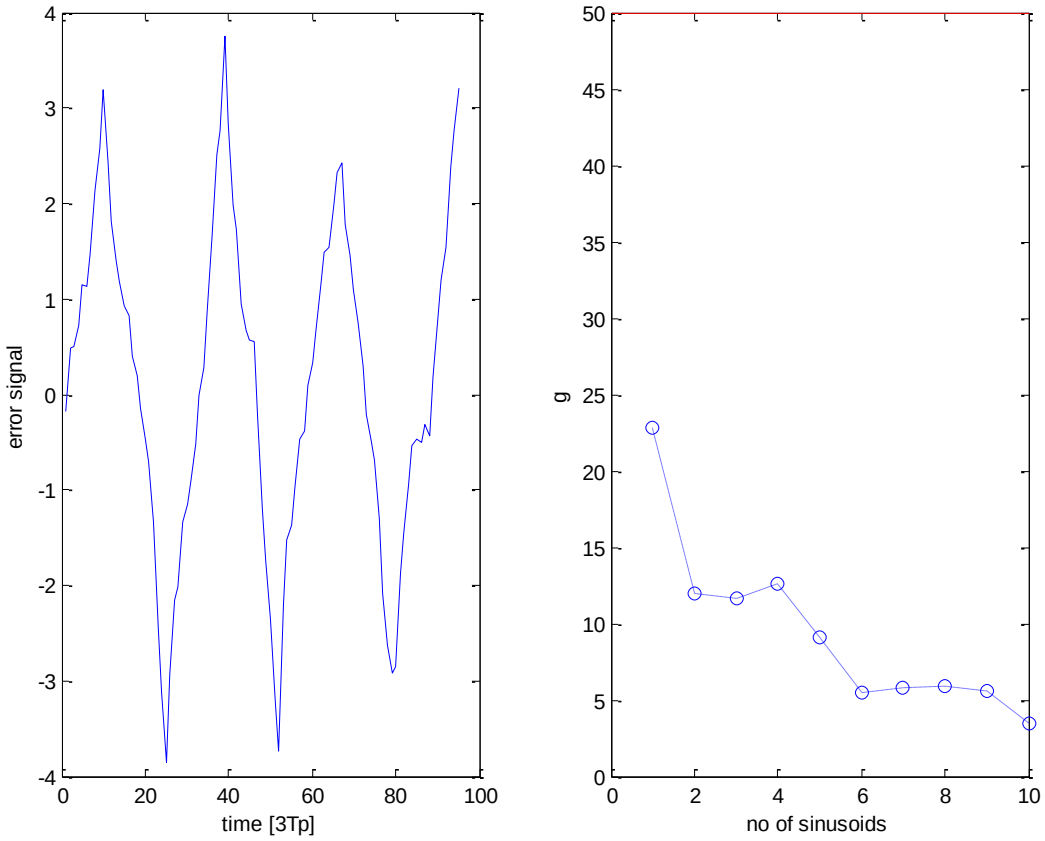

CHEM 23	Frequency, w rad/cycle	Amplitudes	Phase, radian	g	w./w(1)	Comment
Flow control	0.0506	0.3417	0	147.6556	1.0000	**Stiction**
	0.1509	0.0966	0.1669	40.3656	**2.9832**	
Ts =12 s	0.9470	0.0628	0.7243	27.5942	18.7204	
	0.0967	0.0401	1.2517	16.0602	1.9122	
	0.1165	0.0381	0	15.6974	2.3032	
	0.2257	0.0360	-1.2627	15.8513	4.4619	
	0.1999	0.0370	0.4948	15.8307	3.9517	
Stiction (likely)	0.9601	0.0340	-1.1821	17.0634	18.9791	
	0.9723	0.0312	1.5708	15.5303	19.2203	
	0.8963	0.0290	0	13.5910	17.7172	

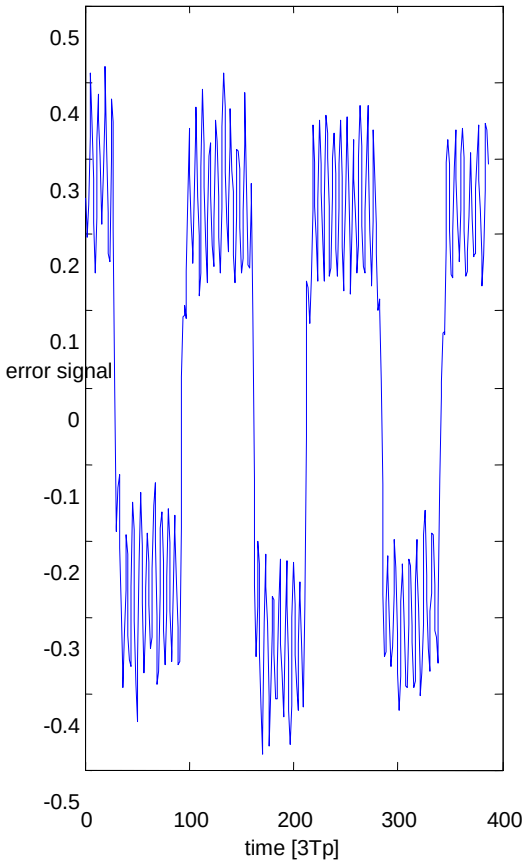

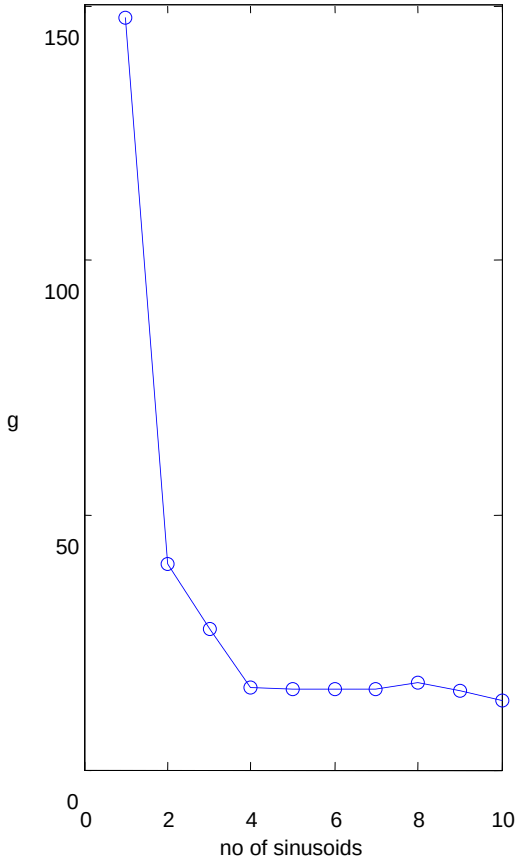

CHEM 24	Frequency, w rad/cycle	Amplitudes	Phase, radian	g	w./w(1)	Comment
Flow control	0.4410	59.1964	-0.0808	10.8973	1.0000	**Stiction**
	0.0720	67.2587	-0.7751	12.1271	0.1633	
Ts = 12 s **Time window: 1 to 41**	0.3043	28.8910	-0.3868	15.4361	0.6899	
	0.4181	9.1737	-1.0948	5.3058	0.9480	
	0.6455	8.7098	-0.0406	5.1134	1.4636	
	0.1722	5.1265	-0.2881	3.8555	0.3904	
	1.3402	**5.0232**	0.6649	4.7437	**3.0389**	
Stiction (likely)	1.1594	3.3022	0.2651	3.3310	2.6288	
	0.9940	4.3406	0.7910	4.5097	2.2538	
	0.8062	4.0081	0.4415	3.3490	1.8280	

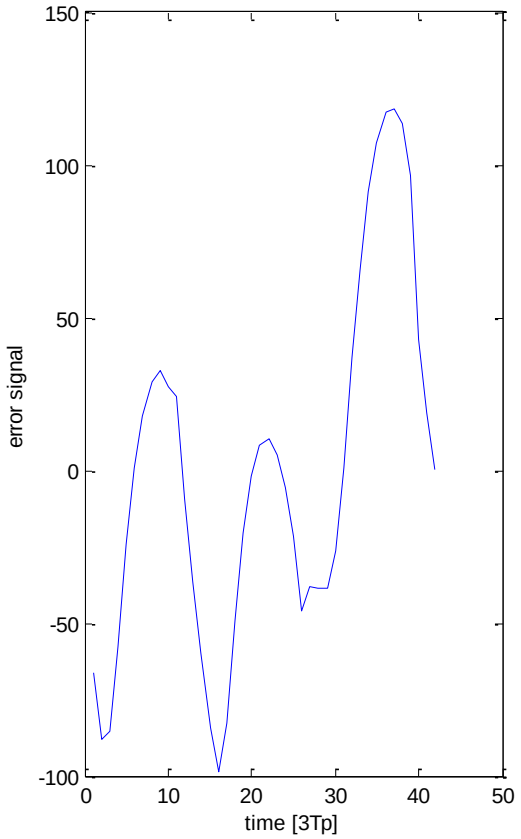

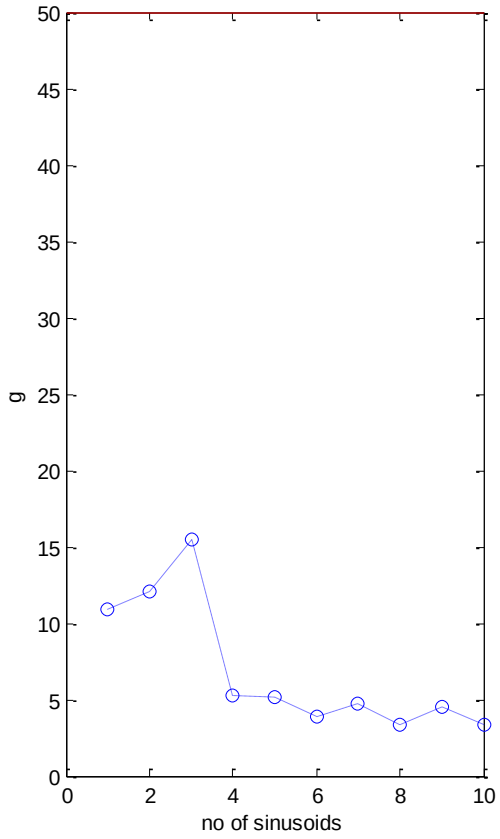

CHEM 28	Frequency, w rad/cycle	Amplitudes	Phase, radian	g	w./w(1)	Comment
Temperature control	0.0473	1.3859	-0.8590	184.9540	1.0000	Stiction not likely to be present
	0.0336	0.1912	0.7250	52.2569	0.7099	
Ts=12 s **Time window: 1 to 390**	0.0740	0.2291	-0.2902	55.0371	1.5663	
	0.0943	**0.1026**	-0.6220	51.0423	**1.9951**	
	0.0629	0.0843	0	44.3750	1.3312	
	0.1487	0.0780	0.9620	37.2721	3.1464	
	0.0148	0.0556	1.1113	36.0225	0.3125	
Stiction (likely)	0.0815	0.0391	0.2653	22.3212	1.7249	
	0.1869	**0.0316**	1.2056	24.9607	**3.9536**	
	0.1722	0.0454	0	31.2273	3.6440	

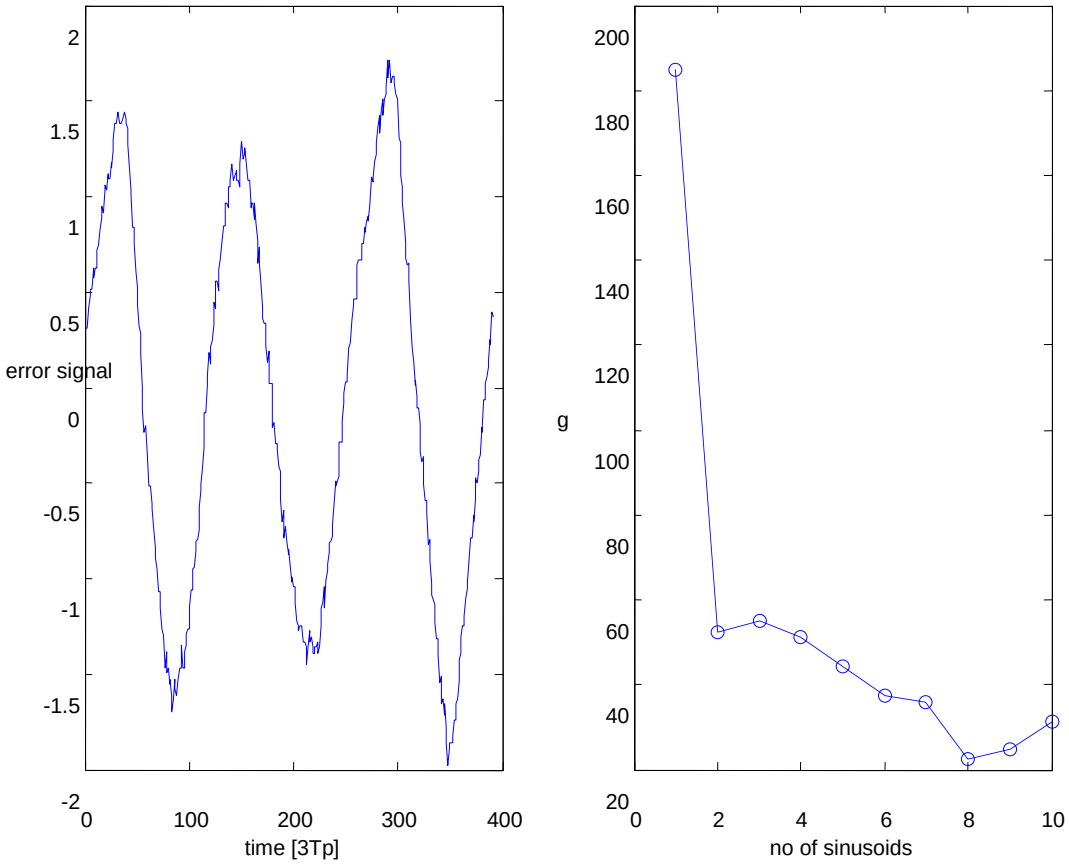

CHEM 29	Frequency, w rad/cycle	Amplitudes	Phase, radian	g	w./w(1)	Comment
Flow control	0.3264	34.4782	-0.5509	13.4385	1.0000	Stiction
	1.1389	16.9605	0.0859	6.1687	3.4888	
Ts=60 s **Time window: 1 to 60**	0.4833	17.2341	0.2963	6.2741	1.4805	
	0.7175	11.5265	-0.4911	5.2744	2.1980	
	0.9678	**11.2627**	-0.3184	**4.3615**	**2.9646**	
	1.5315	9.6996	0.6156	5.2790	4.6916	
	0.1539	9.6516	-1.5242	5.4911	0.4715	
Stiction	0.0692	6.6307	-0.0269	3.4823	0.2121	
	1.7651	5.8706	1.2181	3.8101	5.4074	
	2.1949	7.0079	-0.8773	4.1226	6.7238	

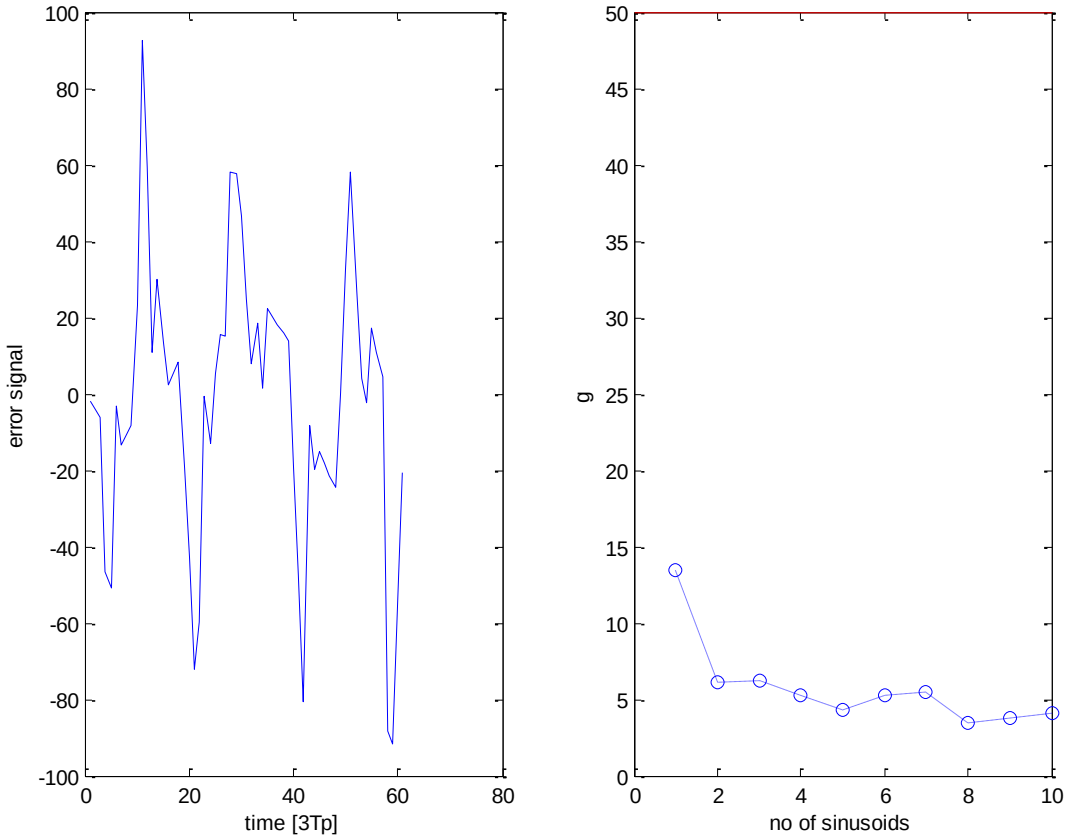

CHEM 32	Frequency, w rad/cycle	Amplitudes	Phase, radian	g	w./w(1)	Comment
Flow control	0.0667	15.1147	-1.1312	131.1149	1.0000	Stiction
	0.2061	**2.2417**	-0.3598	**52.1796**	**3.0901**	
Ts=10 s **Time window: 1 to 272**	0.0476	1.4313	1.1949	30.6255	0.7141	
	0.0853	1.4033	-0.4657	35.9253	1.2792	
	0.0179	1.1312	-0.1541	37.8604	0.2684	
	0.1241	1.0129	-0.3013	29.3424	1.8616	
	0.1643	0.4659	0.7143	14.8640	2.4645	
Stiction (likely)	0.3384	**0.3833**	0.9522	**10.4641**	**5.0750**	
	0.2478	0.3590	-0.7659	9.4014	3.7160	
	0.2822	0.2532	0.2651	6.2350	4.2319	

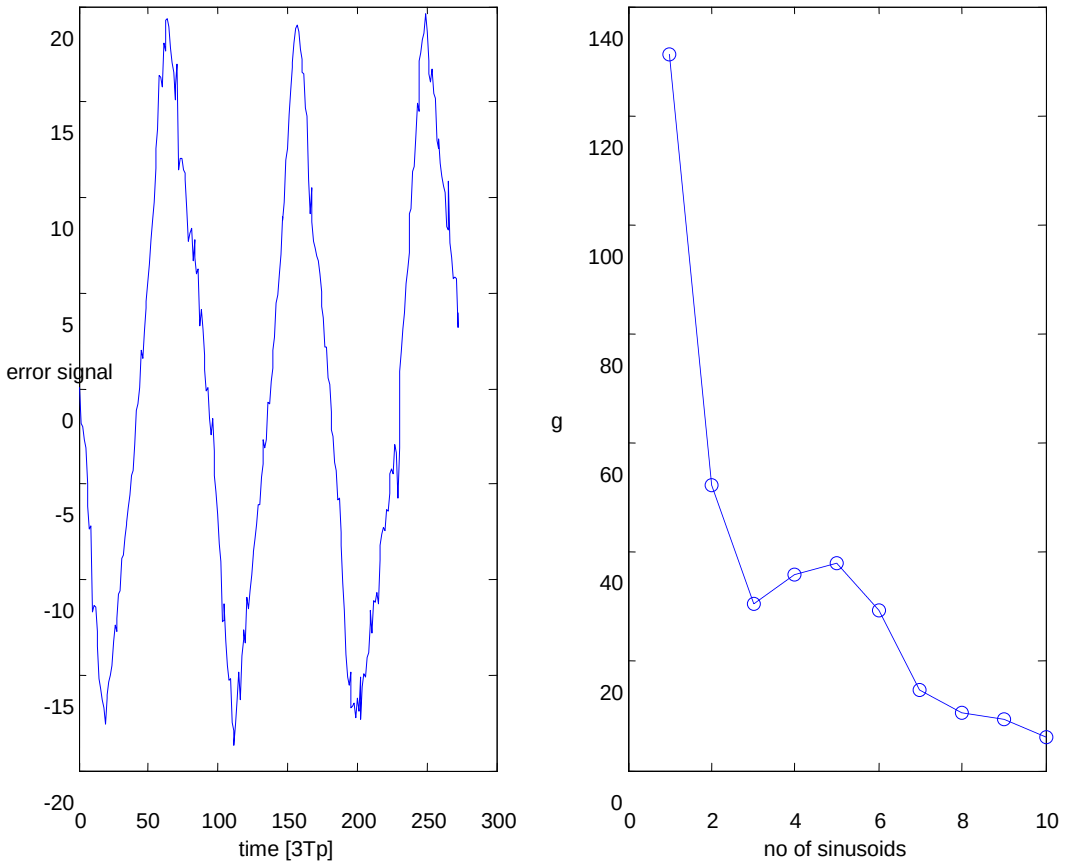

CHEM 33	Frequency, w rad/cycle	Amplitudes	Phase, radian	g	w./w(1)	Comment
Flow control	0.6797	0.2366	-0.5319	6.8708	1.0000	No stiction
	0.4575	0.1179	0	6.5834	0.6731	
Ts = 12 **Time window:1 to 69**	0.5625	0.1082	1.2294	5.1522	0.8275	
	0.7777	0.1108	1.2907	6.0031	1.1441	
	0.1040	0.0660	-1.3058	4.4390	0.1531	
	1.9075	0.0682	1.1688	5.0980	2.8063	
	0.1937	0.0587	-0.5888	6.2590	0.2849	
Disturbance (likely)	1.8169	0.0587	-0.5059	7.1824	2.6730	
	0.3752	0.0566	-1.5708	8.0574	0.5520	
	0.2797	0.0444	0.4760	9.2178	0.4115	

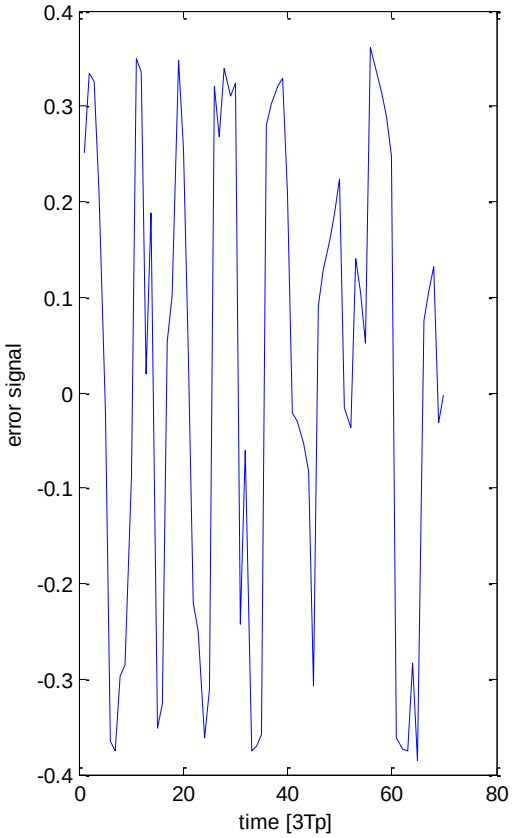

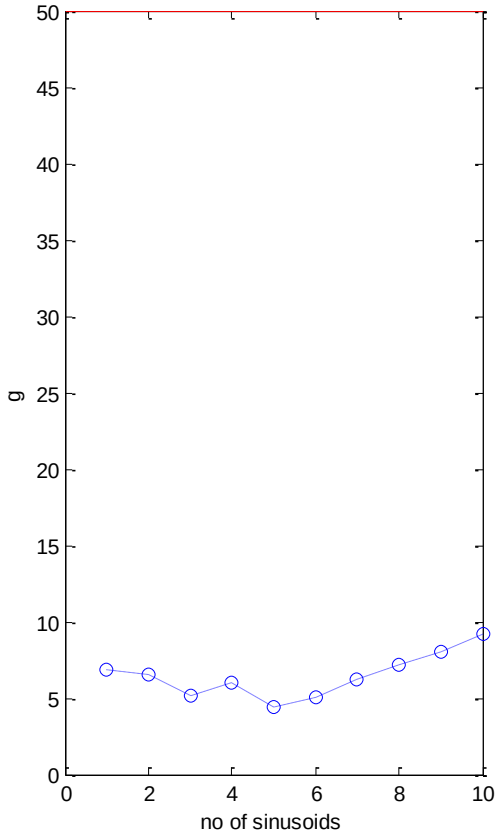

CHEM 40	Frequency, w rad/cycle	Amplitudes	Phase, radian	g	w./w(1)	Comment
Temperature control	0.2904	1.0006	-0.5433	13.6420	1.0000	No stiction
	0.4195	0.8345	0.8856	7.7063	1.4443	
Ts=60 s **Time window: 200 to 267**	0.1040	0.4826	0.3116	11.3024	0.3582	
	0.2232	0.4238	-0.0357	6.0712	0.7685	
	0.3316	0.2802	-1.2188	4.6528	1.1416	
	0.8281	0.1965	-1.4438	6.6593	2.8513	
	0.7057	0.2273	0.3997	8.1785	2.4297	
No clear oscillation (PS)	1.0009	0.1556	-0.8941	7.3793	3.4462	
	0 + 0.0800i	0 + 0.0244i	-1.5708 + 1.6941i	5.5196	0 + 0.2754i	
	0.4938	0.1230	1.5708	6.8656	1.7003	

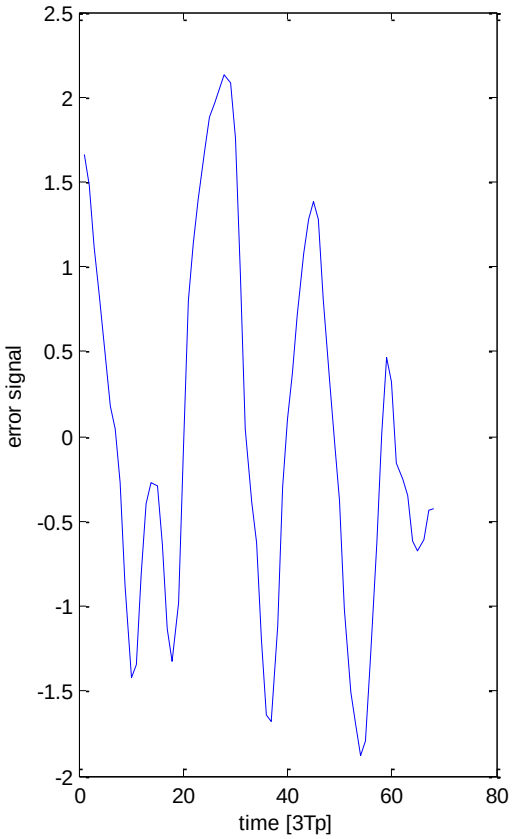

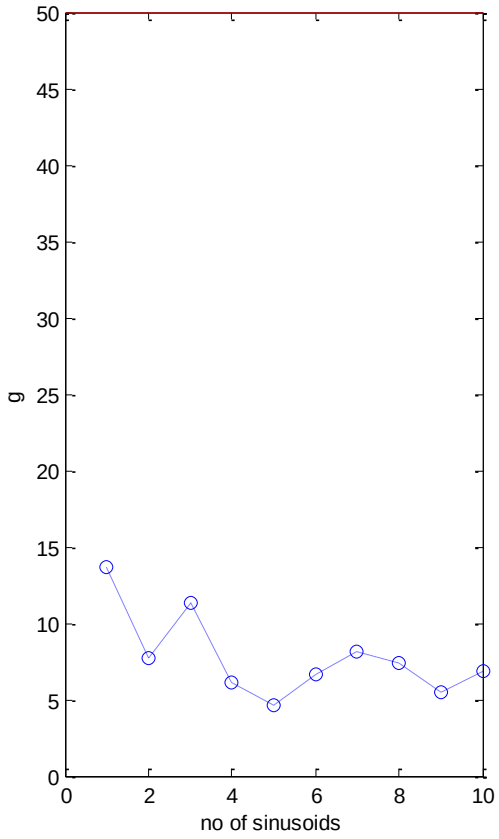

CHEM 54	Frequency, w rad/cycle	Amplitudes	Phase, radian	g	w./w(1)	Comment
Level control	0.2380	1.0583	0.8759	11.5473	1.0000	Correctly detects the absence of stiction.
	0.3377	0.8932	-0.2943	14.6822	1.4192	
Ts= 60 s **Time window: 1 to 50**	0.1314	0.5774	-0.1883	20.6599	0.5522	
	0.6165	0.1654	0.1758	8.1821	2.5907	
	0.2440	0.1329	-1.4225	7.8418	1.0255	
	0.3813	0.1314	0.2967	11.0779	1.6023	
	1.5909	0.0762	0	6.8958	6.6851	
No clear oscillation	0.8914	0.0733	1.4244	6.5428	3.7459	
	1.1213	0.0606	-0.4621	8.2052	4.7120	
	1.4707	0.0425	0.5643	6.1131	6.1803	

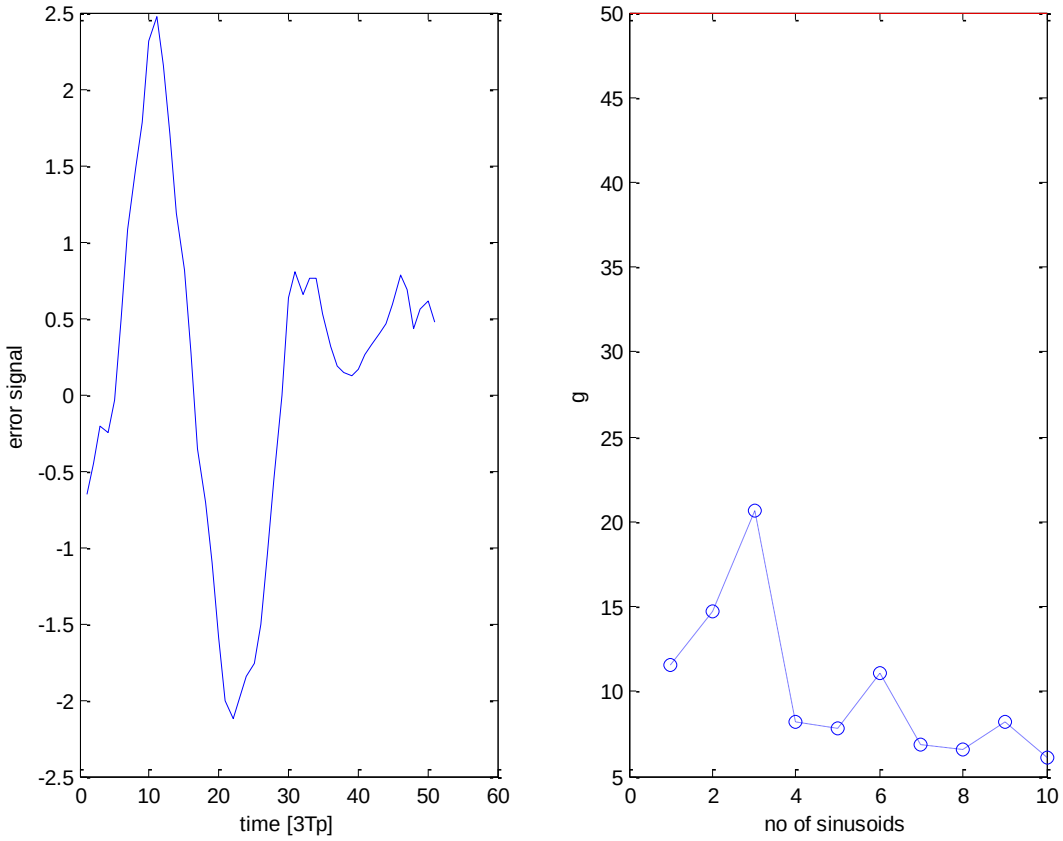

CHEM 62	Frequency, w rad/cycle	Amplitudes	Phase, radian	g	w./w(1)	Comment
Flow control	0.2386	0.3144	0.8806	3.9435	1.0000	Correctly detects the absence of stiction
	0.9828	0.2968	0.3869	4.4041	4.1188	
Ts = 60 **Time window: 1 to 50**	1.0730	0.2926	-0.2579	5.2555	4.4969	
	0.7609	0.2840	-1.4369	4.5506	3.1887	
	0.4291	0.3619	1.2504	5.3858	1.7984	
	0.1267	0.1731	-1.4383	5.6776	0.5311	
	0.5860	0.1640	-0.6544	5.7880	2.4560	
No clear oscillation (PS)	1.4436	**0.1558**	0.5664	**7.1566**	**6.0500**	
	0.8523	0.1231	-0.5563	8.6462	3.5718	
	0.2535	0.0811	-0.4340	5.8169	1.0624	

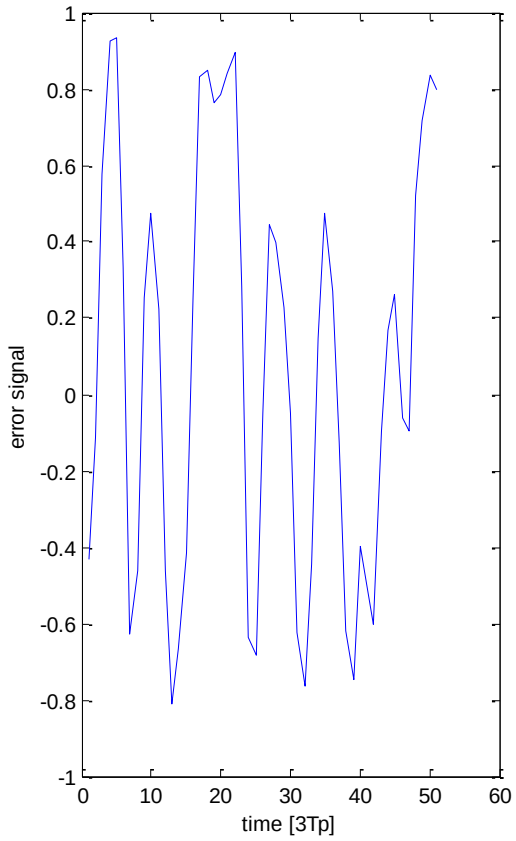

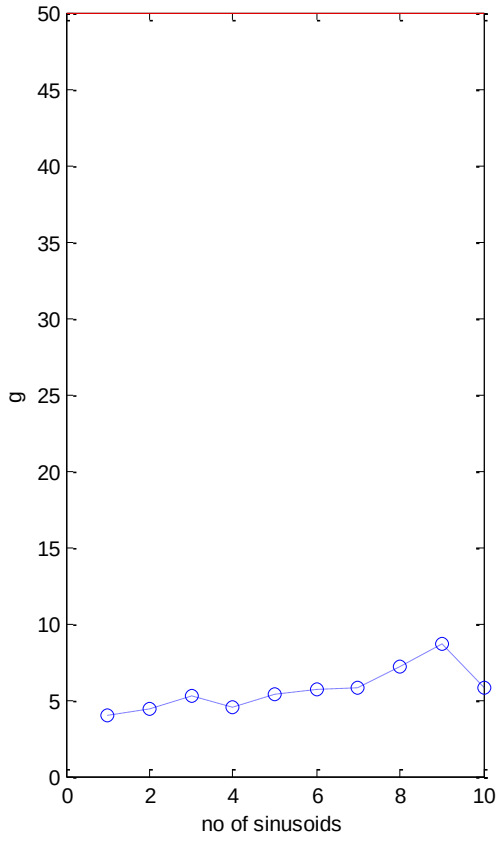

PAP 2	Frequency, w rad/cycle	Amplitudes	Phase, radian	g	w./w(1)	Comment
Flow control	0.1543	1.7286	1.1026	47.2471	1.0000	Stiction
	0.3110	**0.4540**	-0.3429	13.9225	**2.0154**	
Ts = 1 **Time window: 1 to 127**	0.4668	**0.4875**	-1.1878	17.4489	**3.0253**	
	0.1994	0.2327	0.7535	21.6107	1.2926	
	0.6331	**0.1505**	-0.8659	13.8622	**4.1035**	
	0.4215	0.1453	-0.4175	12.4886	2.7319	
	0.6855	0.1037	1.0740	11.5643	4.4426	
Stiction	0.3700	0.1111	1.4485	8.4085	2.3981	
	0.2901	0.0625	-1.5708	7.0150	1.8802	
	1.1062	0.0764	-1.0201	7.0654	7.1696	

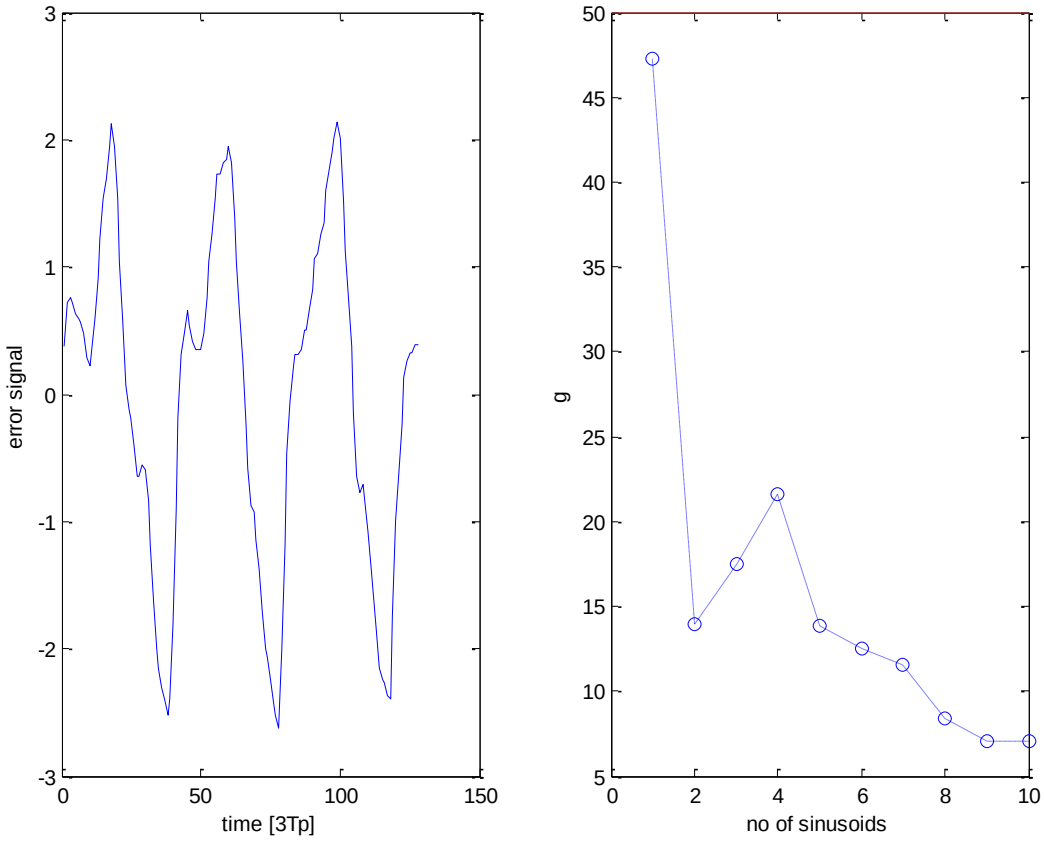

PAP 4	Frequency, w rad/cycle	Amplitudes	Phase, radian	g	w./w(1)	Comment
Concentration control	0.1538	17.2605	-1.2662	54.7195	1.0000	Stiction
	0.3152	2.6689	-0.2691	13.3166	**2.0494**	
Ts=1 **Time window: 1 to 127**	0.4796	**2.4049**	-0.6062	24.2173	**3.1188**	
	0.6299	1.8111	0.3155	26.1214	**4.0957**	
	0.1924	1.3678	-0.6428	28.7453	1.2509	
	0.1004	0.8166	1.3232	16.5472	0.6530	
	0.2857	0.5593	-0.3505	10.8499	1.8578	
Deadzone and tight tuning	0.0499	0.5147	-0.9207	11.7050	0.3242	
	0.4366	0.4636	0.9679	10.9801	2.8389	
	0.7351	0.4003	0.4735	10.6638	4.7803	

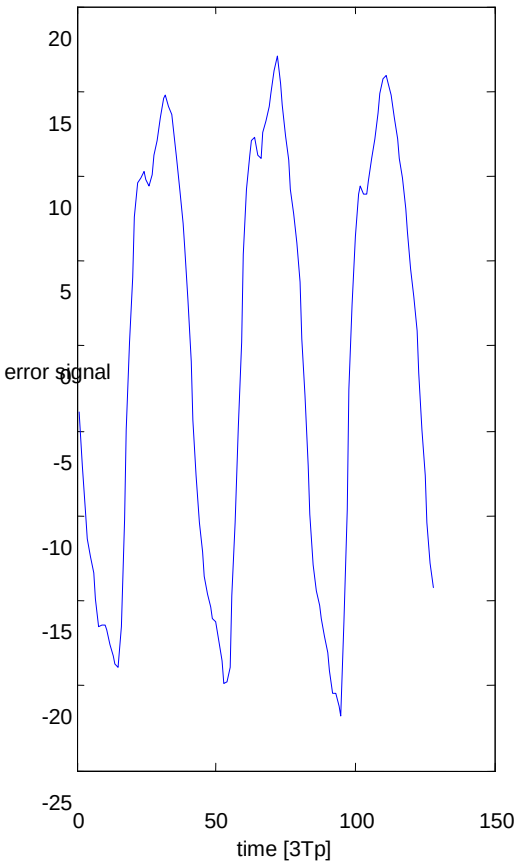

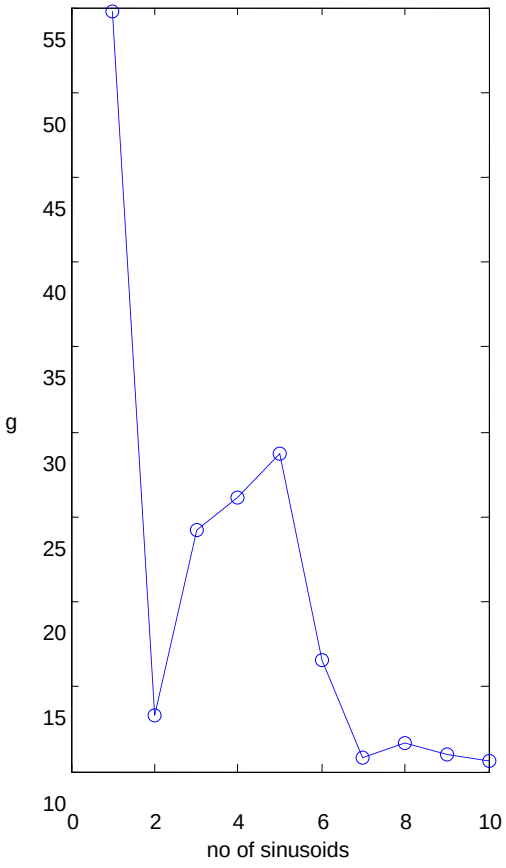

PAP 5	Frequency, w rad/cycle	Amplitudes	Phase, radian	g	w./w(1)	Comment
Concentration control	0.0429	0.0721	-0.2279	155.6501	1.0000	No stiction
	0.0542	0.0120	0	72.5822	1.2641	
Ts= 0.2 **Time window: 9000 to 9486**	0.0883	**0.0085**	0	56.9606	**2.0616**	
	0.0120	0.0069	0	61.7028	0.2799	
	0.1033	0.0055	0	44.3048	2.4108	
	0.1410	0.0056	0	52.8709	3.2896	
	0.1566	0.0044	0	41.1473	3.6547	
Stiction	0.0354	0.0041	0	39.3563	0.8263	
	0.0702	0.0046	0	40.8634	1.6377	
	0.1896	0.0031	0	37.6164	4.4242	

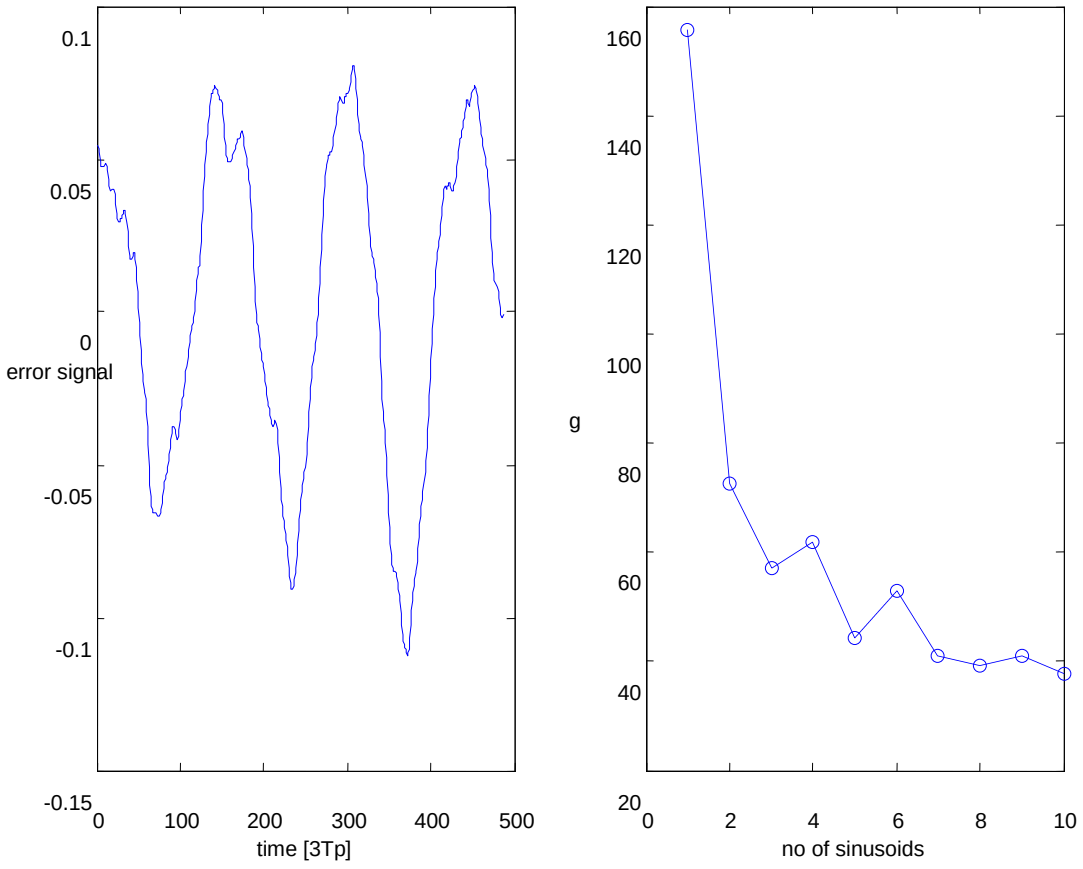

PAP 7	Frequency, w rad/cycle	Amplitudes	Phase, radian	g	w./w(1)	Comment
Flow control	0.0223	0.0120	0	73.6981	1.0000	No stiction
	0.1154	0.0116	0	69.2572	5.1661	
Ts=0.2 s **Time window: 1 to 2728**	0.0044	0.0113	0	69.9635	0.1959	
	0.1059	0.0106	0	71.5287	4.7407	
	0.0208	0.0084	0	47.4595	0.9310	
	0.0274	0.0077	0	38.7057	1.2245	
	0.1395	0.0084	0	37.6232	6.2454	
External disturbance	0.0992	0.0077	0	40.0021	4.4410	
	0.0137	0.0070	0	36.5424	0.6111	
	0.1606	0.0062	0	35.6298	7.1898	

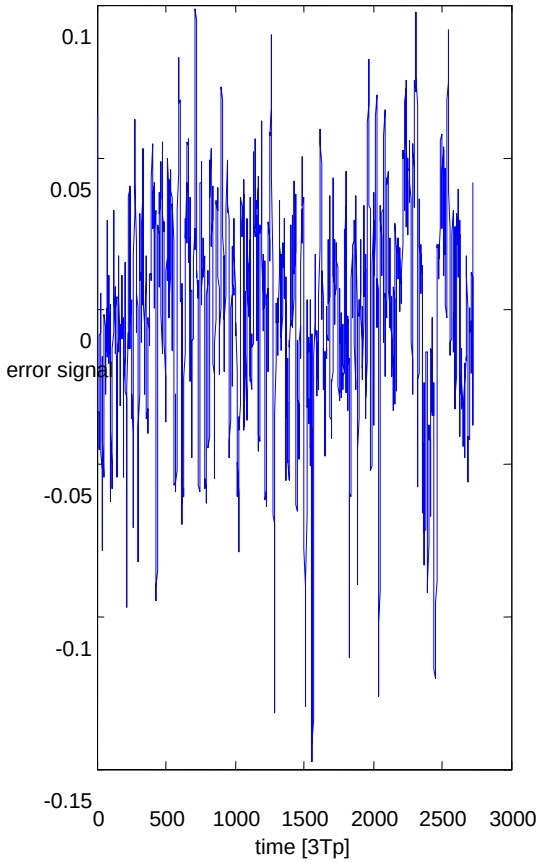

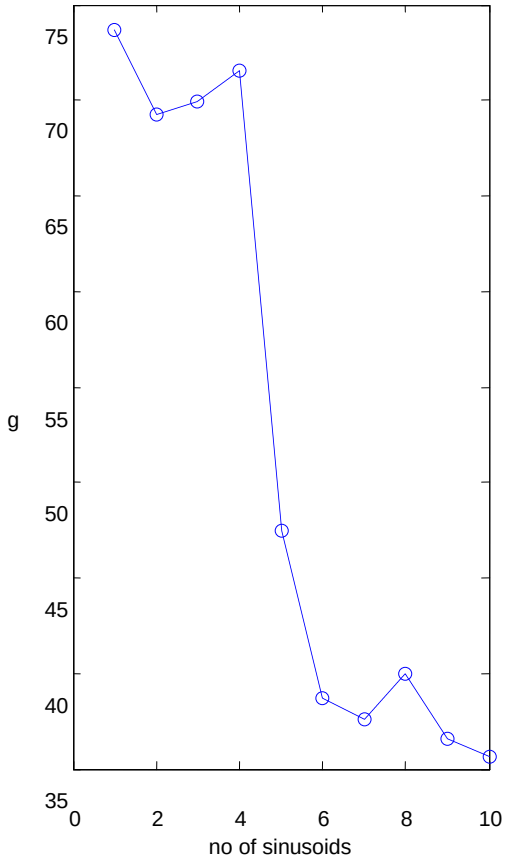

PAP 9	Frequency, w rad/cycle	Amplitudes	Phase, radian	g	w./w(1)	Comment
Temperature control	0.0479	16.9473	-0.3442	178.6745	1.0000	No stiction
	0.0333	4.6596	0.9534	110.9710	0.6965	
Ts = 5 **Time window: 1 to 406**	0.0583	1.9629	-0.7141	72.7985	1.2173	
	0.0172	1.4722	-0.3202	74.6824	0.3587	
	0.1045	1.1964	-0.1951	69.5645	2.1844	
	0.1934	0.5611	1.2722	28.3654	4.0417	
	0.1543	0.5102	-0.2203	25.1522	3.2238	
No stiction	0.0298	0.5064	-0.8793	28.4536	0.6217	
	0.0929	0.5086	-0.0942	33.4753	1.9421	
	0.2429	0.4683	0.0820	35.3727	5.0757	

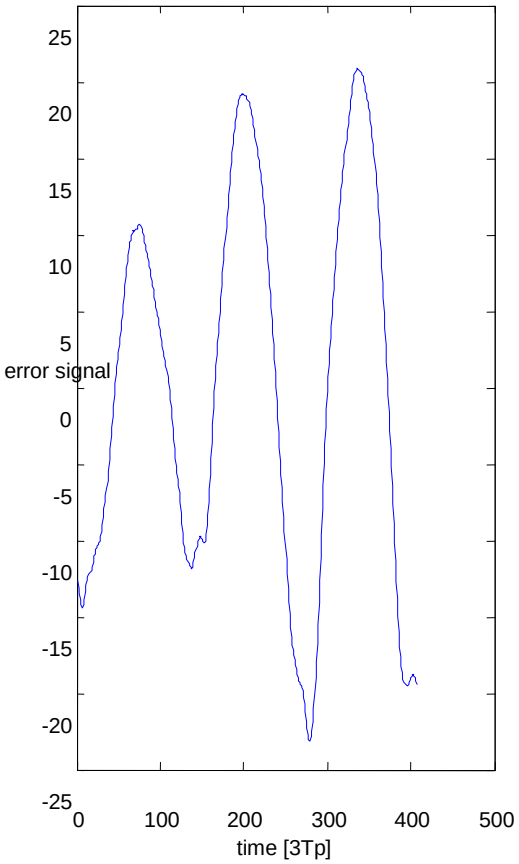

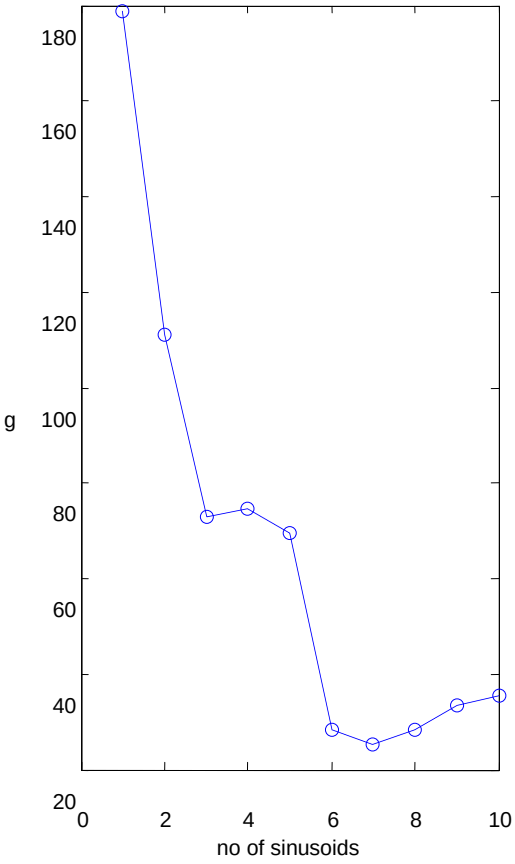

MIN 1	Frequency, w rad/cycle	Amplitudes	Phase, radian	g	w./w(1)	Comment
Temperature control	0.0548	9.1465	-0.0509	99.9486	1.0000	
	0.1110	**4.4924**	-0.4056	**74.2150**	**2.0274**	
Ts=60 **Time window: 670 to 999**	0.0758	2.6421	-1.0179	48.5561	1.3843	
	0.0297	2.4424	-1.2749	29.4361	0.5418	
	0.1550	1.5902	-1.4238	32.0089	2.8318	
	0.0977	1.3413	-0.8528	33.5445	1.7851	
	0.1311	1.1305	-0.8285	27.9564	2.3945	
Stiction	0.1857	1.0459	0.0879	25.7473	3.3922	
	0.2481	0.9064	-1.4119	27.7771	4.5317	
	0.2296	0.7280	-0.3942	22.1837	4.1926	

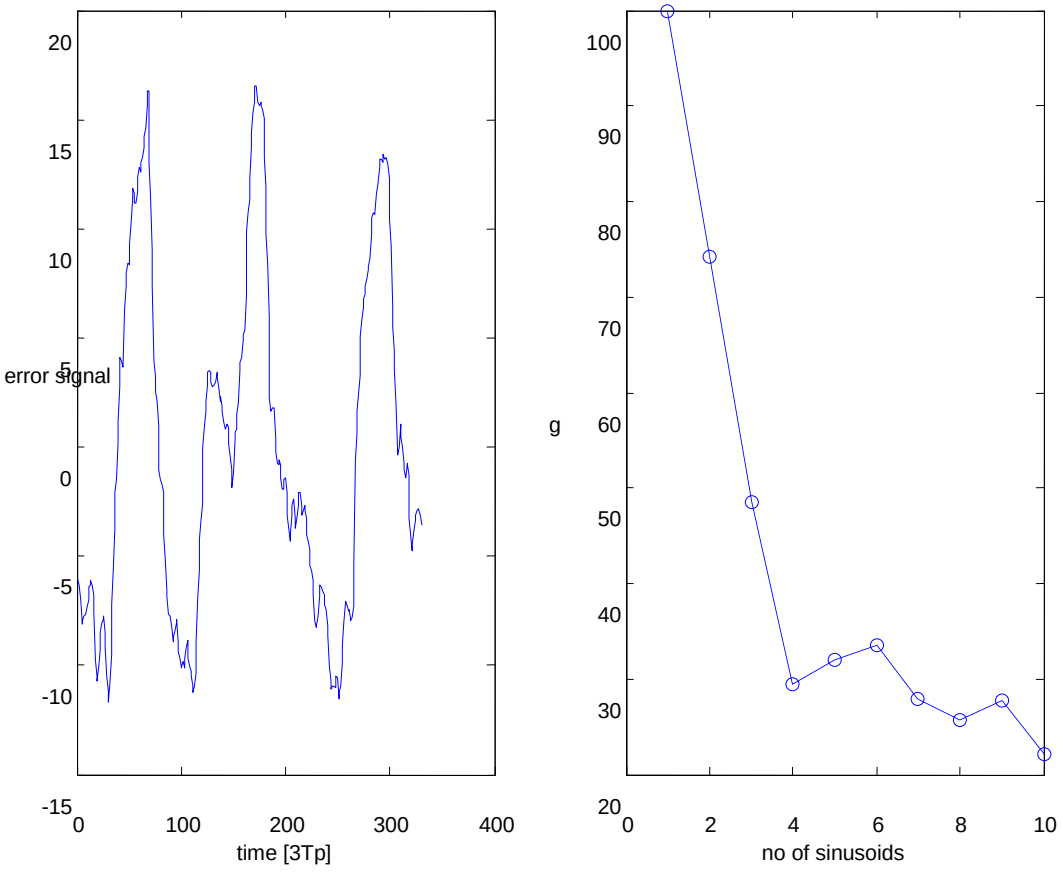

MET 1	Frequency, w rad/cycle	Amplitudes	Phase, radian	g	w./w(1)	Comment
Gauge control	0.0637	0.0118	0	96.5432	1.0000	No stiction
	0.0355	0.0037	0	22.3272	0.5569	
Ts=0.05 **Time window: 1 to 306**	0.0152	0.0024	0	18.7605	0.2394	
	0.1220	**0.0026**	0	**19.2526**	**1.9150**	
	0.3542	0.0023	0	11.2585	5.5605	
	0.2290	0.0017	0	10.3818	3.5951	
	0.1426	0.0014	0	8.4047	2.2397	
External disturbance likely	0.4320	0.0015	0	8.3759	6.7834	
	0.8141	0.0014	0	8.5465	12.7827	
	0.2513	0.0015	0	8.5460	3.9458	

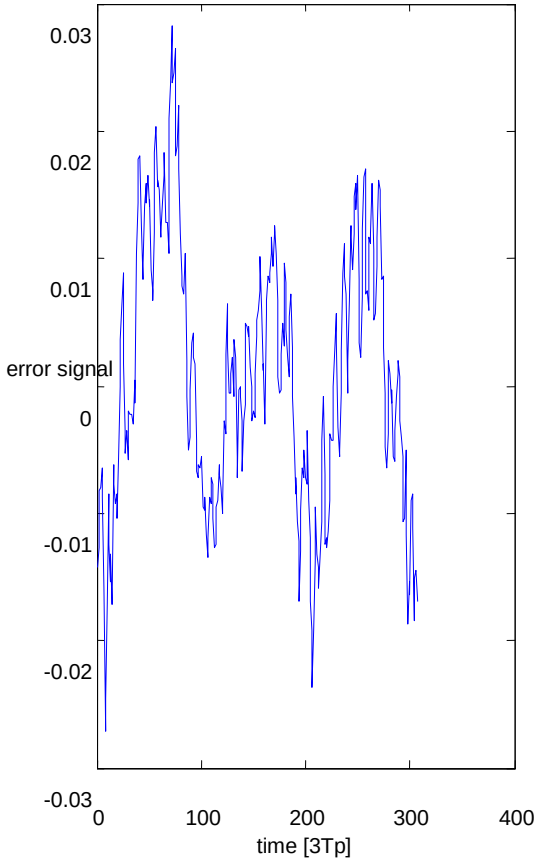

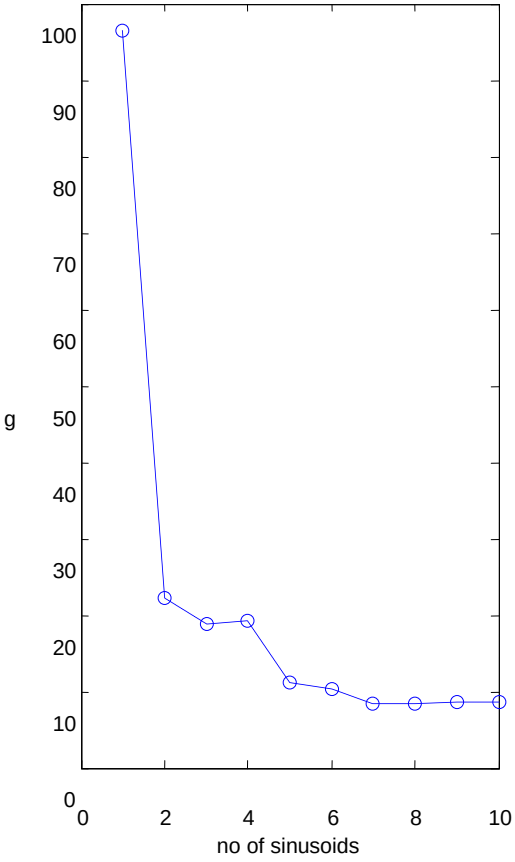

MET 2	Frequency, w rad/cycle	Amplitudes	Phase, radian	g	w./w(1)	Comment
Gauge control	0.2260	0.0027	0	17.0278	1.0000	No stiction
	0.4614	**0.0018**	**0**	**12.9719**	**2.0414**	
Ts =0.05 **Time window: 1 to 81**	0.8409	0.0014	0	11.5388	3.7206	
	0.3566	0.0014	0	11.5558	1.5778	
	0.0536	0.0010	0	11.5362	0.2370	
	0.5975	0.0008	0	11.1368	2.6435	
	0.7404	0.0006	0	7.5181	3.2756	
External disturbance likely	0.1779	0.0005	0	6.0806	0.7871	
	0.9830	0.0004	0	6.1342	4.3491	
	1.0853	0.0003	0	5.1955	4.8017	

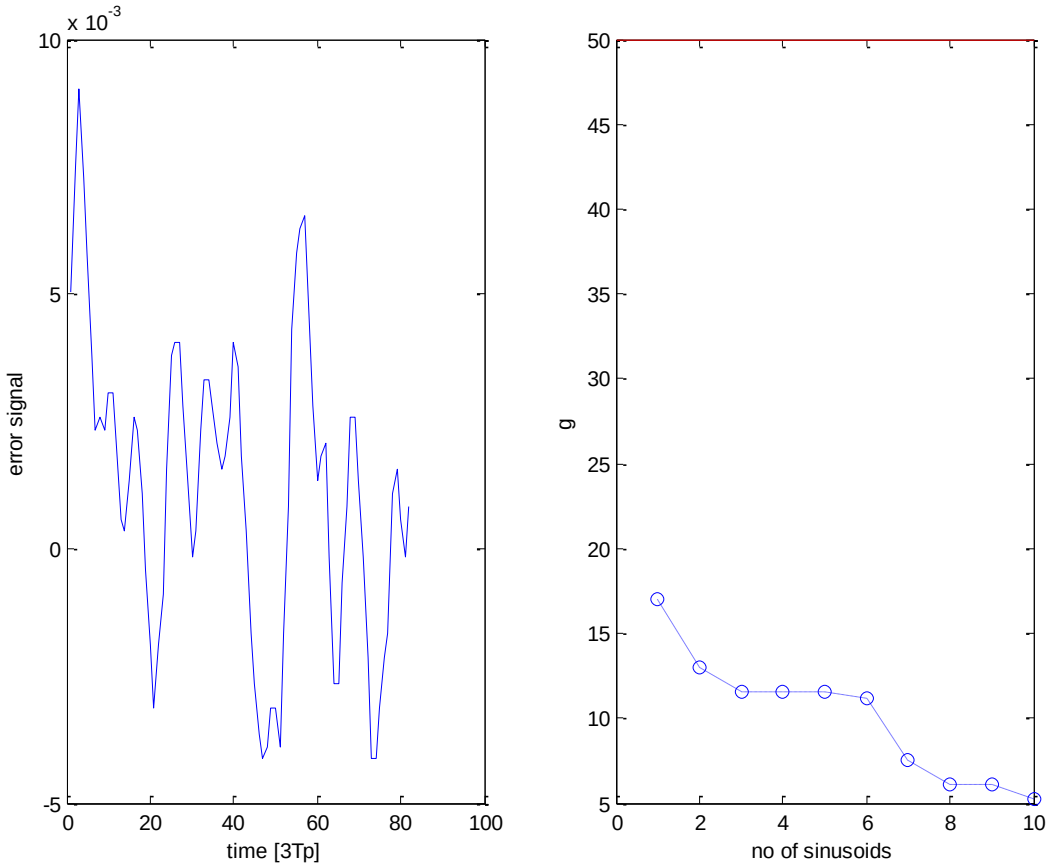

MET 3	Frequency, w rad/cycle	Amplitudes	Phase, radian	g	w./w(1)	Comment
Gauge control	0.1854	0.0026	0	17.5960	1.0000	No stiction
	0.4914	0.0021	0	15.3071	2.6502	
Ts=0.05 **Time window: All**	0.7753	0.0015	0	15.7973	4.1815	
	0.3027	0.0010	0	9.2281	1.6324	
	0 + 0.0067i	0.0219	0	9.5834	0 + 0.0360i	
	0.5975	0.0008	0	10.9159	3.2226	
	0.3516	0.0008	0	13.1981	1.8965	
No oscillation	0.9446	**0.0005**	0	8.4435	**5.0945**	
	0.2423	0.0005	0	8.2249	1.3070	
	0.1305	0.0005	0	8.2067	0.7040